The TMT Laser Guide Star Facility Conceptual Design Rework Report

TMT.AOS.CDD.08.001.REL09

Submitted By:
NOAO

April 23, 2008

Revision: 0.8.

Standard Revision Control

1. Revision Version # 0.0
   Date: 2008-01-07
   Revised by: Dick Joyce
   Reason for / items changed: Initial Release draft outline

2. Revision Version # 0.1
   Date: 2008-01-23
   Revised by: Dick Joyce
   Reason for / items changed: Completed Sections 1, 2, 3, started Appendices.

3. Revision Version # 0.2
   Date: 2008-02-05
   Revised by: Dick Joyce
   Reason for / items changed: Completed Appendix A, Started B, Section 4.

4. Revision Version # 0.3
   Date: 2008-02-12
   Revised by: Dick Joyce
   Reason for / items changed: Completed Appendix B, continued Section 4.

5. Revision Version # 0.4
   Date: 2008-02-29
   Revised by: Dick Joyce
   Reason for / items changed: Continued Section 4, Section 5, Appendix C.

6. Revision Version # 0.5
   Date: 2008-03-25
   Revised by: Dick Joyce
   Reason for / items changed: Sections 4.5, 4.6, Appendices D and E.

7. Revision Version # 0.6
   Date: 2008-03-27
   Revised by: Dick Joyce, Ed Hileman
   Reason for / items changed: Revisions throughout, new figures.

8. Revision Version # 0.7
   Date: 2008-04-17
   Revised by: Corinne Boyer, Dick Joyce, Ed Hileman
   Reason for / items changed: Response to CB comments, revised throughout.
9. Revision Version # 0.8
   Date: 2008-04-23
   Revised by: Dick Joyce, Ed Hileman
   Reason for / items changed: Revised Weight and CG Tables.

Table of Contents

List of Figures

List of Tables

Applicable Documents

[1] AURA-Delta LGSF Conceptual Design, TMT.BUS.CON.07.069.REL01 (16 January 2008).
[2] TMT Laser Guide Star Facility Conceptual Design Report, TMT.AOS.CDD.06.035.REL03 (31 August 2006).

[3] Science-based Requirements Document v15.0, TMT.PSC.DRD.05.001.REL15 (31 Jan 2005).
[4] Initial Functional Performance Requirements Document for the Laser Guide Star Facility, TMT.AOS.CDD.07.002.DRF01 (07 November 2007).
[5] Allen Hankla, Lockheed Martin Coherent Technologies, "Thirty Meter Telescope: Recommendation of Beam Train Optics and Laser Launch Telescope Optics, Final Report", TMT.AOS.CDD.06.049.REL01 (23 May 2006).
[6] Ed Hileman, NOAO, "Laser Guide Star Facility Flexure Analysis Results", TMT.AOS.PRE.08.022.REL01 (12 March 2008).
[7] Ed Hileman, NOAO, "LGSF Flexure Results Spreadsheet", TMT.AOS.MED.08.024.REL03 (09 April 2008).
[8] Operations Concept Document (OCD), TMT.OPS.MGT.07.002
[9] Observatory Requirements Document (ORD), TMT.SEN.DRD.05.001
[10] Observatory Architecture Document (OAD), TMT.SEN.DRD.05.002

Acronyms and Abbreviations

AG	Asterism Generator
AO	Adaptive Optics
AR	Anti-reflection
ASCAM	All Sky Camera
BOCAM	Boresighted Infrared Camera
BS	Beamsplitter
BTO	Beam Transfer Optics
BTOTE	Beam Transfer Optics Top End
CAD	Computer Aided Design
CCD	Charge Coupled Device
CG	Center of Gravity
CoDR	Conceptual Design Review
CSEM	Centre Suisse d'Electronique et de Microtechnique
DCC	TMT Document Management Database (DocuShare)
DM	Deformable Mirror
DOB	Diagnostic Optical Bench
GLAO	Ground Layer Adaptive Optics
ICD	Interface Control Document
IFPRD	Initial Functional Performance Requirements Document
IFU	Integral Field Unit
LGS	Laser Guide Star
LGSF	Laser Guide Star Facility
LLT	Laser Launch Telescope
LMCT	Lockheed Martin Coherent Technologies
LSE	Laser Service Enclosure
M1	Primary Mirror
M2	Secondary Mirror
M2CRS	Secondary Mirror (TMT) Coordinate Reference System
M3	Tertiary Mirror
MCAO	Multi-Conjugate Adaptive Optics
MIRAO	Mid-infrared Adaptive Optics
MIRES	Mid-infrared Echelle Spectrograph
MOAO	Multi-Object Adaptive Optics
NFIRAOS	Narrow Field Adaptive Optics System
NIRES	Near-infrared Echelle Spectrograph
NOAO	National Optical Astronomy Observatory
OAD	Observatory Architecture Document
ORD	Observatory Requirements Document
QWP	Quarter-wave Plate
RC	Richey-Chrétien
SAC	Science Advisory Committee
SOW	Statement of Work
SRD	Science Requirements Document
TBD	To Be Determined

TBR	To Be Reviewed
TEM	Transverse Electromagnetic (laser mode)
TMT	Thirty Meter Telescope
ULAO	Uplink Adaptive Optics
WFOS	Wide Field Optical Spectrograph
WIRC	Wide Field Infrared Camera

1.0 Introduction

1.1 Statement of Work

The conceptual design of the LGSF Top End was based on the assumption that the telescope top end flexure was negligible. Preliminary design work for the telescope structure is on going and preliminary estimates of the telescope top end flexure are now available for the new RC design: ±15 mm decenter and ±2mrad tip/tilt in the M2CRS coordinate system. The current LGSF Top End design must therefore be updated, since neither the LLT field of view nor the dynamic range of the laser guide star pointing mirrors is large enough to compensate for the telescope top end flexure and to maintain the asterism on axis with a good beam quality. It is anticipated that at least the LLT will be mounted on a tip/tilt stage or equivalent.

The Telescope Top End redesign is currently in progress and will be completed by the end of October 2007. The new design will be reviewed during the Telescope Top End Review scheduled November 1, 2007.

This work package is split in two phases:

- Phase 1: Tasks performed before the Telescope Top End Review
    - Develop the optical concept for the LLT flexure compensation
    - Provide the preliminary mechanical concept for the LLT flexure compensation
    - Interact with the TMT Telescope Department to insure that the needs of the BTO are reflected in the requirements for the redesign of the Telescope Top End
    - Develop the initial concepts for the BTO path, BTO mounting points and relay lens locations.
    - Provide initial estimates of changes in the LGSF Top End in terms of mass and cross section for the Telescope Top End Review. Participation in person or via video at this review is expected.
- Phase 2: Tasks performed after the Telescope Top End Review
    - Complete the mechanical conceptual design for the LLT flexure compensation
    - Redesign the BTO and BTO Optical Bench optics as needed: Optimize the placement of the fold mirrors and relay lenses within the BTO path for access and maintenance.
    - Evaluate the dynamic range requirements of the active mirrors of the entire BTO including any additional active devices
    - Provide the clear aperture requirements of all the BTO optics including any additional optics.
    - Finally, provide final estimates of the mass, volume, cross section and center of gravity of the new LGSF top end. Cost estimates for all additional opto-mechanical devices and associated electronics should be provided.

As an input to this work, TMT will provide the most recent top end design (CAD model), the LGSF Conceptual Design Report, a preliminary version of the ICD between the telescope structure and the LGSF and the most recent versions of the ORD and OAD.

1.2 Contact Information

LGSF Team:		
Brent Ellerbroek	626-395-1620	brente@caltech.edu
Corinne Boyer	626-395-1623	cboyer@tmt.org
NOAO Team:		
Jay Elias	520-318-8231	jelias@noao.edu
Ed Hileman	520-318-8186	ehileman@noao.edu
Dick Joyce	520-318-8323	djoyce@noao.edu
Ming Liang	520-318-8394	mliang@noao.edu

1.3 Executive Summary

NOAO submits this upgrade to the Conceptual Design Study of the TMT Laser Guide Star Facility (LGSF) under a contract [1] based on the Statement of Work in section 1.1. The LGSF will be an integral component of TMT, and will be of critical importance in enabling TMT to achieve the adaptive optics performance required to meet the goals set forth in the Science Requirements Document for high resolution imaging and spectroscopy. The LGSF will project up to eight sodium laser guide stars in four different asterisms, as required by the TMT LGS Adaptive Optics (AO) systems which will be used with the first and second-generation instrumentation. The Conceptual Design Report presented a design which could be constructed with current technology, permits rapid switching from one AO asterism to another, and employs multiple lasers to provide contingency for continued AO operation in the event one of the lasers is nonfunctional.

This report represents an incremental rework of the initial conceptual design in the optical and mechanical areas, in response to changes in the basic TMT design and progress within the TMT project in defining the top end structure, flexure modelling of the telescope top end, and systems engineering work addressing operational issues such as access for installation and maintenance. Particular areas of emphasis, following the Statement of Work, include compensation for the effects of telescope structure flexure, mating the optical path up the telescope truss to the BTO/LLT components mounted behind the TMT M2, providing a support structure for the optical bench and LLT to the TMT M2 structure, and considering the issues of personnel access. In addition, the initial conceptual design layout has been modified to reduce the number of optical elements in the high-power laser beam.

Flexure analysis of the LGSF on TMT suggested that the beam deviations within the LGSF BTO are less than 0.32 mrad and should be correctable by the BTO Centering and Pointing mirrors. The flexure could be reduced by stiffening the truss members which support the Diagnostic Bench and Asterism Generator. Flexure of the TMT structure resulted in LLT pointing deviations up to 2.4 mrad. The recommended solution is to mount the LLT in a frame which can be tilted to compensate for this error. Modal analysis of the LGSF Top End showed that acceleration as large as 6.6 g can be expected at the lowest mode frequency of 13.6 Hz in the case of a “lifetime seismic event”, and that even significant stiffening of the structure would be unlikely to reduce this below the 5 – 6 g regime. A detailed analysis of flexure compensation of the beams traversing the vertical and horizontal trusses was not carried out at this time, since

TMT plans to move the LSE off of the telescope elevation structure. This will necessitate a redesign of the transport ducting between the LSE and the vertical truss and the relay lenses and reanalysis of the truss flexure at that time.

Although this report is a supplement to the Conceptual Design Study Report [2], it provides an overview of the conceptual design to make it useful as a stand-alone document. The report will be restricted to work on the optical and mechanical concept which is aligned with the tasks set out in the Statement of Work. Additional redesign efforts, for example, on the Laser System Enclosure are likely to occur as a result of developments in laser technology or novel approaches to the task of beam transport, but these would be the subject of future reports. Prior to the beginning of the LGSF Preliminary Design phase (tentatively scheduled in 2009), these incremental reports would be incorporated into a revised final Conceptual Design Report.

2.0 Overview of Current Project

2.1 Introductory Remarks—The Initial Conceptual Design Report

The Initial Conceptual Design Report [2] presented a working concept for the TMT LGSF which could have been built using the technology available or under contract for delivery at that time (August 2006). This section will provide a brief description of the LGSF concept to provide a context for the redesign work carried out in this project and make this report useful as a stand-alone document. For additional details, the reader may refer to the Conceptual Design Report [2] itself. The following sections will describe the progress in the TMT design development and the subsequent refinements to the LGSF concept which are the conclusions of this report.

The TMT Science Advisory Committee (SAC) has defined eight first- and second-generation instrument capabilities [3] to be implemented within the first decade of TMT operation. These instrumental capabilities were used to derive the requirements for the associated AO systems. Some instruments have AO requirements in common, and a total of four separate AO capabilities were identified:

- Narrow-field Infrared Adaptive Optics System (NFIRAOS): Intended to deliver diffraction-limited images over a small field, sufficient for IFU or slit spectroscopy, with 0.6 – 5 μm operating range as a goal. A Multi-conjugate AO (MCAO) capability may be provided to provide compensation over a larger (~ 2 arc min) field, both to support WIRC and improve sky coverage.
- Wide-field Multiple Object Adaptive Optics (MOAO): Intended to deliver LGS-based tomographic turbulence information over a large (~ 5 arcmin) field, and apply this to delivering excellent wavefront correction over small selected subfields for multiple IFU spectroscopy.
- Small-field Diffraction-limited Mid-infrared Adaptive Optics (MIRAO): Intended for delivering diffraction-limited images over a small field for MIRES, and possibly the long-wavelength component of NIRES.

- Ground-layer Adaptive Optics (GLAO): Intended to provide partial AO correction for WFOS over its wide patrol field. Must avoid LGS interference with WFOS patrol field.

The requirements for the LGSF include the ability to project up to eight sodium laser guide stars in four different asterisms, as required by the TMT LGS AO systems listed above. The table below summarizes the principal top-level requirements of the TMT LGSF as outlined in the SOW at the start of the Conceptual Design Study. A more complete listing is given in the Initial Functional Performance Requirements Document (IFPRD, [4]). Additionally, several requirements have evolved in the course of developing the designs and performance estimates for the LGSF and the TMT LGS AO systems.

Table 2.1-1: LGSF Requirements Summary

Parameter	Requirement
Asterisms	Four separate LGS asterisms as follows: NFIRAOS: 1 on-axis and 5 equally spaced at 35 arcsec radius MOAO: 3 equally spaced at 70 arcsec radius and 5 equally spaced at 150 arcsec radius MIRAO: 3 equally spaced at 70 arcsec radius GLAO: 4 equally spaced at 510 arcsec radius[1]
LGS Power	17W minimum per beacon; 25W goal
Total Laser Power	150W (may be more than one laser)
LGS Image Quality	Far-field $1/e^2$ diameter 0.6 arcsec
Polarization	98 % circularly polarized (TBR)
LLT Diameter	Sufficient to include all the beam with a $1/e^2$ diameter of 300 mm
Operation	Downtime < 5%[2]. Operability may be met using reduced number of lasers as long as a minimum power of 17W per beacon is maintained Switch from one AO asterism to another in 2 min
Safety	Must meet safety requirements for Class 4 lasers with respect to damage to personnel or observatory, illumination of aircraft or satellites, and interference with neighboring telescope operation
Calibration	Must include calibration and diagnostic systems
Observatory	Must support hardware and software interfaces to observatory
General	Must meet TMT requirements for mass, volume, power consumption, heat dissipation, and ease of servicing
Power Upgrade	Include plan for eventual upgrade in laser power by factor of 4 to 5, and allow for higher laser power in materials/coating specifications
ULAO Upgrade	Include plan for eventual incorporation of ULAO and reserve sufficient space in optomechanical layout for this upgrade

[1] This requirement has been updated to include an additional on-axis beacon.

[2] This requirement has been updated since the LGSF Conceptual Design and is now LGSF downtime < 0.5% (refer to the OAD requirement REQ-1-OAD-0350 [10])

The basic opto-mechanical layout of the TMT LGSF is based upon the LGSF systems employed on the Gemini North and Gemini South telescopes. Like the Gemini systems, the TMT LGSF consists of four primary subsystems. The Laser Enclosure housing the sodium lasers is mounted on the telescope structure. The Beam Transport Optics (BTO) direct the laser beams up the telescope truss to a position behind the secondary mirror where the BTO Optical Bench is located. This bench consists of the optics which generate the asterisms, feed the beams to the LLT, maintain the asterism orientation on the sky, and evaluate the beam quality and pointing. Finally, the LLT itself is also located behind the secondary on the optical axis of the telescope. Figure 2.1-1 illustrates these subsystems on the TMT and the beam path up the telescope structure.

The overall approach to laser safety is also based largely upon the Gemini Safe Aircraft Localization and Satellite Avoidance system design. The TMT LGSF will employ (i) one or more all-sky cameras (ASCAM) and a boresighted infrared camera (BOCAM) to detect aircraft or clouds which might intercept the laser beams, (ii) a Laser Traffic Control System dedicated to avoid laser beam interference with neighboring telescopes, and (iii) an Earth-orbiting Satellite Illumination Avoidance System dedicated to predict illumination of satellites by the TMT laser beams. A Laser Interlock System will shutter the laser beams if an event is detected by these or other AO sub-systems.

At the time of the Conceptual Design Report, the 50W sodium laser under contract for delivery to Gemini South was the most powerful commercial unit available, leading us to utilize three of these lasers to achieve the 150W total power requirement. This also permits the concept to address the operating flexibility issue in a fairly straightforward manner. The 150W total power requirement is driven by the goal of operating the six-beacon NFIRAOS asterism at 25W per beacon. However, the minimum power requirement per beacon (17W) can be achieved with a total power of 100W, so it is possible to maintain NFIRAOS operation with one of the three lasers inoperable. Likewise, the MIRAO three-beacon asterism can be generated with any one laser, and the four-beacon GLAO asterism with any two lasers. Only the eight-beacon MOAO asterism requires all three lasers to meet the minimum power requirements. There are thus a total of 11 configurations (four for NFIRAOS, three each for MIRAO and GLAO, one for MOAO) supported by the LGSF.

The method of separating the laser and asterism flexibility issues is to utilize two separate mechanisms. The Laser Switchyard, located in the Laser System Enclosure (LSE), accepts the input beams from the operating laser systems and, utilizing controllable beamsplitters and mirrors, delivers the proper number of beams at the desired power level. The Asterism Generator accepts these beams and directs them, at the proper location and convergence angle, to the input pupil of the LLT for projection on the sky. For this reason, it must be located on the BTO Top End, near the LLT.

Figures 2.1-1 and 2.1-2 show the configuration of the LGSF concept as of August 2006. Although there have been changes in the telescope configuration and in the details of the LGSF concept, the basic functional layout is unchanged. Relocation of the LSE off of the telescope structure is being considered, but this lies outside the scope of this work and, for the purposes of

this report, the LSE remains on the telescope, but attached to the elevation journal. A summary of the functional subsystems is presented below.

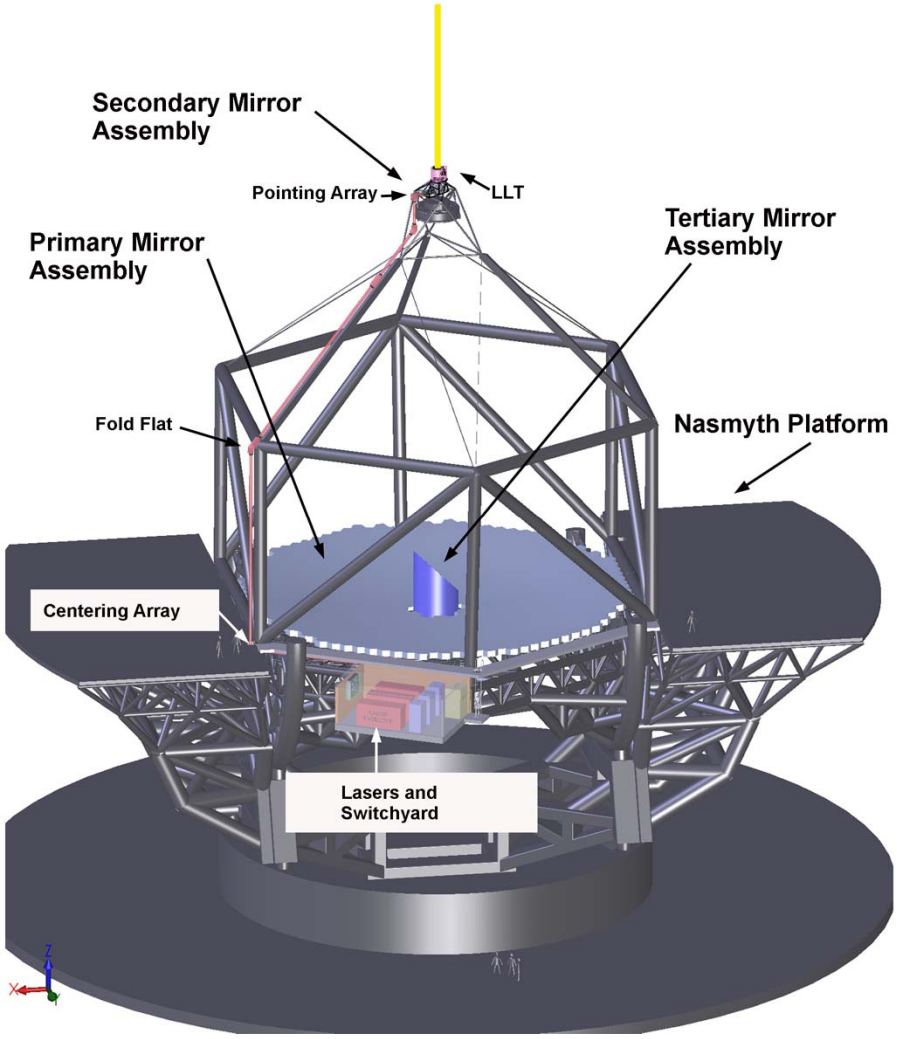

Figure 2.1-1: Overview of the LGSF, illustrating the installation on TMT, as presented in the Initial Conceptual Design Report (August 2006). The primary subsystems are the sodium lasers and associated optics, located on the telescope structure, the Beam Transport Optics (BTO), which convey the laser beams up the telescope structure, and the BTO Top End (BTOTE), located behind the secondary mirror assembly, which contains the diagnostic and asterism generation optics and the LLT.

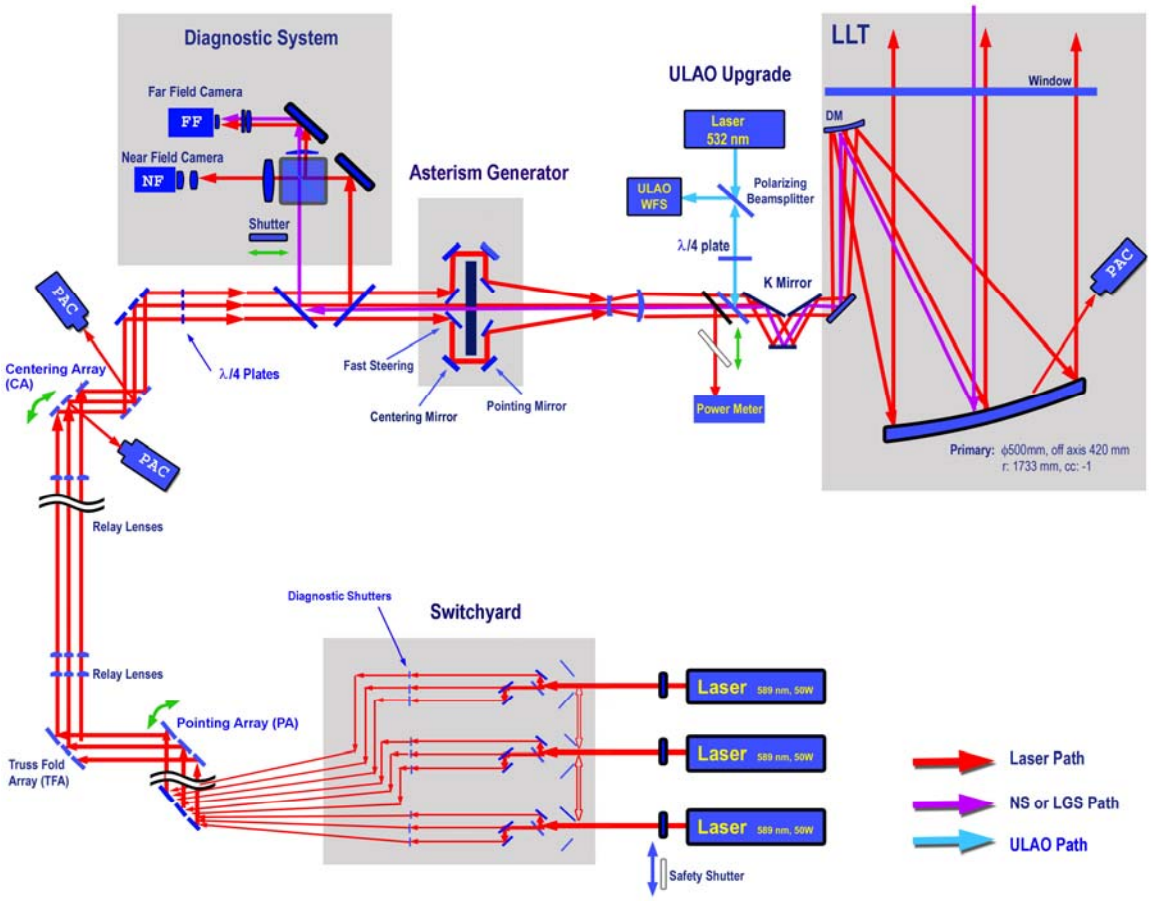

Figure 2.1-2: Functional block diagram of the TMT LGSF as presented in the Initial Conceptual Design Report (August 2006). For clarity, only three beams are shown within the BTO and BTOTE.

Laser Systems: As noted above, the baseline system will utilize three 50W sodium lasers, to be provided by a commercial vendor. The three lasers and associated electronics will be installed in the Laser Service Enclosure (LSE) mounted to the TMT telescope structure. The LSE provides a moderately clean (Class 10000), temperature-controlled environment with provision for removing heat generated by the electronics. The LSE is accessible to maintenance personnel with the telescope pointed at zenith.

Laser Switchyard: This is an optical bench with motor-controlled beamsplitters and mirrors which accept the 50W input beams from the operating lasers and direct them to the proper outputs at the desired power. One can generate either two 25W beams (using a 50/50 beamsplitter) or three 17W beams (using 33/66 and 50/50 beamsplitters). There are nine possible output beam positions. Each AO asterism utilizes dedicated output beam positions, no matter which lasers are in use. Shutters at the output of each beam are used to block off unused outputs or to permit diagnostic measurements of any individual output beam. The switchyard will also have three low-power HeNe "surrogate" lasers which can be switched into the optical path to provide 594.1 nm laser beams (near the sodium laser wavelength) to permit testing of the BTO optics and controls without requiring the sodium lasers to be brought online.

Beam Transport Optics: As the name suggests, these transport the nine possible output beams from the Laser Switchyard out of the LSE and up the telescope truss to the BTO Top End behind the secondary mirror. The BTO mirrors re-form the beam arrangement from the linear switchyard output to a compact geometry for transport up the structure in a conduit which is smaller than the secondary support truss to avoid any vignetting of the telescope primary. A series of three relay lenses in each beam preserves the 5 mm laser beam diameter and exit pupil position over the ~ 50 m path to the secondary.

Two of the mirrors in each beam position within the BTO path are controllable in tip/tilt to maintain both centering and pointing of the beams at the input to the BTO Top End, correcting for the inevitable flexure of the telescope structure with altitude. This is a low-bandwidth correction which may utilize a lookup table. The prealignment cameras can directly view the laser beams on the mirrors as a diagnostic.

Asterism Generator: The asterism generator re-forms the fixed pattern of beams from the BTO into the AO asterism using three mirrors in each of the nine input beams. A fourth mirror is fixed at each of the 18 possible locations for all four AO asterisms, oriented so the beam is directed to the input pupil of the LLT. The third of the four mirrors moves in local azimuth to direct the beam to the proper output mirror. The first mirror is capable of very high bandwidth, low-amplitude tip/tilt motion (Fast Steering) to correct for wind shake and other high frequency telescope motions. The second and third mirrors are adjustable in tip/tilt to maintain centering and pointing on the LLT with telescope altitude in a manner analogous to those in the BTO.

K Mirror: This three-mirror system acts as an image rotator to maintain a fixed asterism orientation with respect to the sky as the telescope moves in altitude and azimuth.

Laser Launch Telescope: The LLT consists of two lenses and an off-axis unobscured reflective telescope. The net demagnification is 60, so that an input angle of 1 degree is projected from the LLT as an angle of 1 arcmin. This permits reasonable separation of the individual laser beams at the location of the asterism generator as well as very fine beam control by the Fast Steering mirrors. The reflective LLT design was chosen because of its nearly achromatic performance for natural star diagnostics, acceptable cost and alignment tolerances, and the suitability of the secondary as a deformable mirror (DM) should the ULAO upgrade be implemented.

Diagnostic System: The diagnostic system directs a small fraction (0.5%) of each of the laser beams through a beamsplitter into two camera systems, one focused at a relatively close distance, the other at infinity. The near-field camera is used to evaluate the intensity profile and quality of the laser beam within the LGSF. The far-field camera views the projected LGS at diffraction-limited resolution to evaluate its image quality. The two cameras together define the pointing of the laser beacon. The diagnostic system contains a second beamsplitter to direct the light of a natural star backwards through the LLT to the near and far-field cameras as an independent check of the LLT image quality and to coalign the pointing of the LGS asterisms with that of the TMT.

Beam Dump: The beam dump is a mirror which directs the laser beams from a position near the LLT collimator lenses to a power meter. The main function of the beam dump mirror is to shutter the laser beams at the telescope top end. Such function is used when switching between observations with the same instrument. This can be used, in conjunction with the shutters in the Switchyard, to measure the power of any individual laser beacon. The beam dump can also permit one to carry out measurements of the laser beams using the diagnostic system without projecting the beams through the LLT to the sky.

Safety System: In addition to the shutters at the output of the Switchyard and the Beam Dump mirror, the LGSF has three shutters at the outputs of the three lasers themselves. These are very fast (0.1 s) shutters which can withstand the full power of the laser beams for a time sufficient for the internal laser shutters (which are slower but more robust) to block the beam. These shutters interface to the Laser Interlock System, which continuously monitors for a variety of potential safety hazards (aircraft or satellite incursion, interference with neighboring telescope operation, personnel in dome, etc.) and immediately closes the shutters if an event is detected.

Polarization: The linearly polarized output of the sodium lasers is converted to circularly polarized light prior to projection by the LLT to maximize the efficiency of exciting the Na D2 resonance in the atmosphere. This is accomplished by quarter-wave plates (QWP) tuned to 589 nm in each output beam. The QWP rotation must be adjustable to account for variations in instrumental polarization as the laser beams are directed through different optical elements in the Switchyard for the various LGS asterisms. Ideally, these should be located as close to the LLT as the beam geometry permits.

Mechanical: For both safety and cleanliness, the entire optical train of the LGSF must be enclosed in a light and (nearly) air-tight mechanical structure. The enclosure will be maintained at a very slight overpressure by a flow of filtered air to minimize any incursion of contaminants and to carry away any heat generated by the motors, cameras, or the small fraction of sodium laser light absorbed by the optics. The diameter of the conduit transporting the beams up the telescope structure will be less than that of the truss elements. To protect the LLT mirror coatings and to maintain cleanliness within the entire LGSF, the LLT will have an AR-coated window. This window will be easily replaceable should the coating deteriorate due to exposure to the environment.

2.2 Changes Since the Initial Conceptual Design Report

Since the Conceptual Design Review, the design of the TMT itself has continued to evolve. As the telescope concept converges on its final configuration, the LGSF concept must evolve in parallel to maintain consistency. In addition, parts of the LGSF concept which were left uncompleted at the Conceptual Design because of the lack of any interface information are now in a position to be included and analyzed in a quantitative fashion.

The major changes motivating the current work package are:

- The TMT telescope design was changed from a Gregorian to a Ritchey-Chrétien configuration. This significantly decreases the overall telescope height and the optical path length from the LSE to the M2 assembly.
- A final configuration for the TMT top end and M2 support was defined. This will permit the interfacing of the laser beams coming up the telescope truss with the optical bench behind M2 as well as the design of the support structure for the BTO Top End and LLT.
- The flexure of the TMT structure due to gravity is now known sufficiently well to allow the design of compensating mechanisms to meet the LGSF pointing accuracy requirements.
- The design of the telescope enclosure has continued to mature to now include elevators, handling equipment, etc. The operational issues of access for installation and maintenance must now be incorporated into the LGSF design.
- The structures group has carried out a modal analysis of the TMT telescope structure response to anticipated seismic events. The LGSF subsystems, particularly those on the top end structure, must meet the "survival" load requirements.

2.3 Summary of LGSF Redesign Work

This section presents a summary of the changes to the initial LGSF concept resulting from this work. Sections 3 and 4 will provide a detailed description of the optical and mechanical work. For reference, Figures 2.3-1 and 2.3-2 are current illustrations of the overview of the LGSF on the revised TMT concept and the functional layout of the LGSF. One may compare these to their earlier counterparts Figures 2.1-1 and 2.1-2.

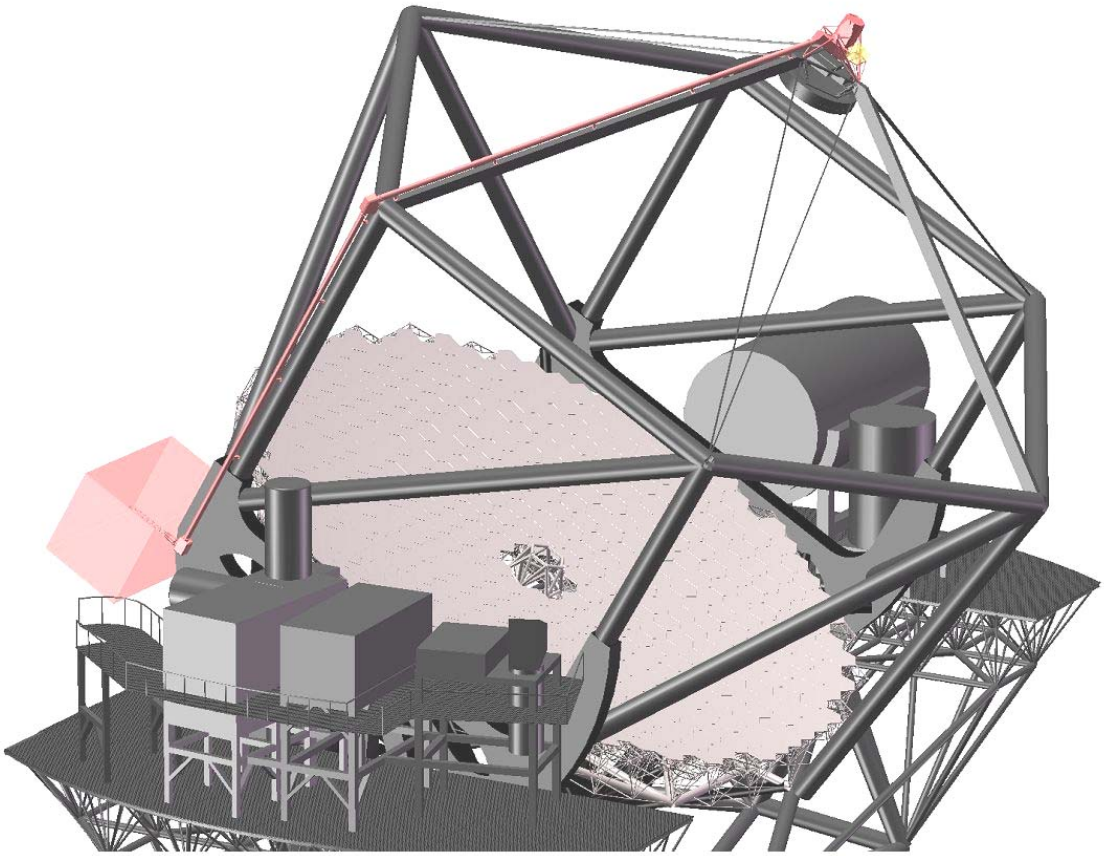

Figure 2.3-1: Current concept overview of the LGSF on TMT. Note the much more compact telescope structure resulting from the change from a Gregorian to a Ritchey-Chrétien optical design and the direct connection of the upper tripod structure to the M2 hexapod. The LSE (red box on left) is still located on the telescope structure, but attached to the elevation journal.

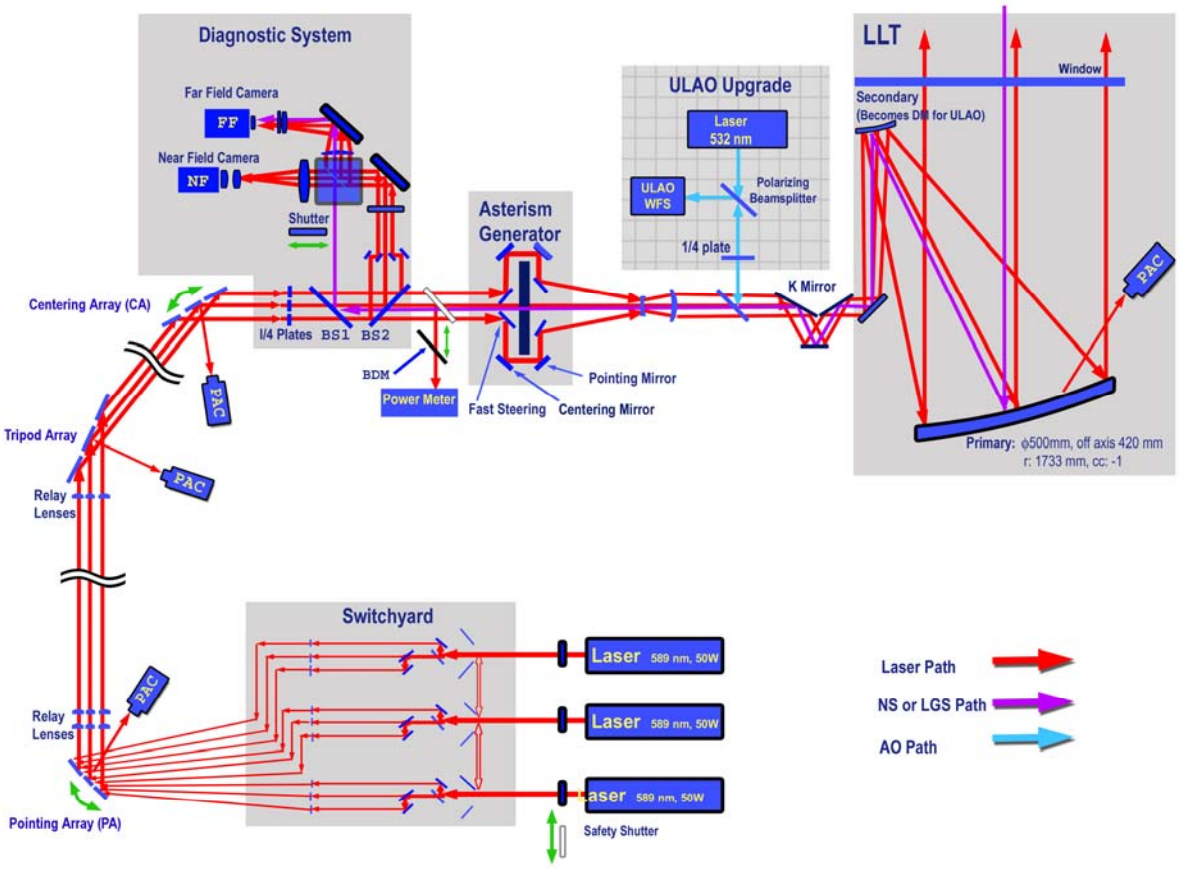

Figure 2.3-2: Functional block diagram of the current LGSF concept. For clarity, only three beams are shown within the BTO and BTOTE. Most of the functional design changes are in the diagnostic system.

- As a result of the reconfiguration to a Ritchey-Chrétien design, the optical path from the LSE to the TMT top end has been reduced from ~ 50 m to 44.5 m. The relay lenses which reimage the laser beam onto the LLT pupil were redesigned for this shorter path length. Their location was also changed to put the L1/L2 pair next to the truss fold mirror array at the base of the vertical truss structure and L3 near the non-active Tripod Fold Array at the transition from the vertical to tripod leg. This will make the relay lenses much more accessible for maintenance or replacement.
- With the choice of the "tripod" design for the telescope top end and M2 support structure, it was possible to define the complete laser beam path from the LSE to the input of the BTO top end. The diagnostic bench/asterism generator subassembly (Fig 2.1-2) was rotated in the XY plane to match up the diagnostic bench input to the beam coming up the truss and tilted to minimize the incidence angle on the centering mirrors at the top of the truss transport duct.
- While the centering mirror array is technically part of the truss transfer subassembly, it is now mounted on a fixture attached to the diagnostic bench for stability.
- The asterism generator was scaled down (by ~ 15 %) to minimize size and weight, consistent with the need to converge the beams at the LLT input pupil. The net reduction was a combination of a 25% decrease in focal length and an increase in field of view

from 7.2 to 8.5 arcmin radius. The LLT input collimator focal length was reduced proportionally to maintain the 60:1 magnification.

- Several components of the diagnostic system were modified. The "periscope" mirrors used to reduce the beam footprint into the diagnostic system were relocated downstream of the input beamsplitters. This removes four mirrors from each high-power laser beam and permits the use of less exotic coatings on these mirrors. The beamsplitter BS1, which directs a natural star from the LLT into the diagnostic system for pointing and image quality evaluation, was mechanized to remove it from the beam when the laser beams are being projected to the sky, removing another transmitting optic from the laser path.
- The LLT was installed on a pivot mount to allow it to be tilted slightly in the altitude axis. This provides first-order correction for the tilt component of flexure in the TMT structure due to gravity.
- The support structure for the truss beam transport, BTO top end, and LLT was designed to interface with the new TMT top end structure, with due consideration for installation and access. Weight, balance, and wind cross-sections were calculated.
- Equivalent static design loading to be considered for the LGSF top end equipment has been estimated by modal analysis of the LGSF top end structure and the response spectrum of the telescope top end to limiting case seismic events.

3.0 Optical Design Rework

The fundamental optical layout of the LGSF remains essentially unchanged from that in the original concept, as a comparison of Figures 2.1-2 and 2.3-2 shows. The primary changes have been in rescaling the truss relay lenses to accommodate the shorter path length from the LSE to the M2 structure in the Ritchey-Chrétien design and the asterism generator to fit its focal length into the space between the diagnostic subsystem and the LLT collimator. The beamsplitters feeding the diagnostic subsystem have been redesigned to eliminate several mirrors from the high-power laser beam path to achieve benefits in both throughput and cost.

3.1 Relay Lenses

The current estimate of the distance from the LSE to the input pupil of the LLT is 44.5 m. Although this is reduced from the value for the initial TMT design, the Gaussian laser beam, with a $1/e^2$ beam waist diameter of 5 mm, will diverge to 8.2 mm diameter over this distance (Appendix A.1). We will employ a set of three relay lenses in each laser beam to reimage the laser beam from the LSE onto the entrance pupil of the LLT and maintain the 5 mm beam waist diameter. The first two lenses will also act somewhat as a field lens and reduce the tip/tilt sensitivity of the pointing mirrors at the bottom of the vertical truss structure.

The three lens design is also preferred for safety reasons, since it acts as a relay system without forming a real intermediate focus with consequent concerns about the local beam power density. The minimum beam waist diameter is 3.6 mm.

The relay lens design is shown in Figure 3.1-2 and Table 3.1-1. A physical propagation analysis of the relay is given in Appendix A.1.

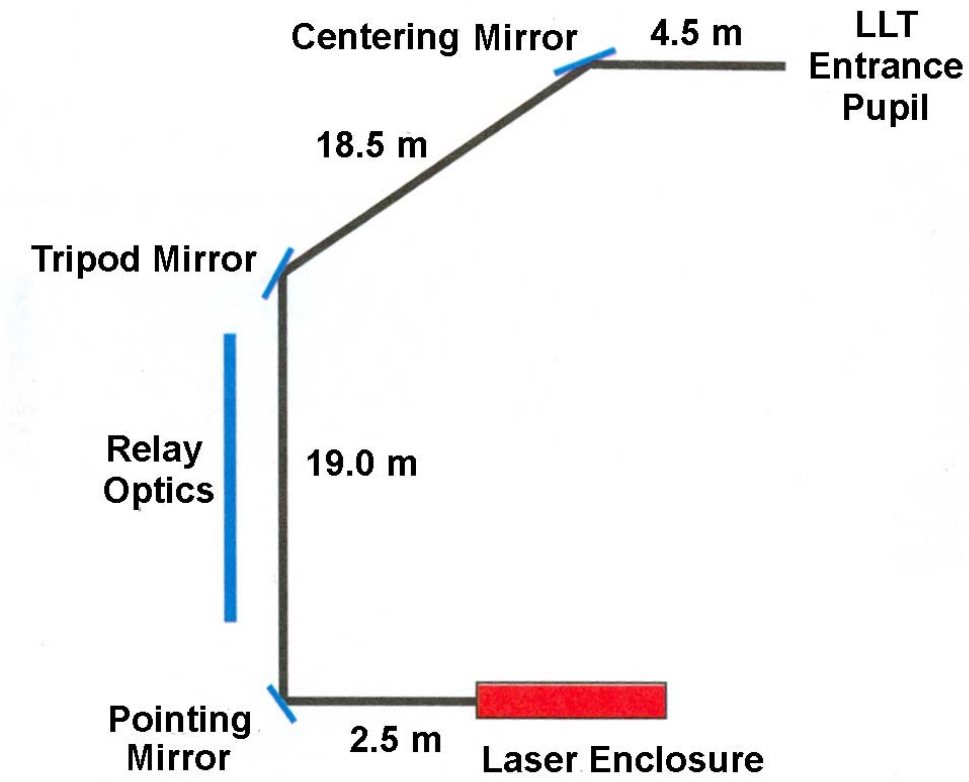

Figure 3.1-1: Schematic layout of the BTO truss optical path, showing the locations of the relay optics. The total optical path length is approximately 44.5 m.

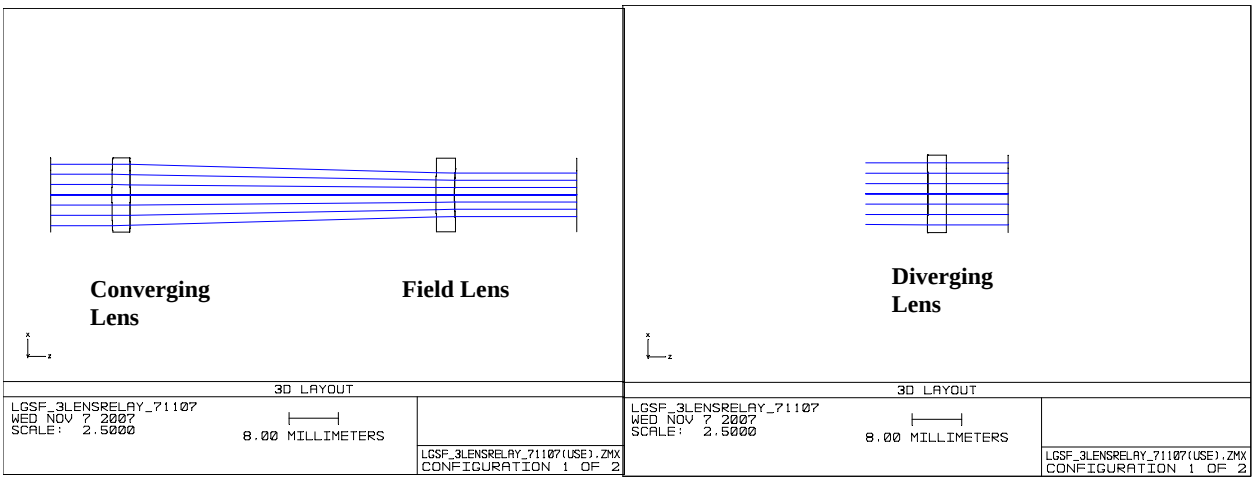

Figure 3.1-2: Schematic of the three LGSF relay lenses. The L1/L2 pair is separated from L3 by 18.46 m.

Table 3.1-1: Relay Lens Optical Prescription

Relay System Prescription				
Surface	**Radius (mm)**	**Separation (mm)**	**Glass**	**Diameter**
Pointing Mirror	Plane	200		
Lens 1	130.00	3	Silica	
	-239.65	50		12.0
Lens 2	275.90	3	Silica	
	49.68	18481.98		8.6
Lens 3	-26097.52	3	Silica	
	-4163.44	259.0197		12.5
Centering Mirror	Plane			

3.2 Diagnostics Subsystem

Several aspects of the Diagnostics Subsystem have been redesigned, although the basic functions and the diagnostic elements themselves (cube beamsplitter, near-field and far-field cameras) remain unchanged. Figure 3.2-1 illustrates the functional differences between the original and present concepts.

The nine beams are transported up the truss transport optics on 70 mm centers, giving a square pattern 140 mm on a side. This relatively large spacing is necessary to assure adequate separation for the nine bending mirrors at the bottom, midpoint, and top of the truss (the first and last being the pointing and centering mirrors) with consideration for the beam motion which occurs when correcting for flexure of the truss with telescope altitude. This beam separation is also necessary at the input of the asterism generator to allow spacing for the active mirrors. To make the best use of the diagnostic camera real estate, a series of mirrors were used to condense the beam pattern and then expand it again into the asterism generator (Fig. 3.2-1). The revised concept maintains the larger beam pattern and condenses it after the pickoff beamsplitter BS2. This replaces four mirrors from each high-power laser beam with two mirrors in the low-power diagnostic subsystem for benefits in both throughput and cost.

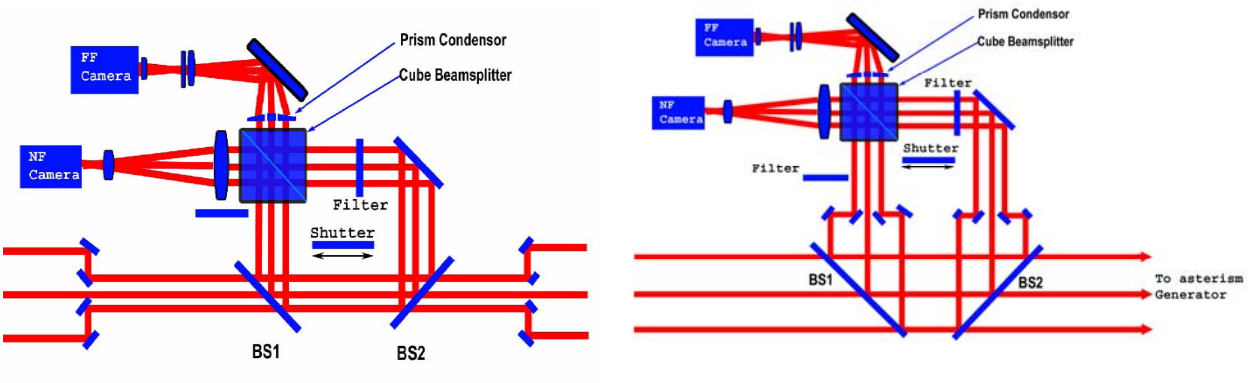

Figure 3.2-1: Functional schematic of the Diagnostic Subsystem in the original concept (left panel) and the present redesigned concept (right panel).

The use of monolithic optics for the beamsplitters BS1 and BS2 is problematic because of the requirement of high-transmission coatings on very large elements. Since the nine beams occupy fixed, widely-spaced locations, these beamsplitters can be fabricated as an array of nine small (25 mm dia) beamsplitters mounted in a plate (Fig 3.2-2). In addition, while all nine beams must be reflected into the diagnostic system by BS2, BS1 is necessary only for on-axis observations of a natural star or the on-axis laser beacon reflected from the back surface of the slightly tilted LLT window. BS1 could consist of a small element mounted only in the on-axis beam, although the introduction of this element would produce a lateral beam shift which would have to be corrected by the AG Pointing/Centering mirrors. We plan to install BS1 on a stage so it can be removed from the beam if operational experience demonstrates that it is not necessary to observe the reflected on-axis beam at all times, giving additional improvement in the throughput. This issue is addressed further in section 4.2.2.

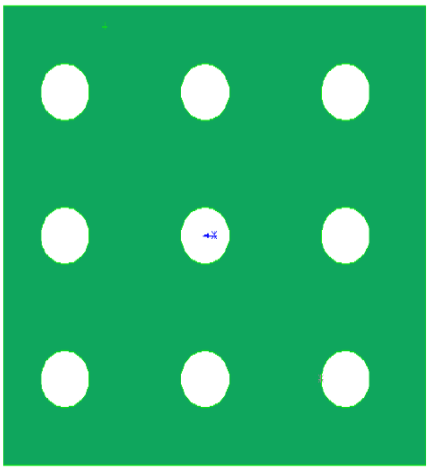

Figure 3.2-2: Schematic illustration of BS2, consisting of small individual optical elements mounted in a larger plate. The same design principle is used for BS1 and the beam dump mirror, which would have a second position to permit the beams to pass through.

The beam dump mirror and power meter were moved from a location near the input pupil of the LLT to the diagnostic bench prior to the input to the Asterism Generator. This was done in part for packaging this subsystem at a more accessible location and in part for safety considerations, since it permits diagnostics of the high-power laser beams without propagating them into the Asterism Generator and LLT collimator optics. The mirrors directing the beams to the power meter will be installed in a frame similar to that in Fig. 3.2-2, except the structure would be largely open to permit the beams to pass through during regular operation (section 4.2).

The Asterism Generator itself was scaled down by ~ 15 % for savings in weight and to match its focal length to the space between it and the LLT collimator. The focal length of the LLT

collimator was reduced proportionally to maintain the 60:1 magnification of the LLT optics. This will be revisited in more detail in section 4.2.

3.3 Physical Optics Modeling

We carried out physical modeling of three subsystems of LGSF:

- Physical propagation of the laser beam profile through the relay lens system
- Wavefront analysis of the laser beam propagation through the LLT for the on-axis beam and beams 35 and 510 arcsec off-axis.
- Energy concentration of the beams projected through the LLT at ground level and at 100 km altitude.

These rather detailed studies can be found in Appendix A at the end of this report.

4.0 Mechanical Design Rework

4.1 LLT Flexure Compensation

At the time of the Conceptual Design Review (September 2006), the TMT was a Gregorian design with a M2 support design which was still quite tentative. The LGSF beam transport was through the use of mirrors which guide the beams up the telescope truss to the BTO optical bench behind M2, enclosed in a tube (for safety and cleanliness considerations) smaller than the width of the truss members, so as to not give additional vignetting of the telescope primary. The detailed design of matching the truss beam transport to the input of the BTO top end was never completed, since the (correct) consensus at the time was that the M2 support structure would be changed in the future. In addition, although it was clear that there would be some gravitationally-induced flexure of the telescope structure with attitude, the lack of a firm design made it impractical to model the flexure quantitatively, although one could envision the general effects which the revised LGSF design would have to address:

- The truss members (which support the truss BTO optics) will flex as the telescope moves from zenith to horizon pointing.
- The LGSF optics behind M2 (BTO top end and LLT) will flex due to gravitational loading.
- The flexure of the telescope truss will translate the center of the M2 structure (where the LLT is mounted) with respect to the TMT optical axis.
- The flexure of the telescope truss will tilt the M2 structure, which will deviate the LLT optical axis from that of TMT.

Although a full model of the telescope structural behavior is still in progress, the selection of the Ritchey-Chrétien optical design and the consequent definition of the vertical and horizontal truss structure allow the estimate of reasonable upper limits for the magnitude of the flexure. For the M2 structure (bullets 3 and 4 above), these were 15 mm in translation and 2 mrad in tilt (section 1.1; Statement of Work). Correction for the first two bulleted items is through sets of tip/tilt

mirrors; this concept is largely unchanged since the Conceptual Design Report, so it will be covered only briefly below. The M2 structure deflection compensation, which is the major motivation for this report, will be covered in more detail.

4.1.1 Truss and BTO Flexure Compensation

The laser beams are transported from the LSE on the telescope structure to the BTO top end on the M2 support structure by three mirrors (per beam). These mirrors are at the bottom of the vertical truss, at the transition from the vertical to the tripod leg, and at the end of the tripod leg (Figs. 2.3-1 and 3.1-1). Since the mirrors are attached to the truss, the flexure will result in translation and tilt of (primarily) the upper two mirrors and of the laser beam entering the optical bench. This will be corrected by the use of tip/tilt adjustments of the mirrors at the bottom of the vertical truss and at the top of the tripod leg, which together can correct for both translation (centering) and tilt (pointing) of the beam.

The diagnostic cameras (far- and near-field) provide feedback to the centering and pointing adjustments to ensure that the laser beams are properly centered and directed. In practice, once the centering and pointing mirror compensations have been determined empirically during commissioning, they can be controlled by means of a lookup table during normal operation. Because the mirrors and relay lenses will be moving with the flexing truss structure, the required adjustment of (particularly) the Centering mirror may be significant. For this reason, the truss mirrors and the relay lenses are specified to be larger (50 mm diameter). However, a quantitative analysis of the requirements will await the redesign of the optical path between the LSE and the vertical truss which will occur with the decision to move the LSE off of the telescope elevation structure (section 5.1).

A similar flexure-induced misalignment of the laser beams can occur within the BTO top end between the diagnostic system and the input pupil of the LLT (section 4.5). This will be corrected, in the same manner as with the telescope truss, by a pair of tip/tilt mirrors located on the Asterism Generator.

4.1.2 LLT Flexure Compensation

Flexure of the TMT truss with gravity will result in both a translation and tilt of the M2 structure. The M2 hexapod will maintain the proper alignment with respect to M1, but the LGSF BTO optical bench and LLT will be fixed to the M2 structure and move with it. Preliminary modeling suggests conservative values of 15 mm in translation in the LLT X-direction and 2 mrad in tilt in the LLT Y-direction. The translation of the LLT with respect to the TMT optical axis can be safely ignored (15 mm at a range of 100 km is approximately 30 arc msec). However, 2 mrad (412 arcsec) is far larger than the 1 arcsec LGS position accuracy requirement dictated by the acquisition field of view of the AO WFS systems and requires that the LLT pointing be corrected to at least this precision.

Several options were considered, including tip/tilt of the LLT optics and tilting the entire LLT itself. Figure 4.1-1 shows the LLT components and the local coordinate system, and Fig. 4.1-2 shows spot diagrams of the LLT image quality for comparison with the performance resulting from the various compensation techniques. Note that in the local LLT coordinate system, gravitational flexure causes a tilt around the Y-axis.

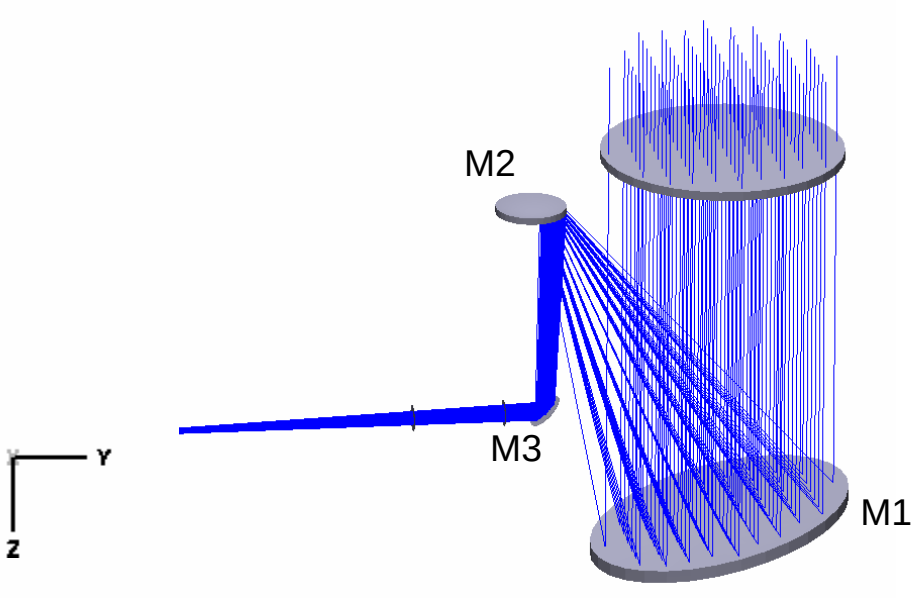

Figure 4.1-1: Schematic of the LLT components, showing the local coordinate system.

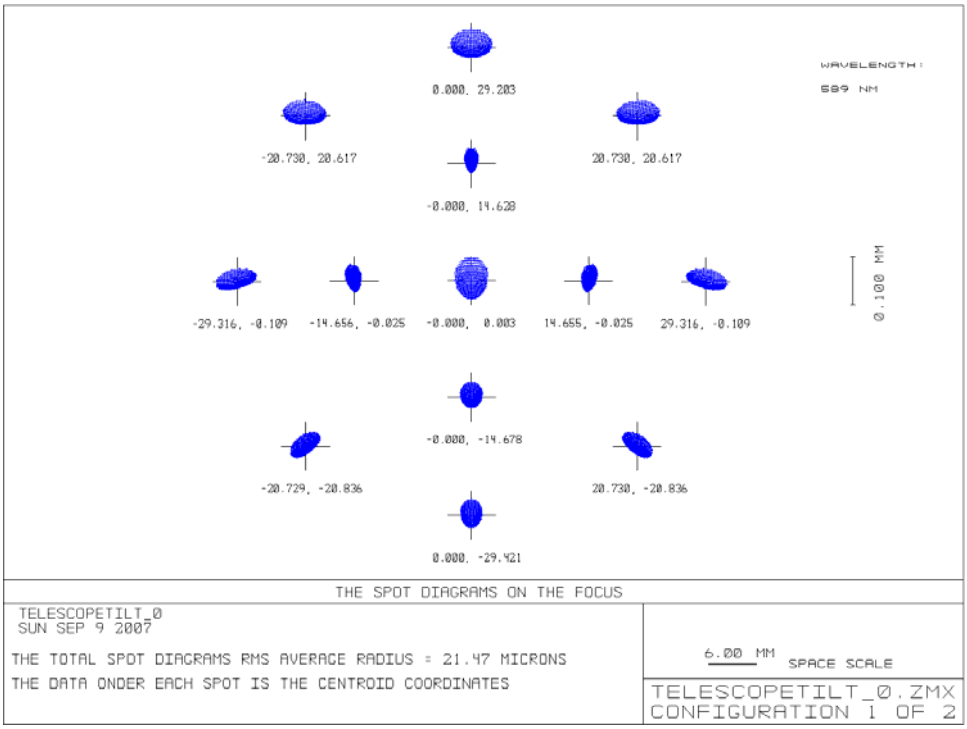

Figure 4.1-2: Spot diagrams of ideal LLT images. The Y-axis (second coordinate) is along the line joining M1 and M2.

4.1.2.1 BTO Centering/Pointing Correction

The idea of using the centering/pointing mirror arrays in the BTO top end (section 4.1.1) was dismissed quickly, primarily because of the large angular corrections needed, comparable to the radius of the GLAO asterism. Because these mirrors are before the collimator, which provides a 60:1 field reduction, the actual angular motions would have to be 60 times greater than the desired flexure correction.

4.1.2.2 Tip/tilt Correction Using LLT M2/M3

One flexure correction option is to effectively operate the LLT off-axis by an amount equal to the tilt component of the flexure by tilting the input flat M3. Unfortunately, the degree of tilt required to achieve 2 mrad of off-axis operation significantly degrades the image quality of the LLT (Fig. 4.1-3). It is possible to adequately compensate for the image degradation by tilting M2 in the opposite sense (Fig. 4.1-3). However, this results in a tilted focal plane at the input to the LLT, which would require further correction earlier in the optical path. In effect, one has corrected the pointing error effects of flexure of the TMT structure at the cost of introducing an additional problem.

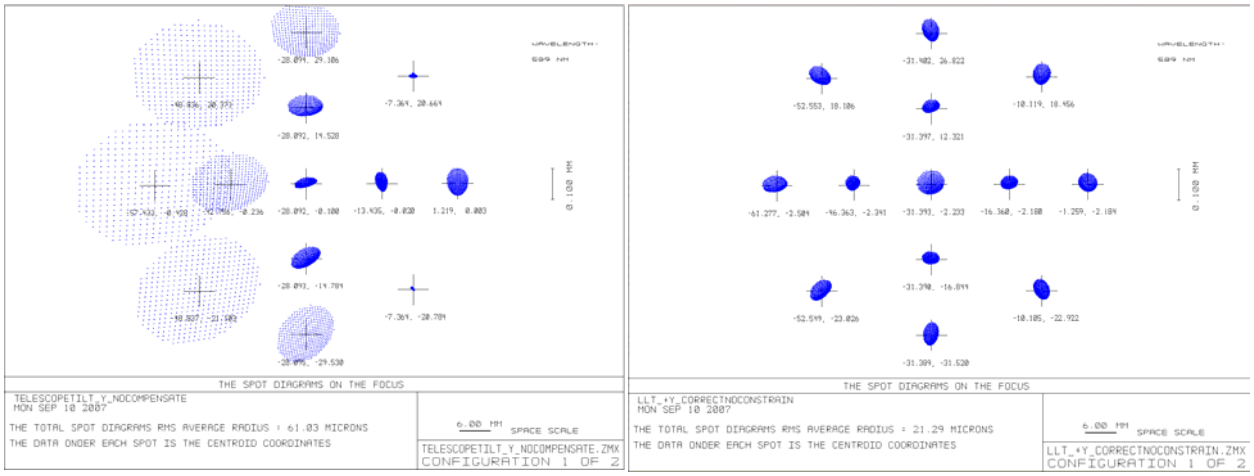

Figure 4.1-3: Spot diagrams for the LLT after a tilt of M3 to correct for 412 arcsec of TMT top end tilt (left panel) and after a compensating tilt of M2 (right panel). This results in a tilt of the input focal plane with respect to the optical axis of the LLT collimator, which would require additional optical adjustment in the BTO.

4.1.2.3 Tip/tilt Correction by Rotation of LLT M1/M2

Another correction option is to tilt the LLT M1 and provide a counter-tilt of M2 to correct for most of the image degradation. Both mirrors would have to rotate around the LLT Y-axis on their respective vertices, since the TMT flexure will be in the LLT X-direction. The resulting image quality is somewhat degraded (Fig. 4.1-4), but acceptable. One can improve this somewhat by recentering the chief ray using M3 or the centering/pointing mirrors on the Asterism Generator.

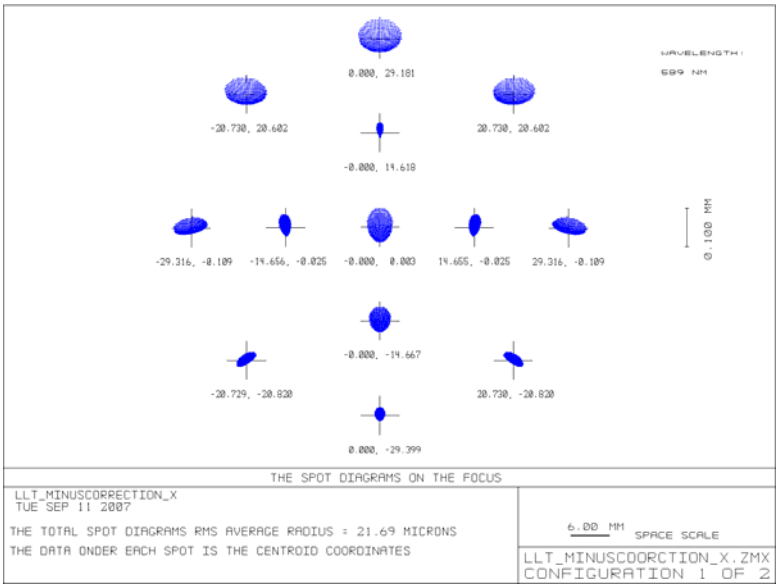

Figure 4.1-4: Spot diagram of LLT images where a tilt of 412 arcsec of the TMT top end (in the LLT X-direction) has been compensated by rotations of the LLT M1 and M2 around the local Y-axis.

While this technique appears to work, it has significant complications from the viewpoint of the mechanical engineering. Both M1 and M2 would have to be mounted in cells which could be accurately tilted about their respective vertices without introducing stresses on the mirrors and their tilts would require precision control to maintain image quality while applying the appropriate off-axis field angle to compensate for the TMT flexure.

4.1.2.4 Tilt of LLT Assembly

The simplest solution from an engineering standpoint is to simply tilt the entire LLT by an amount necessary to compensate for the tilt component of the TMT flexure. Although this requires that the LLT be installed in a rotating frame, the LLT itself remains in fixed alignment, permitting it to be aligned separately, if necessary, and installed into the LGSF top end. The space frame supporting the LLT is extended, ending in two flexures which mount onto the LGSF BTO framework (Fig. 4.1-5). The axis of rotation is coincident with the optical axis of the beam through the K-mirror and LLT M3, so the LLT can be rotated to compensate for the TMT top end flexure without any optical misalignment. Any rotation of the asterism which may occur as a result of this can be corrected by a small adjustment of the K-mirror.

Our approach to tilt compensation is to use a linear actuator to apply force to the bottom of the LLT frame perpendicular to the rotational axis of the flex mounting (Fig. 4.1-6). This force must be sufficient to 1) overcome any inbalance of the LLT about the tilt axis (which should be small) and 2) overcome the resisting moment of the flexures themselves. If one considers the actuator as a linear spring with the rest of the mechanism considered rigid, we can determine the actuator spring stiffness necessary to maintain the LLT rocking frequency above a certain value. The stiffness requirements listed in Table 4.1-1 are based on a preliminary frequency goal of 20 Hz.

The CSEM A45 or A60 actuators (Table 4.1-2) meet the requirements easily, with the possible exception of the repeatability.

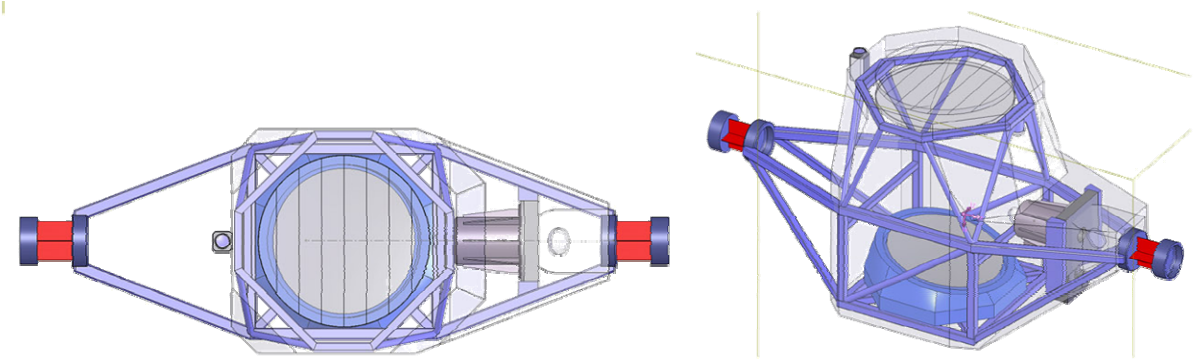

Figure 4.1-5: Top view (left) and isometric view (right) of the LLT mounted in its space frame, with the two flexures along the input optical axis.

Table 4.1-1: Requirements for LLT Tilt Mechanism

LLT Rotation	3.0 mrad (conservative)
Moment arm, actuator to tilt axis	551 mm
Minimum actuator travel	1.65 mm
Design actuator travel	3.00 mm
Linear resolution for 1 arcsec tilt	2.7 μm
Repeatability	5.0 μm
Minimum force	±100 N (or 0 – 200 N in one direction)
Minimum axial stiffness	3.85 N/μm

Table 4.1-2: Specifications for CSEM A45 and A60 Actuators

Model	*A45*	*A60*
		
Actuator length	120 mm	125 mm
Actuator diameter	45 mm	63.5 mm
Stroke length	4 mm or custom	12 mm or custom
Resolution	< 200 nm	< 200 nm
Absolute accuracy	< 5 μm	< 5 μm
Repeatability	< 3 μm	< 3 μm
Axial stiffness	> 50 N/μm	150 N/μm
Maximum load	250 N	> 1700 N
Temperature range	-60 C to 70 C	-60 C to 70 C

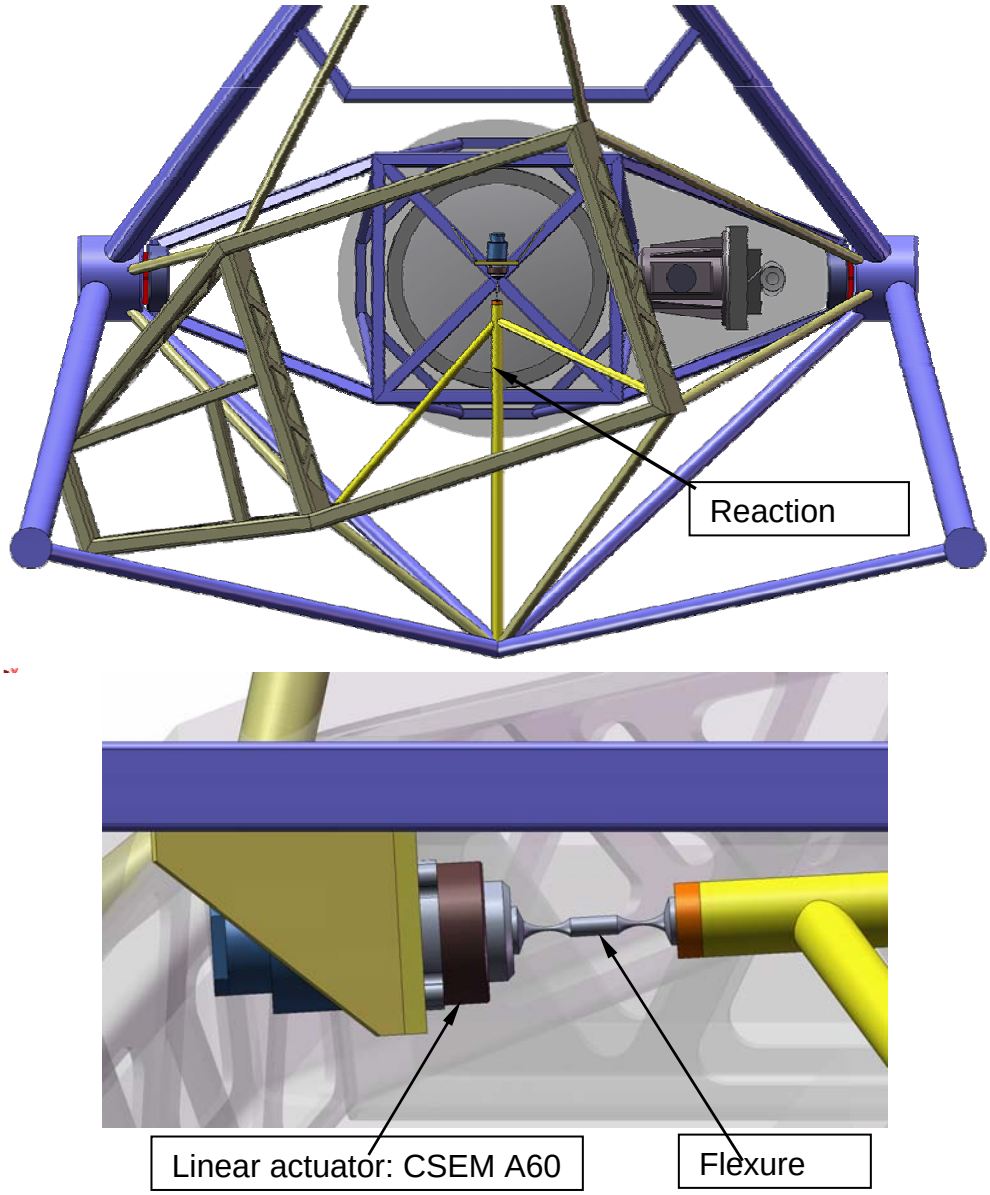

Figure 4.1-6: (top panel): View of the LLT space frame/rotation fixture from below. The linear actuator pushes against a reaction truss designed to minimize bending or buckling. (bottom panel): Magnified view of the linear actuator and flexure coupling to the reaction truss.

4.1.2.5 M2 Hexapod Tilt Correction

Since the flexure of the TMT top end will, to first order, tilt both the LGSF optics (including the LLT) and the TMT M2 itself, it is possible to consider mounting the entire LGSF top end assembly on the M2 hexapod and utilize the latter to correct the tilt of both M2 and the LLT. While this approach may be viable, we did not investigate it in any detail, nor is this report officially recommending this as a solution. We felt it important to recommend a concept which is self-contained and does not require significant modifications to the existing requirements for

the M2 hexapod design. If this concept is pursued in the future, there are some implications for the LGSF:

- Tying the LGSF top end to the M2 hexapod would of course increase the mass and wind loading on the hexapod.
- The function of the M2 hexapod goes beyond simple tilt correction of M2. Small translation and tilt motions of M2 are also used to optimize the image quality of TMT; these would also affect the LGSF and could result in a net tilt which is different from that required to correct the LLT pointing.
- If tilt corrections for M2 are performed about its vertex, they will introduce significant translational motions of the LGSF top end at the point where the beams enter from the tripod leg. This would likely require corrections of the truss centering and pointing mirrors in addition to those required to compensate for the truss flexure.

4.2 BTO Top End Redesign

4.2.1 Mating of Truss Transport to BTO Top End

The conversion to a Ritchey-Chrétien design results in a shorter telescope structure with more horizontal tripod members. After several design studies, the Telescope Structures Group has settled on a straightforward tripod design (designated TRI_2) which mounts to a planar triangular frame (Fig. 4.2-1). This design also simplifies the task of directing the LGSF beams to the BTO top end; the previous concepts would have required the transport ducting to vignette the TMT primary over several meters and an additional set of mirrors to reach the top end.

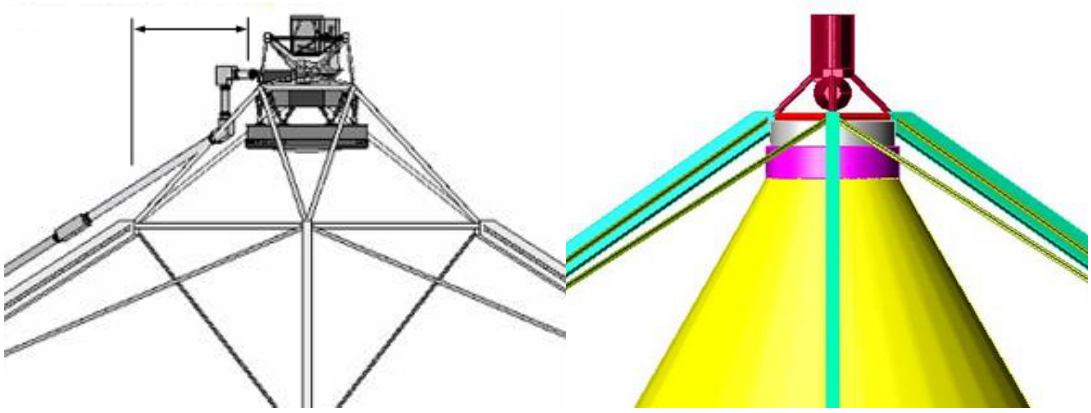

Figure 4.2-1: One of the original M2 support concepts (left panel) and the current TRI_2 concept (right panel). The arrow in the left panel represents the space over which the laser ducting would have obscured the TMT primary. Also note the awkward vertical section to match up with the BTO top end.

Because the BTO ducting will come up one of the two truss members in the +Y dimension (i.e., above the M2 structure when the telescope is pointed at the horizon), the beam will intercept the BTO top end at a 30º angle from the X-axis. One way to address this is to rotate the entire BTO top end structure, including the LLT, by this amount to provide a straight-line path into the

diagnostic bench. However, because we plan to tilt the LLT about the X-axis as part of the flexure compensation strategy (section 4.1), we decided to rotate the diagnostic bench/Asterism Generator subsystems about an axis centered on the large flat following the Asterism Generator to mate the input of the diagnostic bench with the BTO truss transport ducting, while keeping the rest of the optical system (K-mirror, LLT) oriented as before. Figure 4.2-2 illustrates this design concept.

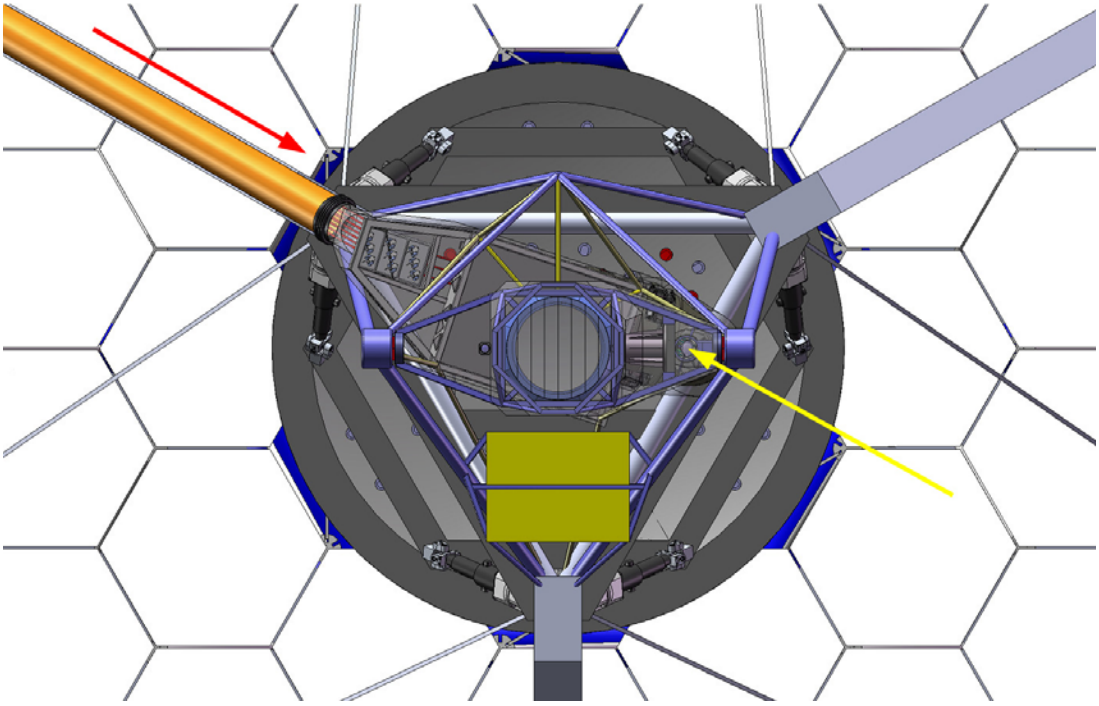

Figure 4.2-2: Top view of the LGSF, showing the BTO transfer ducting (red arrow) meeting the input to the diagnostic bench. The TMT X-axis runs horizontally through the LLT in the figure, and the tripod truss member on the bottom of the figure is below M2 when the telescope is pointing to the horizon. The primary-secondary orientation of the LLT remains along the telescope X-axis, whereas the diagnostic bench and Asterism Generator are rotated approximately 25º about the vertical optical axis (yellow arrow) at the output of the Asterism Generator fold mirror.

The redesign of the TMT top end results in a more compact telescope structure, but the revised angle of the horizontal truss results in a large angle of incidence for the centering mirrors directing the laser beams into the BTO top end. Such a large angle of incidence in the high-power laser beam path would require high-reflectivity coatings customized to this geometry and could introduce unwanted elliptical polarization. By tilting the entire BTO top end assembly, the angle of incidence can be reduced by 10º to 62.7º (Fig. 4.2-3). This angle may still require custom high-reflectivity coatings for the mirrors, but the major axis footprint is reduced by 50% with a consequent relaxation of the safety margin for keeping the laser beams centered on these mirrors.

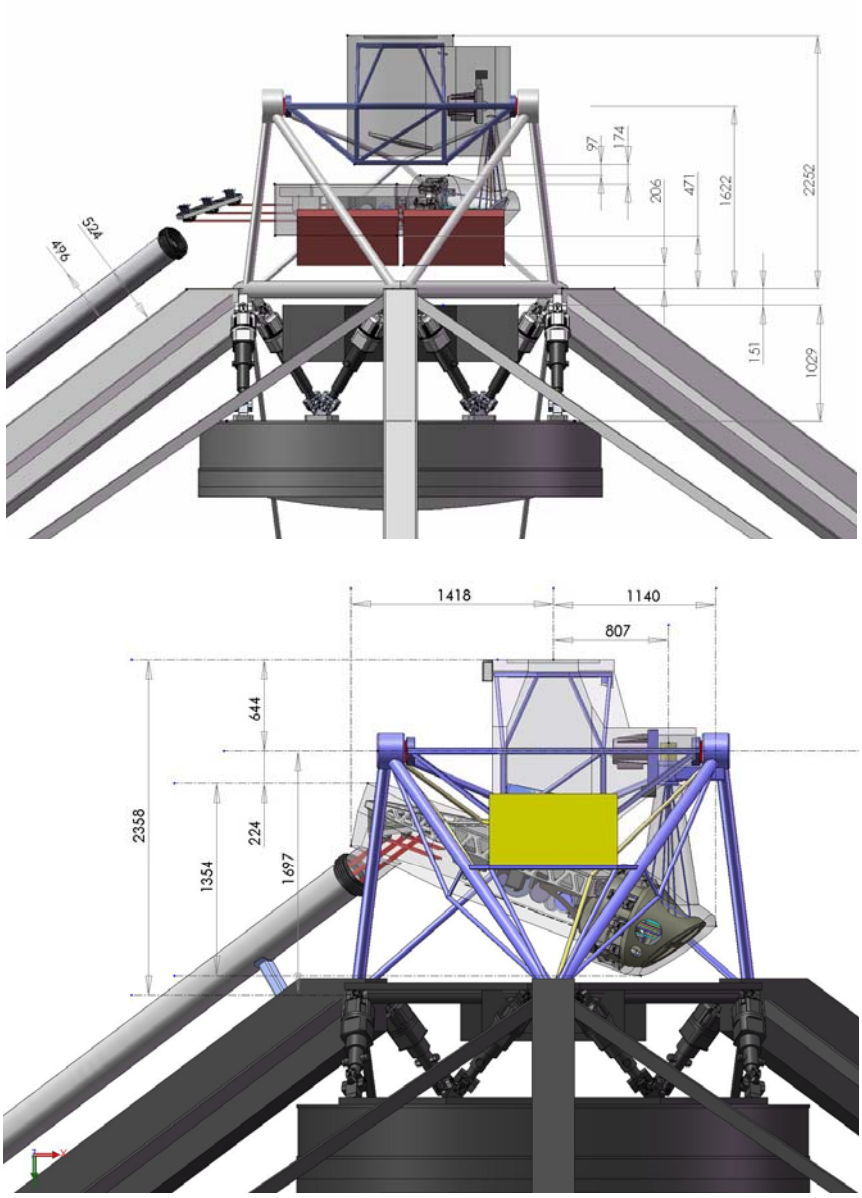

Figure 4.2-3: (top panel) The LGSF top end and the beam transport up the tripod structure with the original horizontal bench. The angle of incidence on the centering array mirrors is 72.7º. (bottom panel) Revised layout after tilting the Diagnostic Bench/Asterism Generator subassembly. This reduces the angle of incidence on the centering array mirrors to 62.7º.

4.2.2 Diagnostic Bench Design

As described briefly in section 3.2, the fundamental design of the diagnostic system is unchanged from the Conceptual Design Review, but the bench itself has been expanded and modified:

- The original design employed an optical "periscope" to compress the 3 × 3 beam pattern from a wide (70 mm centers) to a more compact (25 mm centers) format to reduce the

size of the diagnostic optics and to make more efficient use of the diagnostic camera CCD real estate. A second periscope followed the diagnostic bench to enlarge the beam pattern to meet the minimum spacing requirements of the input mirrors in the Asterism Generator. The redesigned Diagnostic Bench maintains the 70 mm center beam pattern throughout and moves the step-down periscope after the beamsplitter pickoff. This removes four mirrors from each beam in the high-power laser beam path, replacing them with two mirrors in a low-power environment, for gains in both throughput and cost (Fig. 4.2-4, 4.2-7).

- The quarter-wave plates for each beam are now explicitly included in the Diagnostic Bench design.
  - Individual waveplates are mounted in an annular ring supported by radial ball bearings (Kaydon JHA15CL0)
  - Parker LV11 stepper motors rotate each waveplate individually via a worm gear drive.
  - Either limit switch or encoder on the drive motors (TBD) may be used for calibration of the waveplate angle.
- The beamsplitters BS1 and BS2 are no longer a monolithic optical element, but an array of nine small (25 mm diameter) beamsplitters installed in a frame.
  - We present an option for installing BS1 as a two-position mechanism with an open (normal) position and a dichroic position for diagnostics (Fig. 4.2-8).
- The beam dump assembly has been moved from the region of the LLT collimator to the Diagnostic Bench between BS2 and the Asterism Generator (Fig. 4.2-6).
  - Geared motor drives the slide between the normal (through) beam position and the beam dump position
  - Power meter is liquid-cooled thermopile sensor (Coherent Technologies PM-300).

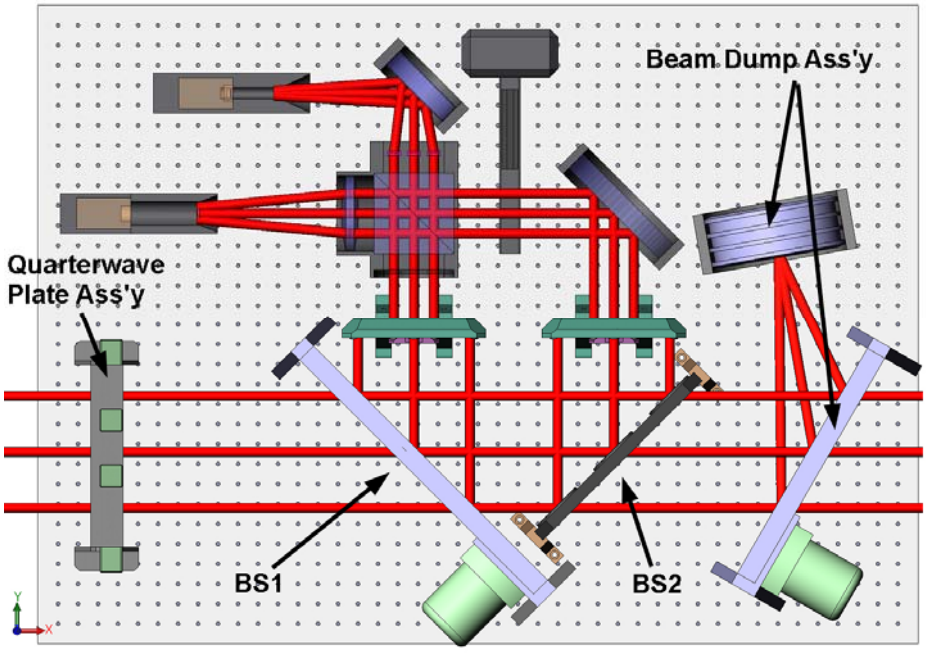

Figure 4.2-4: Layout of revised Diagnostic Bench, with the subassemblies indicated.

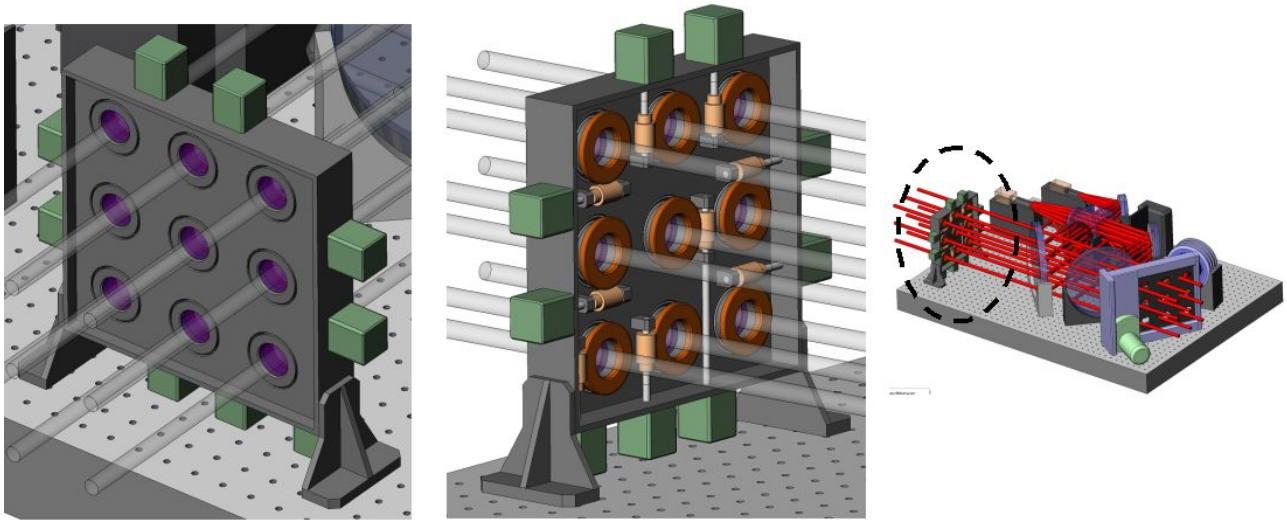

Figure 4.2-5: Entrance and exit views (left and middle panels, respectively) of the quarter-wave plate array on the Diagnostic Bench. The right panel shows the location of this subassembly on the bench.

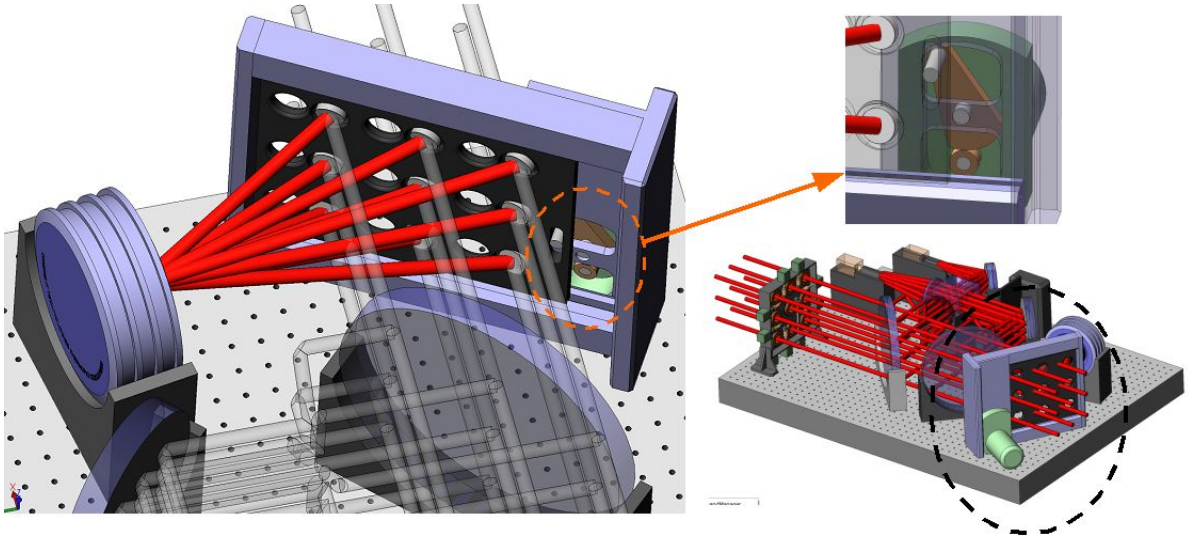

Figure 4.2-6: The beam dump assembly at the output of the Diagnostic Optical Bench (left panel). Each beam position has a dedicated mirror angled to reflect the beam to the power meter. The optical assembly slides in a frame, driven by a motor with an actuator pin (detailed in upper right) to allow rapid deployment of the beam dump. The lower right panel shows the location of the beam dump subassembly on the bench.

Figure 4.2.7 shows a closeup of the two periscopes between the beamsplitters BS1/BS2 and the beamsplitter cube in the Diagnostic section. Figure 4.2-8 shows details of the beamsplitter mounts for BS1 and BS2; the view is from the camera side of the bench, so the main laser beams travel from right to left. The BS1 mechanism is a two-position slide with a choice of open holes for normal operation and dichroics for observing a natural star.

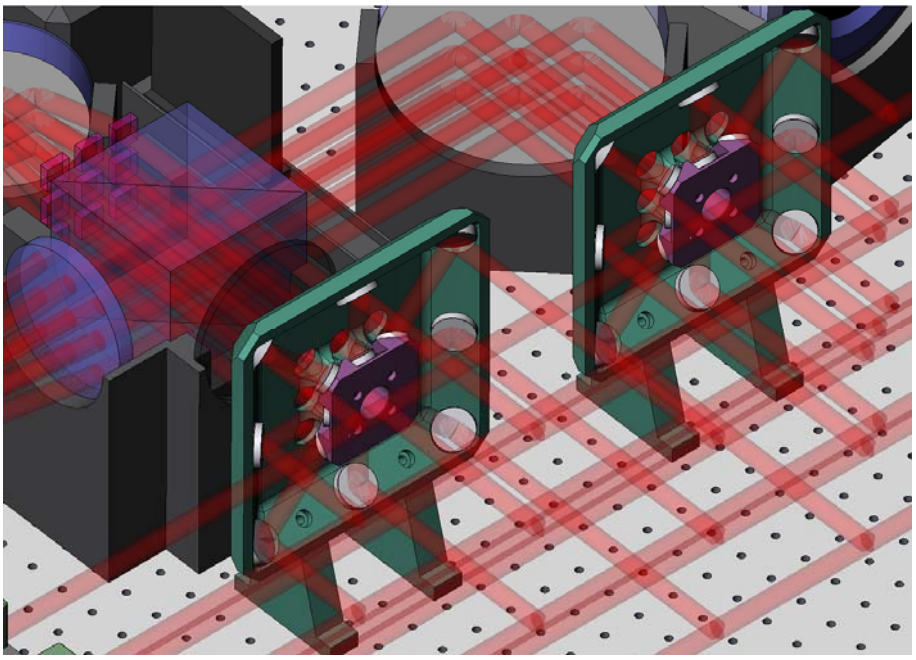

Figure 4.2-7: Closeup of the two periscope assemblies which feed the diagnostic section with a more compact beam geometry. Beamsplitters BS1 and BS2, which would lie in the lower right of the figure, are not shown for clarity.

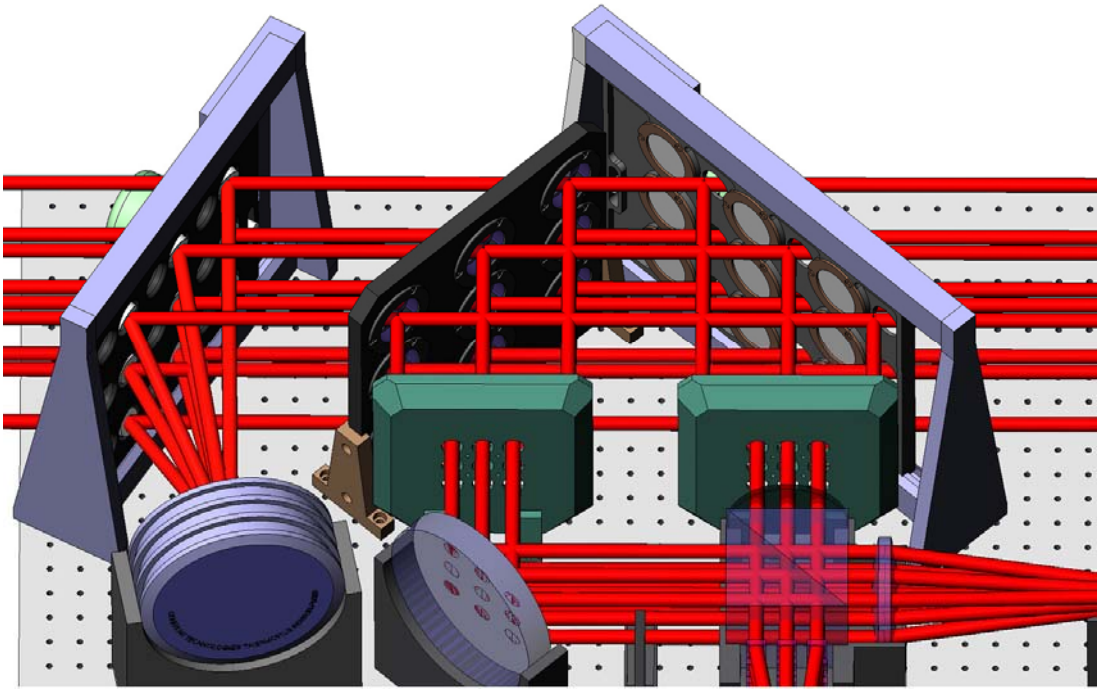

Figure 4.2-8: Closeup view of (from right to left) BS1, BS2, and the Beam Dump.

An isometric view of the redesigned Diagnostic Optical Bench is shown in Fig. 4.2-9.

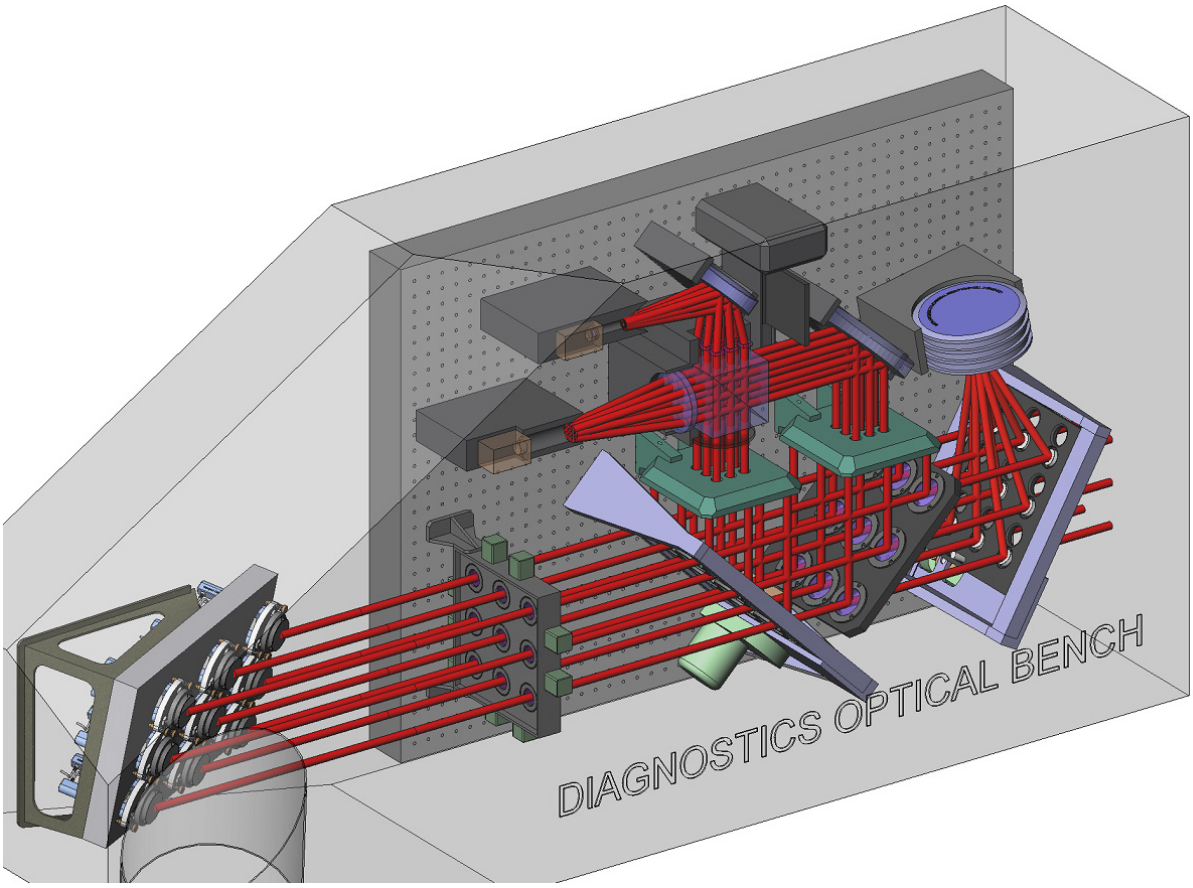

Figure 4.2-9: Isometric view of the redesigned Diagnostic Optical Bench. The beam travel is from left to right.

4.2.3 Asterism Generator

The size of the Asterism Generator was determined by mechanical constraints defined by the output mirrors. The NFIRAOS asterism consists of a central on-axis beacon and five equally-spaced beacons at a radius of 35 arcsec. The 60:1 magnification of the LLT collimator increases this angle to 35 arcmin in BTO space. A minimum center-to-center spacing of the output mirrors of 20 mm requires an Asterism Generator "focal length" of 1964 mm. This spacing was necessary to accommodate individual mirrors 15 mm along the minor axis (to allow for beam wander as the centering and pointing mirrors maintain alignment with the LLT input pupil) and some room for mounting fixtures. Now that the geometry of the truss ducting and LLT mounting has been determined, the overall length of the optical path between them is limited. In order to fit the Asterism Generator into the space between the Diagnostic Bench and the LLT, this "focal length" was shortened from 1964.36 to 1480.67 mm. Maintaining the 60:1 magnification results in the output mirrors for the NFIRAOS asterism being spaced by 15 mm. This is not felt to be a serious problem, as it should be possible to machine the support structure for the mirrors as a single piece (Fig 4.2-10) and mount the mirrors to their respective facets. This will permit a smaller separation between the individual mirrors, since each will not have to be individually mounted to the output face of the Asterism Generator.

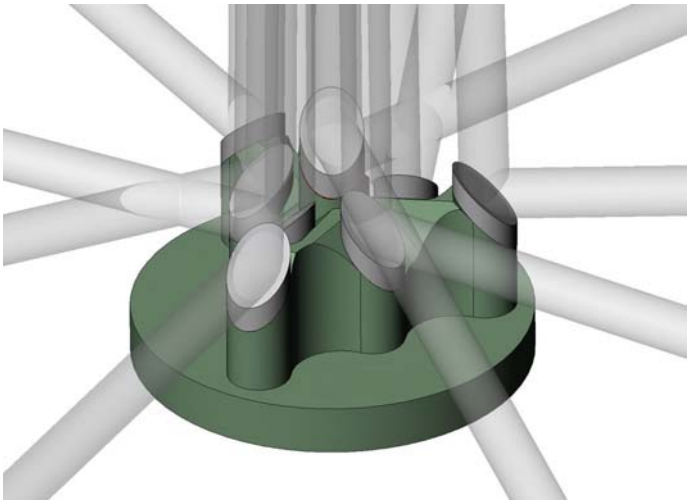

Figure 4.2-10: Concept of a monolithic mounting for the six NFIRAOS and three inner MOAO mirrors at the output of the Asterism Generator.

The decreased spacing between the Asterism Generator plate and the large fold mirror and the smaller angle of incidence of the beams onto the fold mirror (resulting from the tilt of the Diagnostic Bench/Asterism Generator assembly) created a conflict between one of the centering/pointing mirror assemblies on the periphery of the plate and one of the GLAO beams. This was alleviated by clocking the entire Asterism Generator plate slightly (Fig 4.2-11).

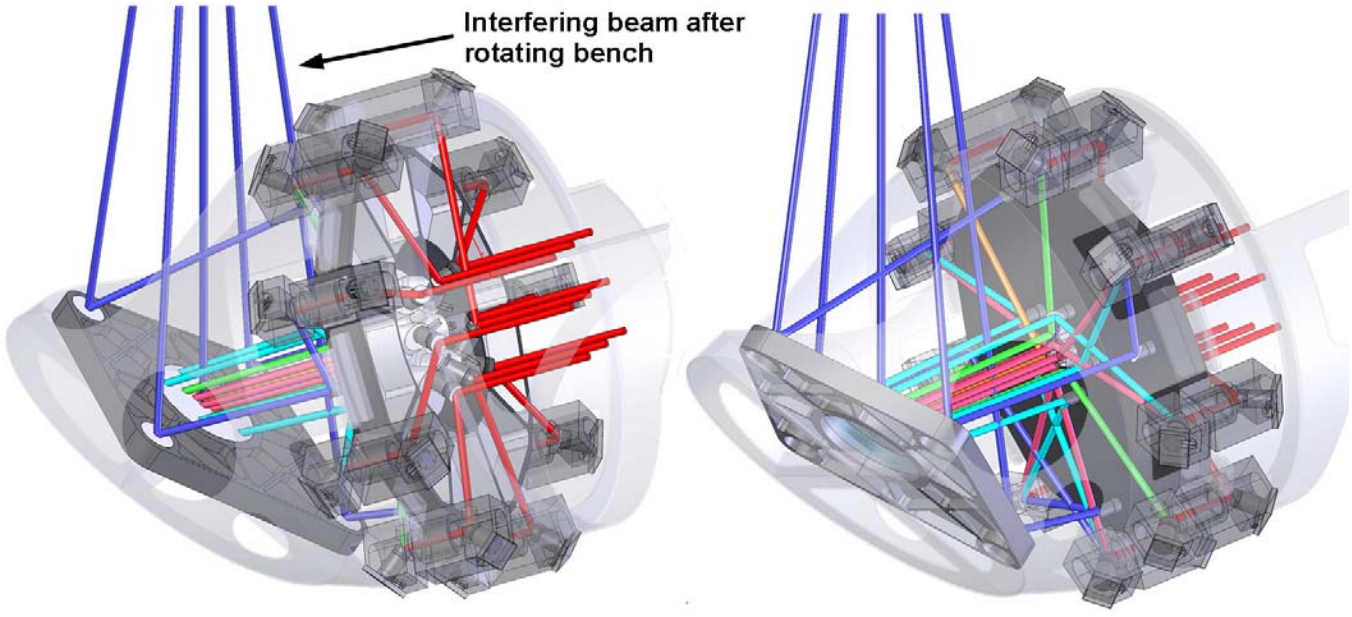

Figure 4.2-11: Detail of the Asterism Generator. The basic design is unchanged from that of the Conceptual Design Review, but the large folding flat has been replaced by an array of smaller mirrors and the entire generator assembly was clocked several degrees to avoid interference between one of the GLAO beams and a mirror subassembly.

4.3 LGSF Interface to Telescope Structure:

4.3.1 Truss Transport Ducting

The definition of the telescope top end structure has allowed us to provide a detailed concept for the transport of the laser beams up the truss and the interface to the BTO top end. However, a complete concept for the transport is dependent on the location of the LSE, which is a subject of current discussion. This report will assume the LSE location specified shortly after the Conceptual Design Review, on one of the two rocker arms which provide the telescope elevation motion (Fig. 4.3-1).

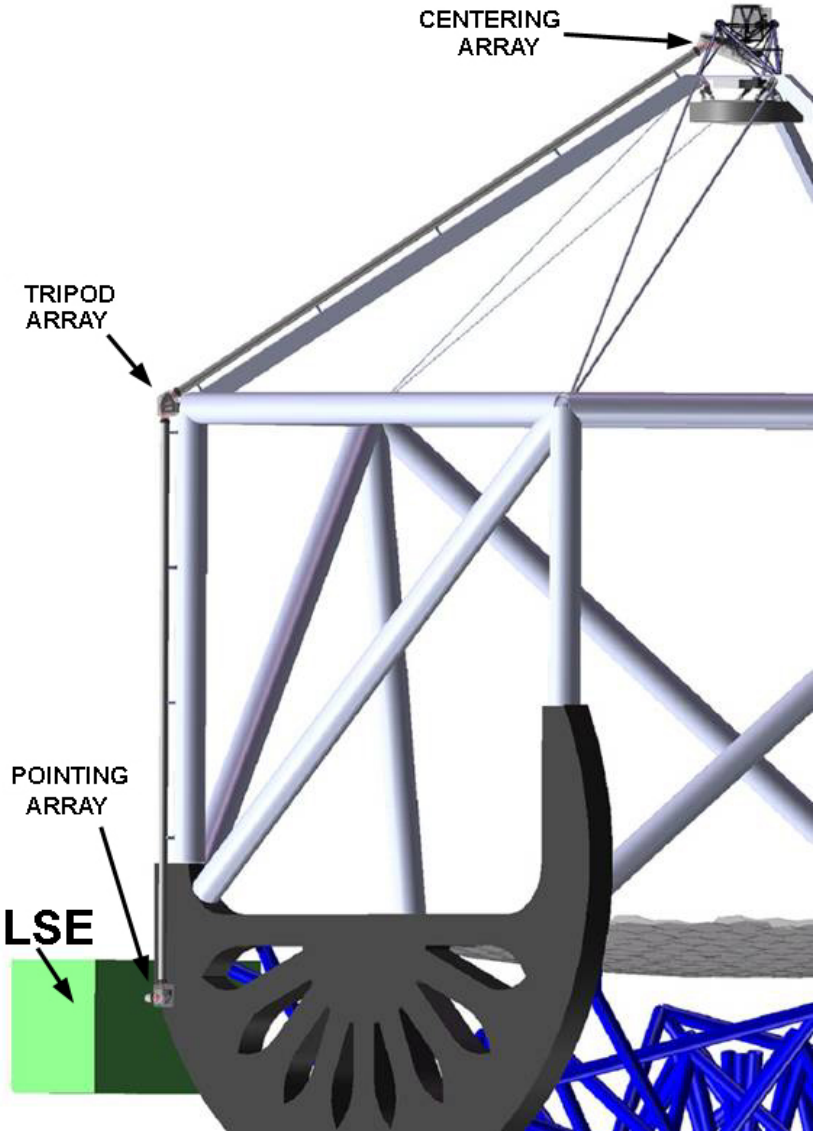

Figure 4.3-1: Overview of the LSE and transport ducting on the TMT.

The ducting path consists of three straight sections: a short horizontal section from the output of the LSE; a vertical section running up the outside of the vertical truss member closest to the

LSE; an angled section running up one of the tripod leg on the "high" side of the elevation axis. At each of the interfaces between sections, the beams are redirected by an array of mirrors, two of which employ mirror mounts adjustable in tip/tilt (the aforementioned Pointing and Centering Arrays). The Tripod Fold Array at the junction of the vertical column and tripod leg members is fixed; the compound angle of reflection at this point will result in a "clocking" of the beam pattern going up the tripod leg to the Centering Array.

Figure 4.3-2 shows details of the Pointing and Tripod Fold Arrays, including their mounting to the telescope structure and the mounting details of the duct tubing to the telescope structure. Both the mirror array and ducting supports mount to the telescope, but they are isolated from each other so that wind or gravitational loading on the ducting will not affect the mirrors. The Pointing and Tripod Fold Arrays are enclosed in boxes attached to the telescope and to the duct tubing by flexible Elastomer bellows. These boxes provide the environmental shielding required for both safety and cleanliness and have covers to provide access for maintenance or replacement of the optical elements. The Relay Lenses are also mounted within the access boxes for the Pointing (L1/L2) and Tripod Fold (L3) Arrays.

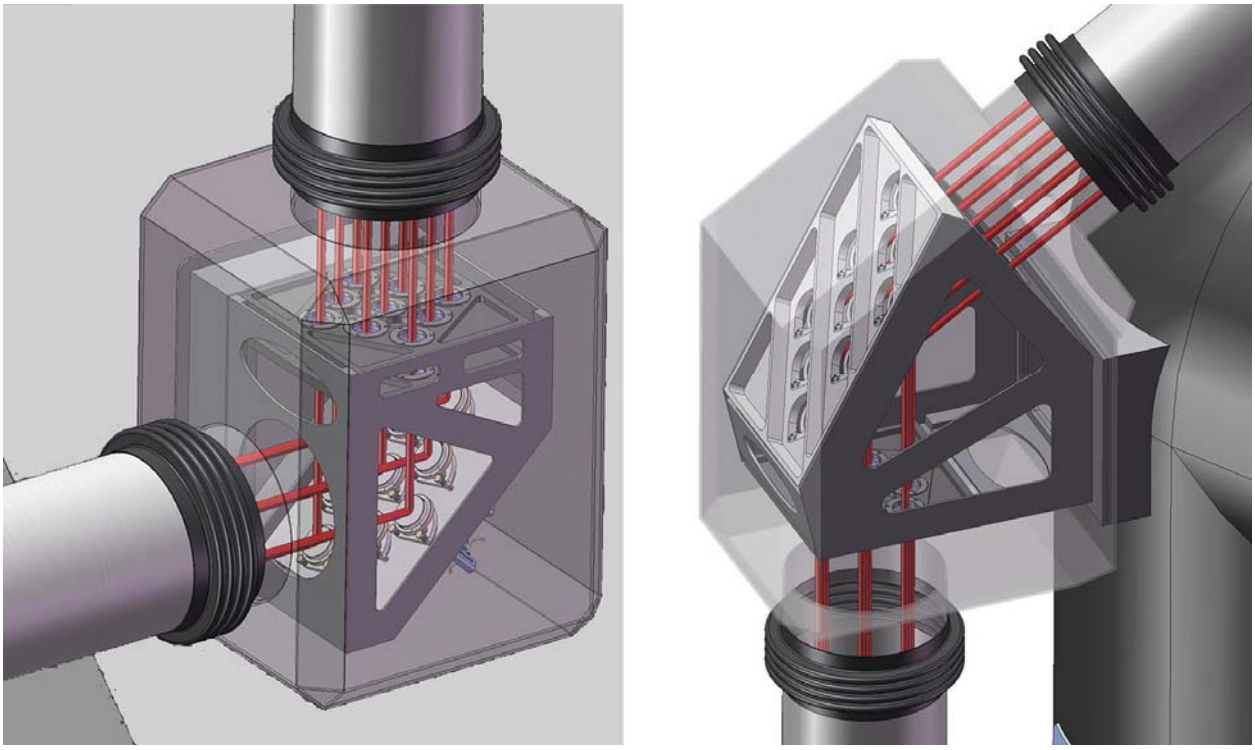

Figure 4.3-2: Closeup of the Pointing Array (left panel) and Tripod Fold Array (right panel) showing the mounting of the arrays, relay lenses, and the duct tubing to the telescope structure. The enclosures at these junctions will have doors for maintenance access.

Pursuant to the recommendations of the LGSF Review by LMCT [5], the three mirror arrays on the truss transport have been sized to permit the use of 50 mm diameter optics, providing a larger margin of safety as the telescope structure flexes with gravity.

The transport ducting is 270 mm diameter, allowing it to remain in the shadow of the 300 mm wide horizontal truss members and avoid additional vignetting of the telescope beam.

4.3.1.1 Truss Transport Safety Issues

For the weight and CG calculations (section 4.4), the transport ducting is assumed to be 1 mm thickness material rolled into tubular sections. The use of thin material raises safety concerns about the possibility of the high-power 25W laser beams burning through the tubing should a malfunction direct one of the beams onto the interior surface of the duct tubing. Investigation of this possibility with simple thermal modeling (conduction only, no radiation) shows that a 25W laser beam with 8 mm diameter normally incident on 1 mm thick Al plate will burn through in a few seconds; for a 2 mm thick plate, this time is increased to approximately 60 sec. While this result suggests that the duct tubing should be 2 mm thick for safety, this approach raises additional issues. Aside from doubling the weight of the duct tubing (section 4.4), the rolling of 2 mm stock into long tubes could be difficult. We feel that retaining the original 1 mm ducting wall thickness does not pose serious safety issues:

- The model analysis assumed normal incidence of the laser beam on a completely absorbing surface, ignoring radiation losses, an extremely conservative scenario.
- Within the transport ducting, the laser beam trajectories are such that an optical malfunction or breakage would likely result in glancing incidence of the beam on the interior duct wall.
- The duct wall may not be black (TBD), so most of the light would be reflected in the event of a malfunction.
- The walls of the junction boxes, which could be subjected to normal laser beam incidence in the event of a malfunction, should be of thicker (~2 mm) material.
- The near-field Diagnostic Camera, which is continuously monitoring the active LGS beams, could be programmed to detect a "missing" beacon and immediately close the safety shutters. This is currently a requirement of the diagnostic control system at a sampling rate of 1 Hz.

4.3.2 LGSF Top End Support Frames

The LGSF top end mechanical structure can be broken into three components: the LLT support frame; the Diagnostic Bench/Asterism Generator support frame; and the LGSF Top End Support Structure which supports these two and attaches to the TMT top end triangle. The Centering Array is mounted in the Diagnostic Bench support frame, but is not part of the bench itself, which would become significantly more massive if it were extended to carry the Centering Array. The top end framework is an axially acting space frame comprised of thin wall mechanical tubing. Bending moments have been minimized to provide a stiff, light yet efficient structure.

The following section (4.4) will discuss the weight and center of mass calculations and will provide illustrations which show the details of the mechanical structure subassemblies and how they fit together.

4.4 Weight, Center of Gravity, and Cross-section

The following figures (Fig. 4.4-1 through 4.4-5) show isometric views of the LLT, Diagnostic Bench/Asterism Generator, LGSF Top End Support Structure, the entire Top End Assembly, and the BTO Truss Subassembly. In these figures, a small triad marks the center of mass of each subassembly. The mass and center of gravity information are summarized in tables immediately following the figures.

Figure 4.4-6 shows the estimates of the cross-section for wind loading calculations.

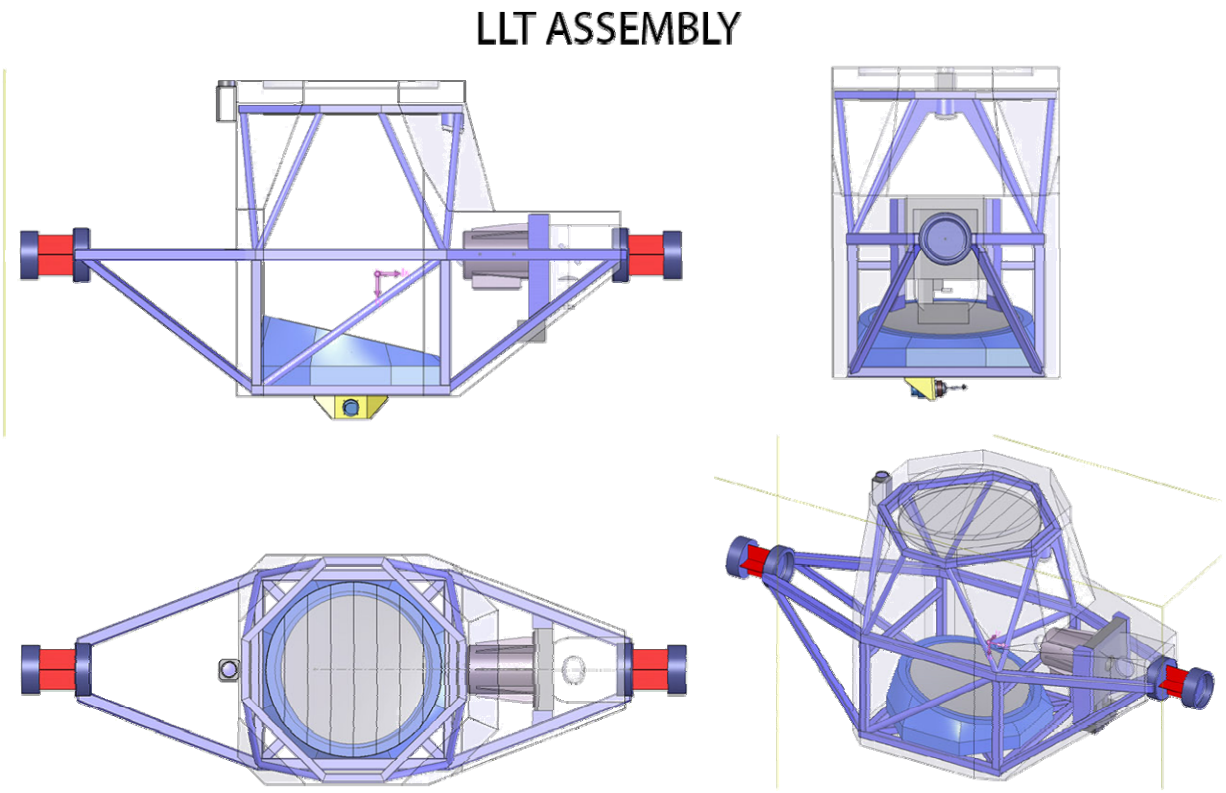

Figure 4.4-1: Isometric views of the LLT assembly. The small triad in this figure and in Figs. 4.4-2 through 4.4-5 mark the center of mass of the assembly.

Table 4.4-1: Weight and CG of LLT Assembly

LLT ASSEMBLY		CG location			Moment		
Item	Wt (kg)	X (m)	Y (m)	Z (m)	WX	WY	WZ
Optics: M1,M2,	31.1	0.04	0.00	26.50	1.18	0.00	823.09
K mirror assy + Rotary Table	21.7	0.65	0.00	26.76	14.15	-0.07	579.98
LLT Environmental Window	16.3	0.00	0.00	27.33	0.00	0.00	445.21
Bore sight camera	2.0	-0.46	0.00	27.37	-0.92	0.00	54.73
LLT Envelope (side paneling to enclose frame, also includes environmental cover)	27.5	0.08	0.00	26.83	2.28	0.00	736.61
M1 Cell	26.5	-0.02	0.00	26.40	-0.64	0.00	700.42
M2 Cell	0.9	0.38	0.00	27.30	0.35	0.00	25.12
Tilt Drive Assy	2.5	0.00	-0.06	26.24	0.00	-0.15	64.54
LLT Cradle Frame Structure	70.0	0.05	0.00	26.76	3.15	0.00	1871.72
LLT ASSY TOTAL	**198.3**	**0.10**	**0.00**	**26.73**	19.55	-0.22	5301.41

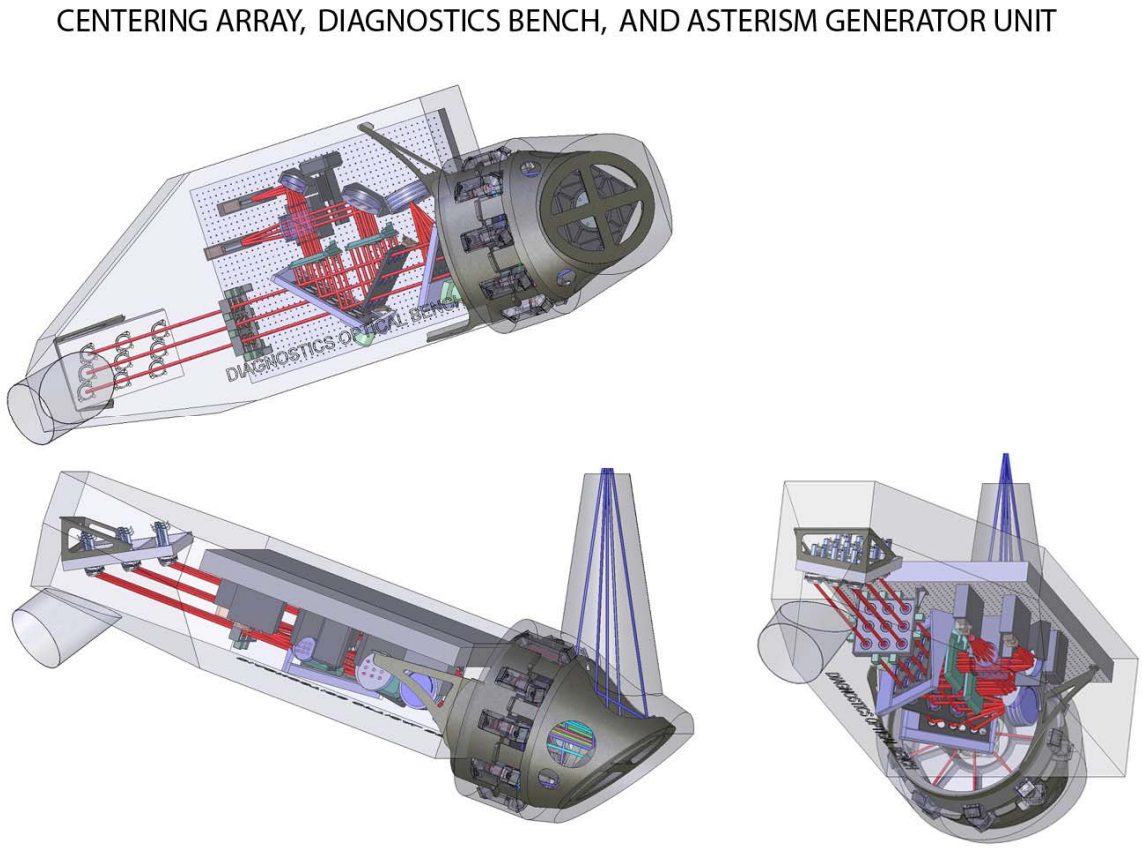

Figure 4.4-2: Isometric views of the Centering Array, Diagnostic Bench, and Asterism Generator in their operating configuration.

Table 4.4-2: Weight and CG of Diagnostic Bench Assembly

CENTERING ARRAY, DIAGNOSTICS BENCH, AND ASTERISM GENERATOR UNIT		**CG location**			**Moment**		
Item	**Wt (kg)**	**X (m)**	**Y (m)**	**Z (m)**	**WX**	**WY**	**WZ**
Centering Array and Support Bracket	10.5	-1.20	0.59	26.25	-12.56	6.20	276.02
Diagnostics Optical Bench (Breadboard)	65.0	-0.14	0.14	26.05	-9.17	9.04	1693.19
DOB Containment Box (Envelope)	37.2	-0.40	0.25	25.99	-14.93	9.24	967.80
DOB Cameras and Upper Train Optics	15.8	-0.34	-0.01	25.97	-5.44	-0.11	410.42
NF and FF Cameras, NFC-1 & FFC-1							
Beam Splitter, BS-3							
Fold Mirrors, FM-3 and 4							
Field Prism Array, FPA-1							
Field Lens, FL-1							
ND Filter							
Beam Shutter, SH-1							
Mounting Hardware for above							
DOB Lower Train Optics							
Large Pattern Beam Splitter, BS-2	3.5	-0.10	0.29	25.89	-0.35	1.02	89.58
Flip up fold mirror, FM-5	3.0	-0.10	0.29	25.89	-0.30	0.88	77.67
Beam Dump Assy (includes actuator and Thermopile), FM-6	9.1	0.19	0.14	25.76	1.70	1.29	234.74
Quarterwave Plate Array Assy, QWA-1	3.9	-0.56	0.45	26.05	-2.16	1.73	100.53
Asterism Generator Containment Box (Envelope)	33.2	0.65	0.05	25.64	21.55	1.69	851.60
AG Bench Support Bracket	36.0	0.54	0.08	25.60	19.46	2.88	922.22
Asterism Generator	49.4	0.57	0.08	25.60	28.20	3.70	1264.21
Centering Array	2.4						
Steering and Tip Tilt Modules	28.2						
Asterism Fold mirrors	0.4						
Generator Bench	7.6						
Output Fold Mirror	10.8						
CENTERING ARRAY, DIAGNOSTICS BENCH, AND ASTERISM GENERATOR UNIT	**266.6**	**0.10**	**0.14**	**25.83**	26.01	37.57	6888.00

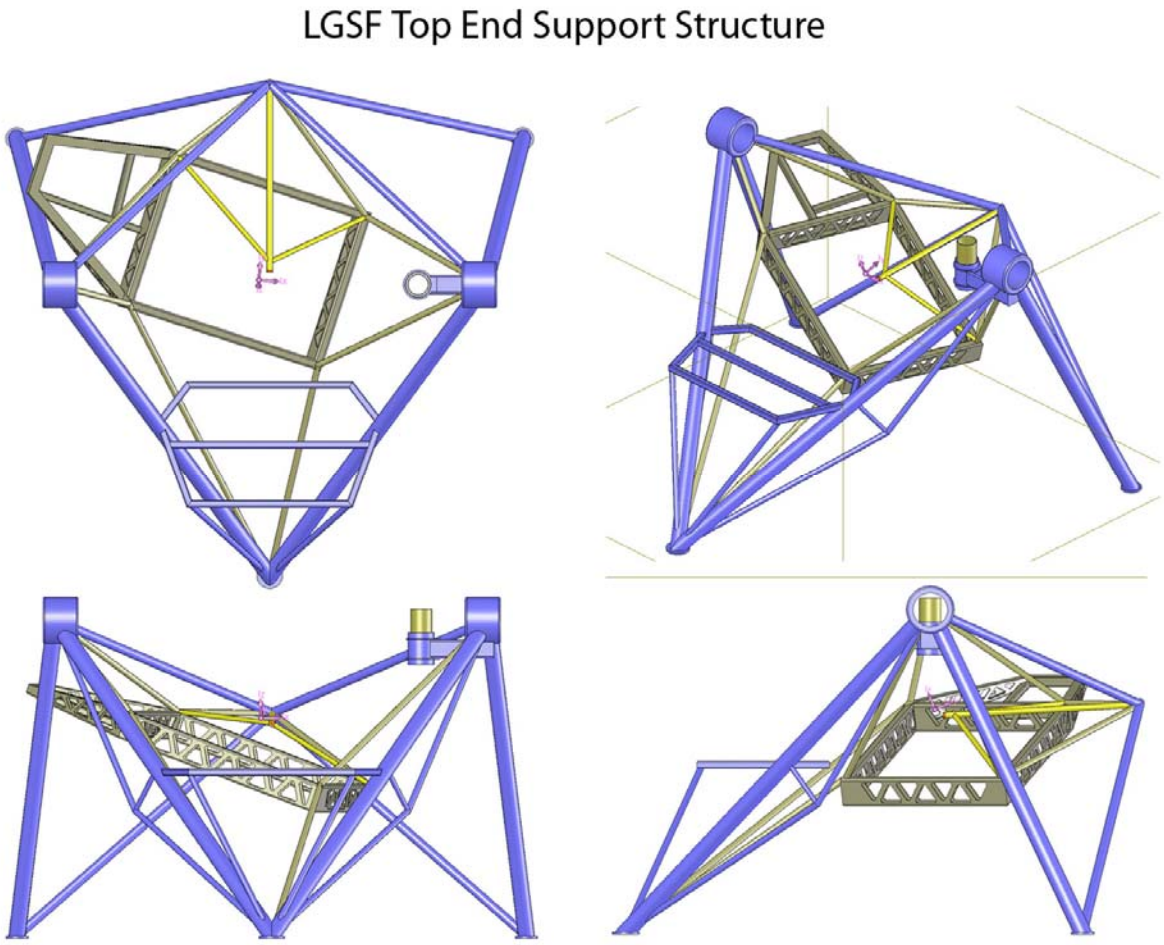

Figure 4.4-3: Isometric views of the LGSF Top End Support Structure. The LLT support frame flexures (Fig. 4.4-1) fit into the two sockets at the top. The Centering Array/Diagnostic Bench/Asterism Generator subassembly support frame is shown in grey. The reaction truss for the LLT tilt mechanism is shown in yellow. The flat bench frame (lower part of upper left panel) supports the electronics boxes. The three tripod legs mount to the TMT top end triangle frame.

Table 4.4-3: Weight and CG of Top End Support Structure

LGSF Top End Support Structure		CG location			Moment		
Item	Wt (kg)	X (m)	Y (m)	Z (m)	WX	WY	WZ
Support Steel for LLT, Diagnostics Bench, Asterism Generator, and Electoronics Cabinets	172.6	-0.06	0.02	26.27	-10.08	4.30	4535.00
LGSF Top End Support Structure	**172.6**	**-0.06**	**0.02**	**26.27**	-10.08	4.30	4535.00

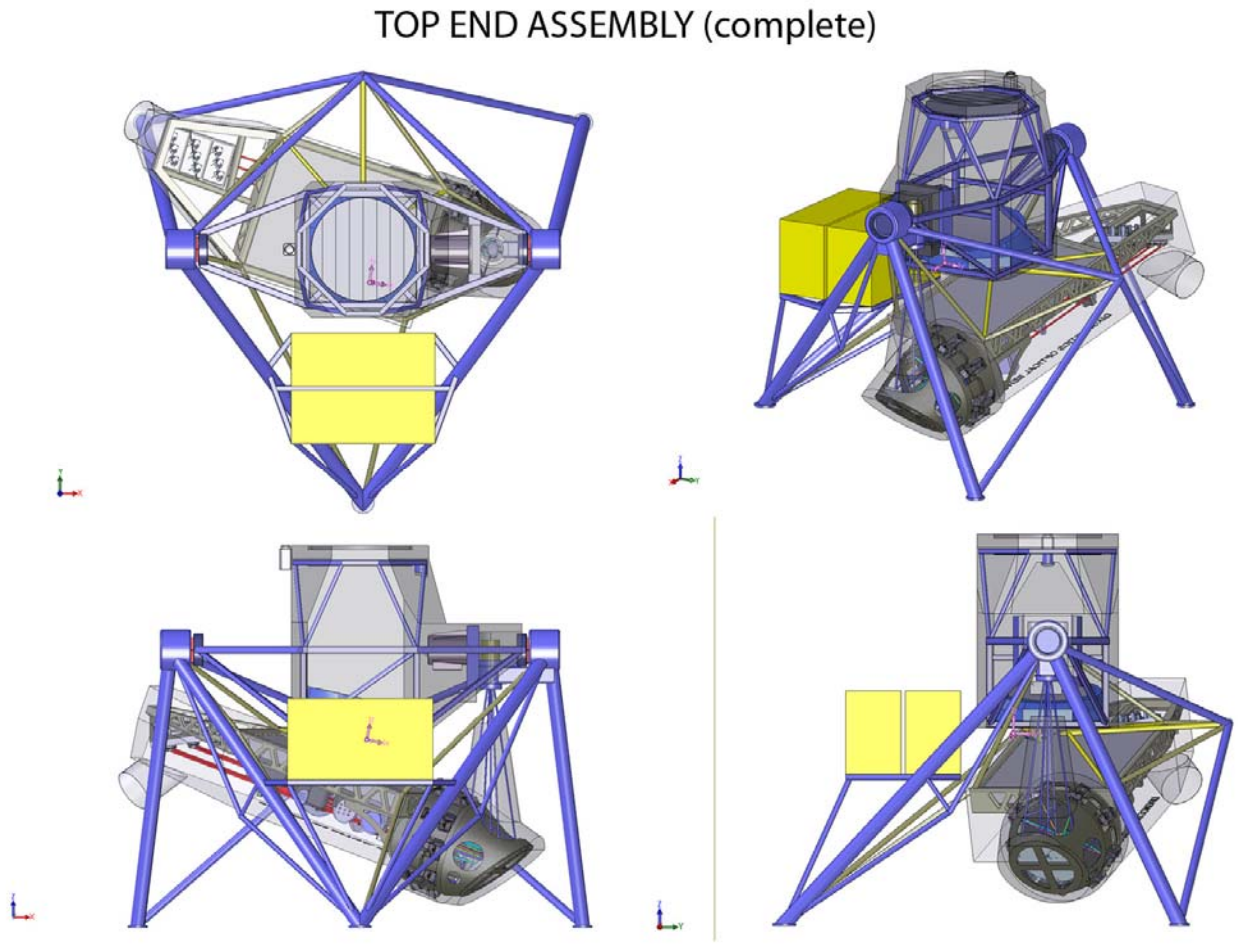

Figure 4.4-4: Isometric views of the complete LGSF Top End Assembly with all components installed. The yellow boxes are the LGSF electronics cabinets.

Table 4.4-4: Weight and CG of LGSF Top End Assembly

TOP END complete		CG location			Moment		
Item	Wt (kg)	X (m)	Y (m)	Z (m)	WX	WY	WZ
LLT ASSY TOTAL	198.3	0.099	-0.001	26.729	19.55	-0.22	5301.41
CENTERING ARRAY, DIAGNOSTICS BENCH, AND ASTERISM GENERATOR UNIT	266.6	0.098	0.141	25.834	26.01	37.57	6888.00
LGSF Top End Support Structure	172.6	-0.058	0.025	26.275	-10.08	4.30	4535.00
ELECTRONICS BOXES	264.9	0.000	-0.871	26.250	0.00	-230.67	6953.63
TOP END complete	**902.5**	**0.039**	**-0.209**	**26.237**	35.48	-189.03	23678.03

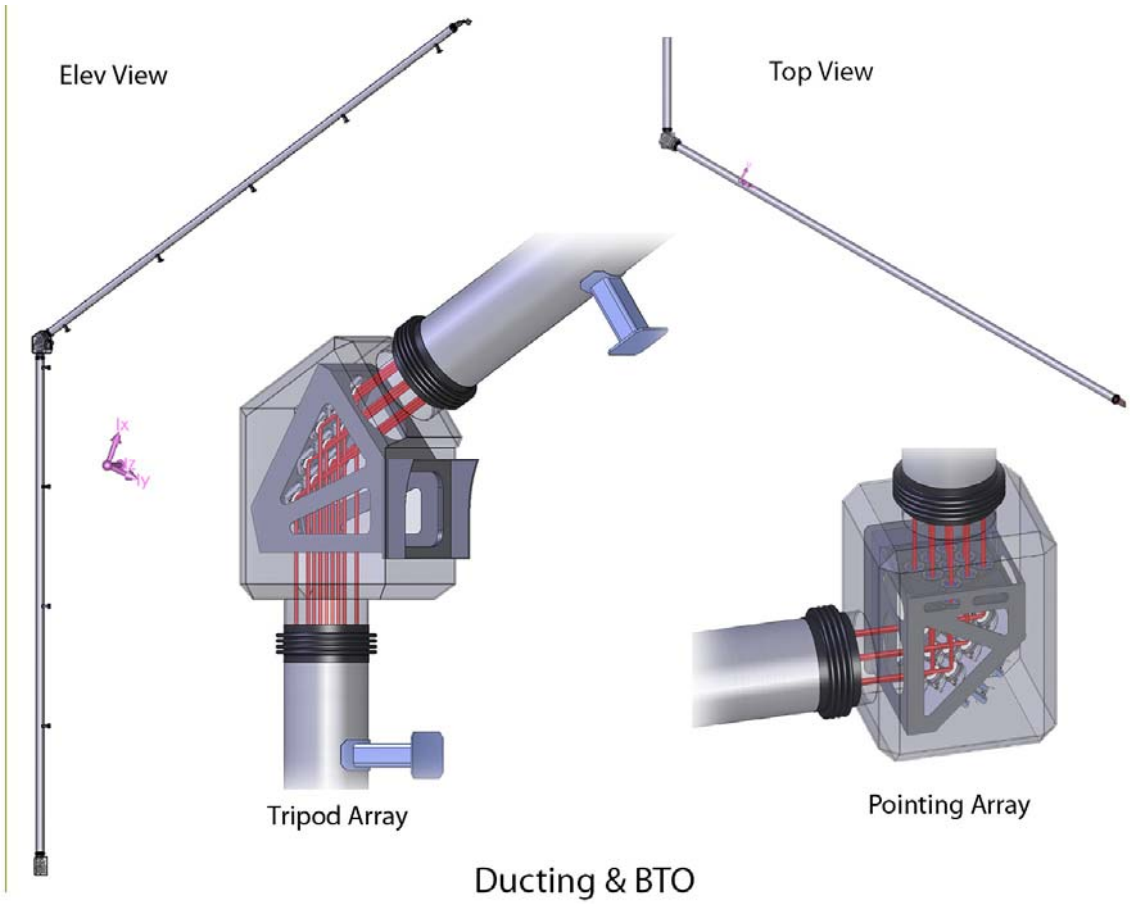

Figure 4.4-5: Model of the Truss Transport Ducting and the two mirror array subassemblies included in this assembly.

Table 4.4-5: Weight and CG of BTO Duct Assembly

Ducting & BTO		**CG location**			**Moment**		
Item	**Wt (kg)**	**X (m)**	**Y (m)**	**Z (m)**	**WX**	**WY**	**WZ**
Duct tubes, Array Enclosures, and Connection Bellows	131.4	-13.55	7.92	10.23	-1780.62	1041.12	1343.97
Duct tubes	92.8						
Pointing Array Enclosure	16.8						
Turning Array Enclosure	19.1						
Bellows	2.7						
Pointing Array	8.0	-16.25	9.35	-4.31	-129.26	74.39	-34.31
Pointing Array Support Bracket	17.2	-16.17	9.42	-4.20	-277.95	161.88	-72.27
Tripod Array	9.1	-16.27	9.39	14.73	-147.60	85.18	133.63
Tripod Array Support Bracket	27.6	-16.07	9.27	14.57	-443.41	255.93	402.17
Ducting Support Brackets	53.2	-11.50	6.64	15.01	-611.58	353.09	797.74
Relay Optics Group 1&2	5.1	-16.25	9.38	-4.05	-83.42	48.16	-20.79
Relay Optics Group 3	2.5	-16.25	9.38	14.38	-41.23	23.80	36.47
Ducting & BTO	**254.1**	**-13.84**	**8.04**	**10.18**	-3515.06	2043.56	2586.61

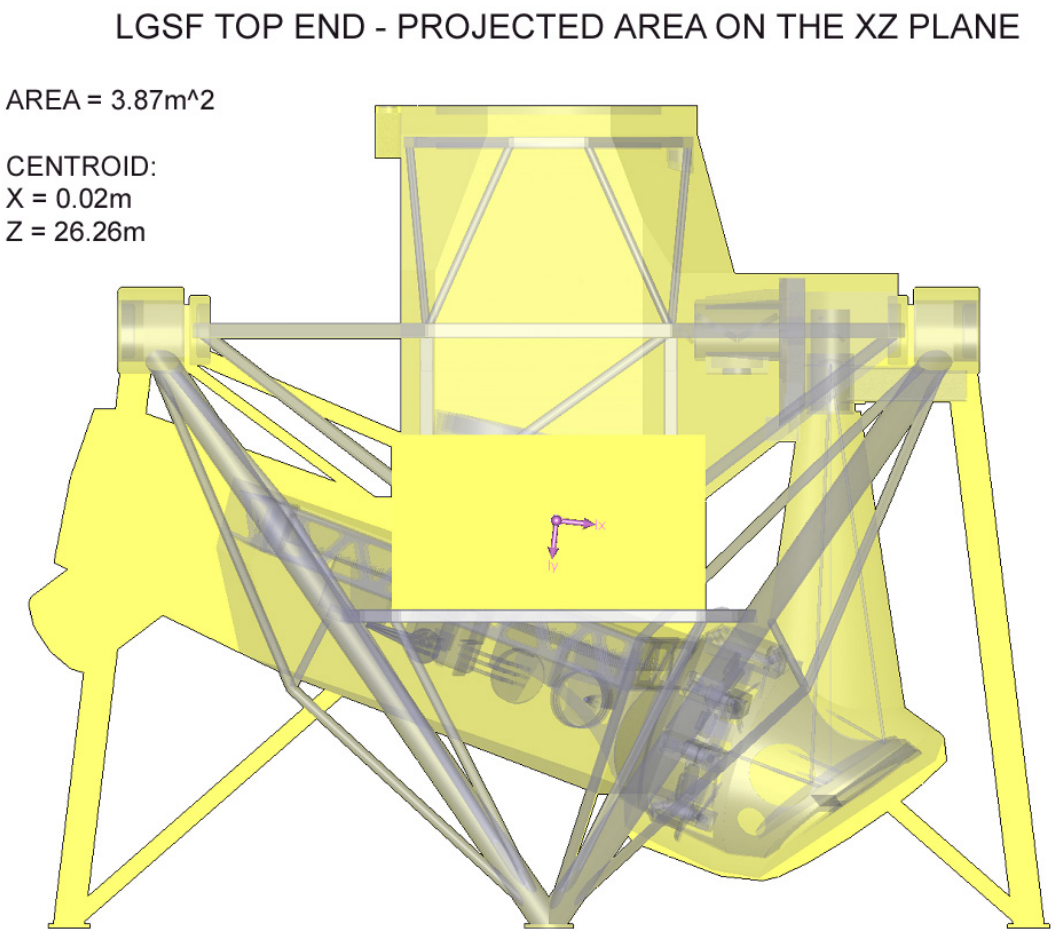

Figure 4.4-6: Projected area of the LGSF Top End Assembly on the XZ plane for the purposes of wind loading calculations.

4.5 Dynamic Analysis of Telescope and LGSF Flexure

With the current conceptual designs for the LGSF and TMT, it is now possible to calculate the displacements and rotations of the LGSF elements due to gravity as the telescope moves over its operational elevation range. This is a necessary prelude to the Final Design Phase to ensure that the Pointing and Centering mirrors are capable of maintaining the correct alignment of the laser beams into the LLT entrance aperture, the design of the LLT tilt mechanism (section 4.1.2.4) is adequate, and that there is no significant displacement or defocus within the LGSF itself. The approach was to assume a linear behavior for calculating the deflections:

- Calculate the deflections for the load case in which one turns gravity on and off with the telescope pointing at the zenith.
- Calculate the deflections for the load case in which one turns gravity on and off with the telescope pointing at a zenith distance of 65º (elevation 25º).

- Linearly combine the two results by subtracting the deflections for the zenith-pointing configuration from those for the 65º zenith distance configuration. These are the results one can anticipate with the telescope at a zenith distance of 65º, provided the LGSF is perfectly aligned when pointing at zenith.

These calculations were carried out for two scenarios:

- With the telescope structure fixed. This will allow us to more easily visualize deflection of the LGSF structure itself without the complication of superimposed telescope flexure.
- With the telescope flexure included. These are the results one would actually use to evaluate the laser beam centering and pointing errors within the LGSF and on the sky, as well as any deterioration in image quality.

4.5.1 LGSF Flexure Analysis Model

The Finite Element model is based from the CAD solid model of the LGSF top end equipment and the fixed tripod array of the BTO. Structural tubing is modeled as beam elements. Solid and plate elements are also employed as needed, primarily in the Diagnostics Bench and the Asterism Generator.

Small scale mechanical devices and structures, such as optics, beam splitters, fold mirrors, and mirror arrays are modeled as lumped masses rigidly attached to nearby structure to which they will actually mount. Thus, their weight is included acting upon the framework, but their own local flexibility is not. The error introduced by this simplification is judged to be small compared with displacements of the structural framework and telescope. The 'breadboard' of the DOB and the main 'bench' of the AG are modeled so the flexure contributions of these items are included.

Non-structural, massless 'pointer' beams (thin red lines) are attached to some of the key optics (M1, M2, Centering Array, Tripod Fold Array, Asterism Generator Fold Mirror, etc.) to aid visualization of optic rotations.

The mass and CG of the FEA model is verified to match the estimated mass budget for all subassemblies as generated by the CAD model.

This report includes a few figures to display the main conclusions of the flexure analysis, as well as a table of the calculated translation and rotation of selected nodes within the LGSF structure. A more complete version of the figures is provided as an ancillary document [6] to this report, in a format which permits the reader to activate an animation of the flexure as gravity varies through its range. In addition, the tables of displacements/rotations are also provided as a separate document [7] in a format which will allow them to be imported into other analysis programs.

4.5.2 Model Overview

Figures 4.5-1 and 4.5-2 provide an overview of the model used in the flexure analysis. Note that the Pointing Array at the base of the vertical truss is *not* included in the analysis, as it is assumed that the effects of telescope flexure on the lower portion of the elevation structure will be small compared to that at the top end. Furthermore, if the LSE is relocated off of the elevation structure (section 5.1), the location of the Pointing Array may change as well. The magenta lines in Fig. 4.5-1 are the "pointer beams" which represent the optical line of sight for an axial input beam (from the Pointing Array into the Tripod Fold Array on the left side of the figure, and into the LLT on the right side). The LGSF is assumed to be perfectly aligned in the gravity-free situation portrayed in Fig. 4.5-1, so the pointer beams match up perfectly.

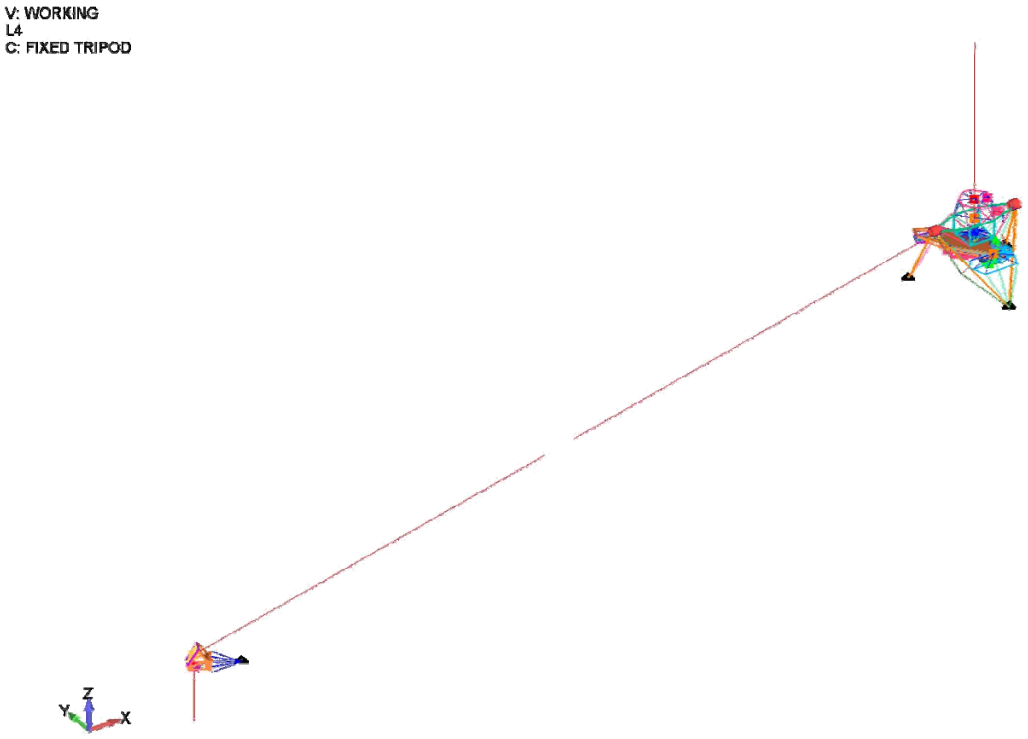

Figure 4.5-1: Overview of the model used in the flexure analysis, showing the Tripod Array at the transition from the vertical to horizontal truss structure on the left and the LGSF Top End Assembly on the right. This illustrates the system in a perfectly aligned gravity-free scenario.

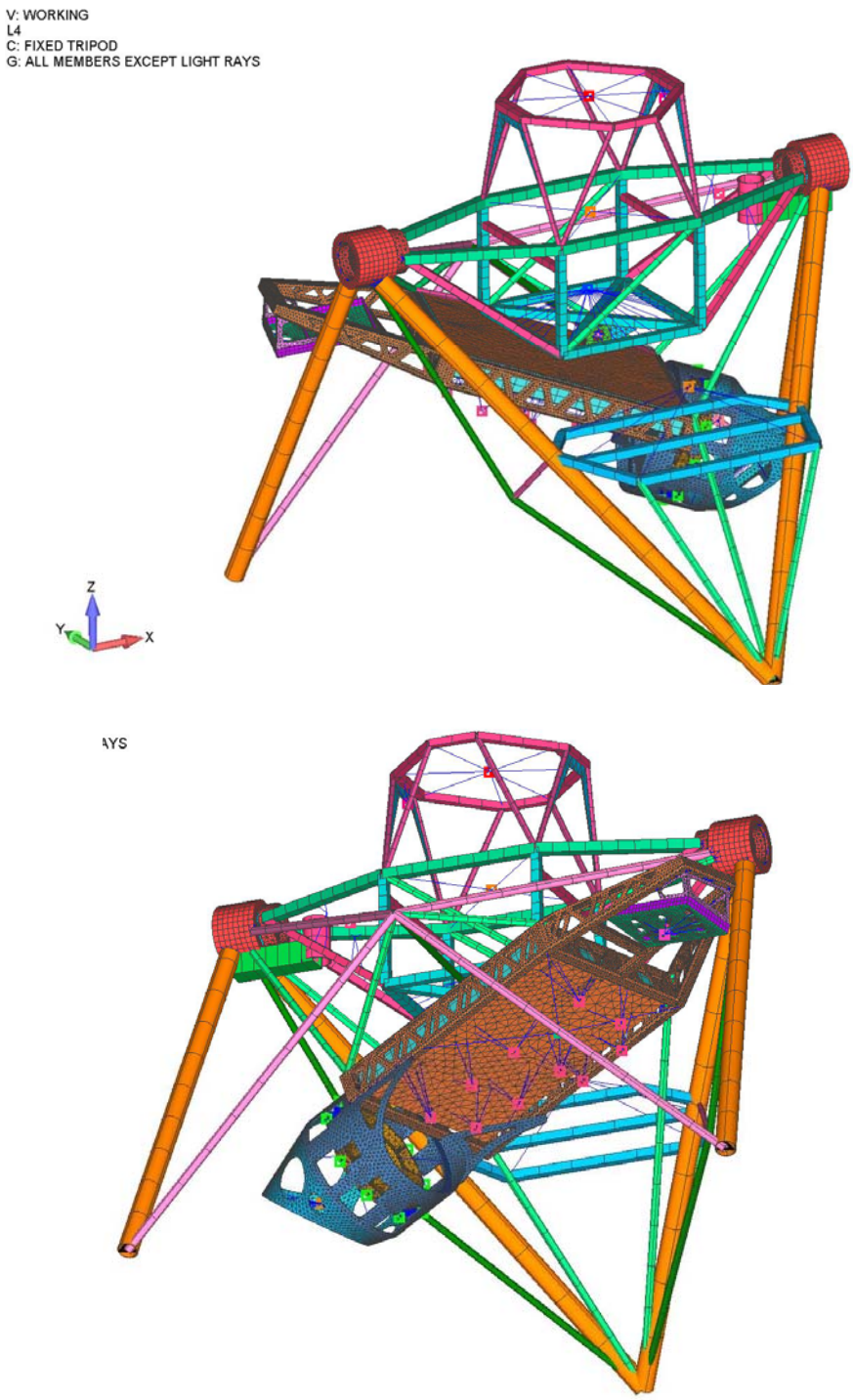

Figure 4.5-2: Two views of the LGSF Top End model, showing the structural members as a series of beam elements. The small colored squares represent the optical elements as lumped masses which affect the structure to which they are mounted but do not flex themselves.

4.5.3 Case 1 – No Telescope Flexure

As noted earlier, the analysis utilizes a linear approach in which the initial configuration illustrated in Fig. 4.5-1 is subjected to loads of 1 g in the –Z direction (corresponding to zenith pointing) and at an angle of 65º to the –Z axis in the Y-Z plane (corresponding to the maximum operational zenith angle of 65º). The results of the deformations were then subtracted to yield the net results on a perfectly aligned LGSF system at zenith after slewing the telescope to a zenith angle of 65º. The individual zenith and 65º pointing deformations are shown in Appendix D [6] in a format which allows animation to make the net motions more discernable.

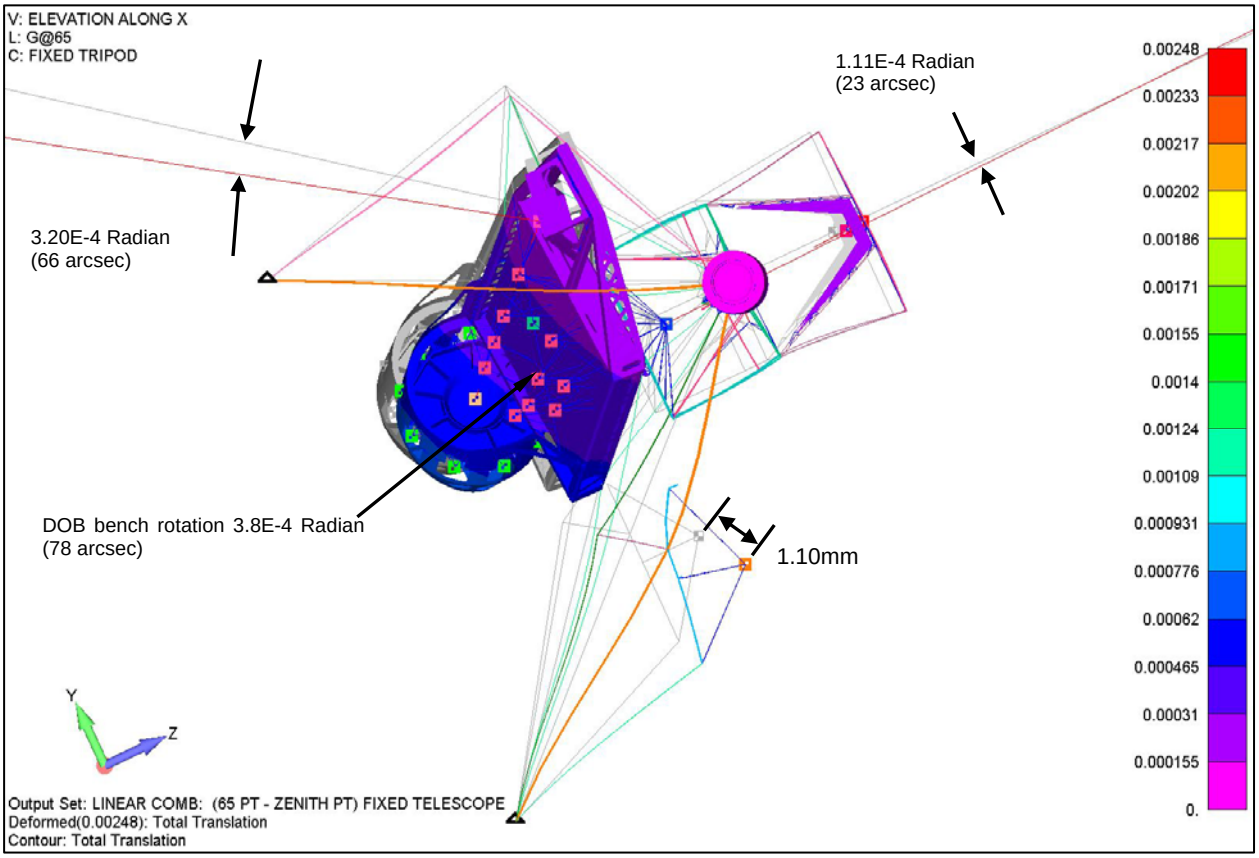

Figure 4.5-3: Net displacements and rotations of several nodes in the LGSF resulting from a telescope motion from the zenith to 65º zenith distance. The light blue lines represent the unloaded structure. Flexure of the TMT structure is not included in this analysis.

The net results are a translation of the structure in the –Y direction and a rotation about the X axis in a manner which deflects the LLT pointing to higher elevation, both driven by the weight of the electronics and the Diagnostic Bench/Asterism Generator assemblies acting below the vertex of the structure which supports the LLT rotation fixture. The results suggest that the flexure within the LGSF Top End structure is relatively small (66 arcsec) and should be well within the correction range of the Top End Centering and Pointing Arrays. The differential rotation of the Diagnostic Bench with respect to the LLT could be reduced by stiffening or improving the geometry of the supporting truss members.

4.5.4 Case 2 – Telescope Flexure Included

The same analysis technique was used to model the LGSF system displacements including the flexure of the telescope, based on the telescope deflections provided by TMT. Not surprisingly, the resulting displacements, shown in Figs. 4.5-4 and 4.5-5, are substantially larger, being dominated by the flexure of the telescope structure. The weight of the M2 assembly, which sits below the triangular truss at the top of the horizontal trusses, results in a substantial translation of the top end as well as a rotational moment which tilts the entire LGSF Top End (including the LLT) to higher elevation angles. The magnitude of this tilt (2.2 mrad) is close to that estimated in the Statement of Work, and is well below the design requirement of 3.0 mrad (Table 4.1-1) for the LLT tilt mechanism. As with the previous analysis, the individual zenith and 65º pointing deformations are shown in Appendix D [6] in a format which allows animation to make the net motions more discernable.

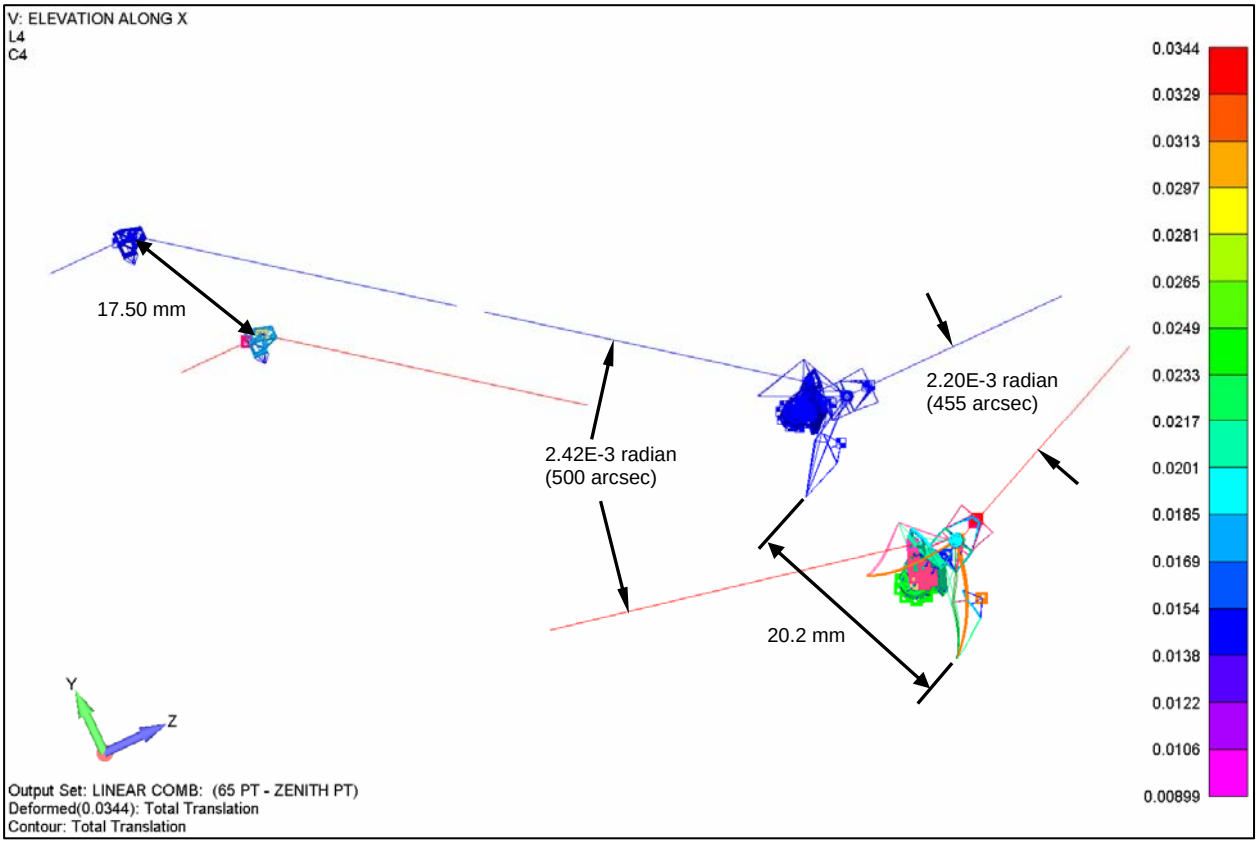

Figure 4.5-4: Net displacements and rotations of the LGSF resulting from a telescope motion from the zenith (dark blue) to 65º zenith distance (multicolored), including the effects of telescope flexure. This view is from a line of sight along the X axis.

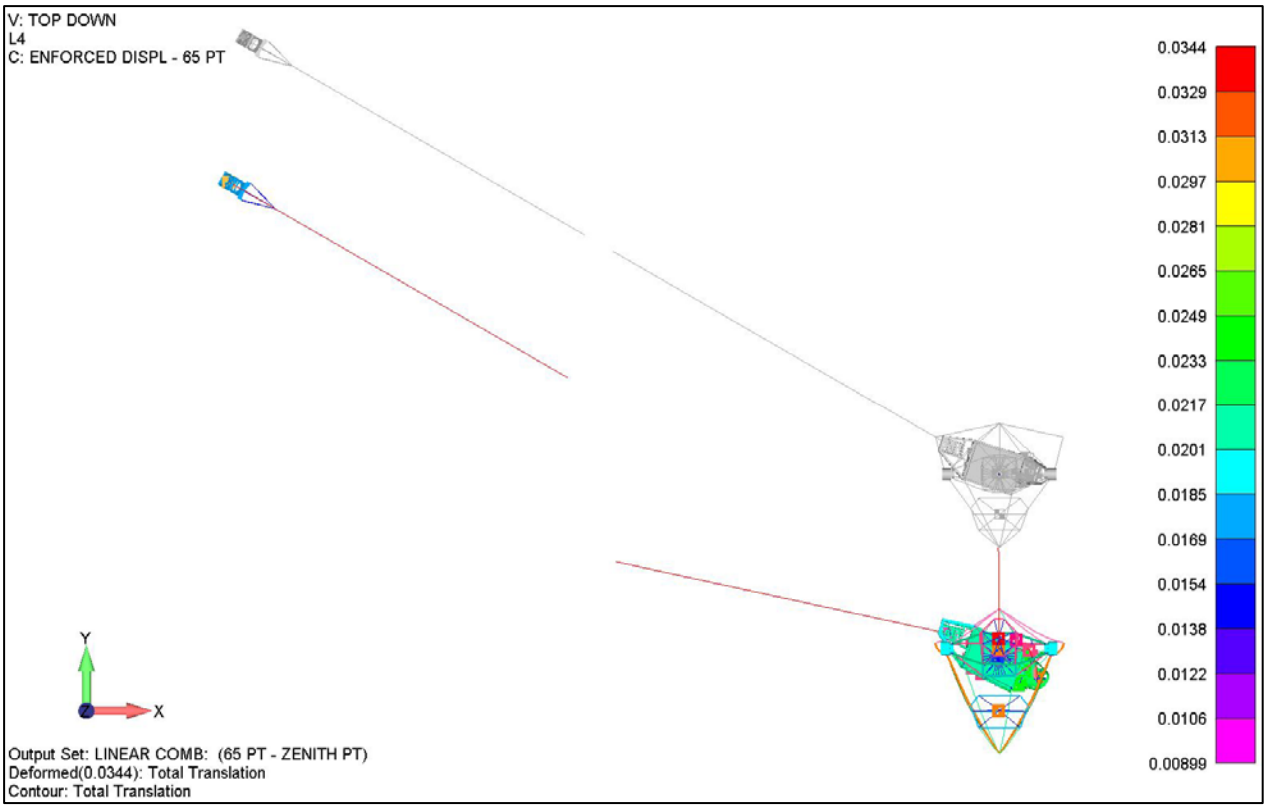

Figure 4.5-5: Net displacements and rotations of the LGSF resulting from a telescope motion from the zenith (grey) to 65º zenith distance (multicolored), including the effects of telescope flexure. This view is from a line of sight along the Z axis.

Below we provide the results for a number of key nodes within the LGSF system (Fig. 4.5-6) as a table of displacements T1, T2, and T3 (meters) along the X, Y, and Z axes, respectively, and rotations R1, R2, and R3 (radians) about the X, Y, and Z axes. This table is for the load case of telescope motion from zenith to 65º zenith distance, including the telescope flexure. The complete tabular summary is provided in Appendix E as a separate document [7].

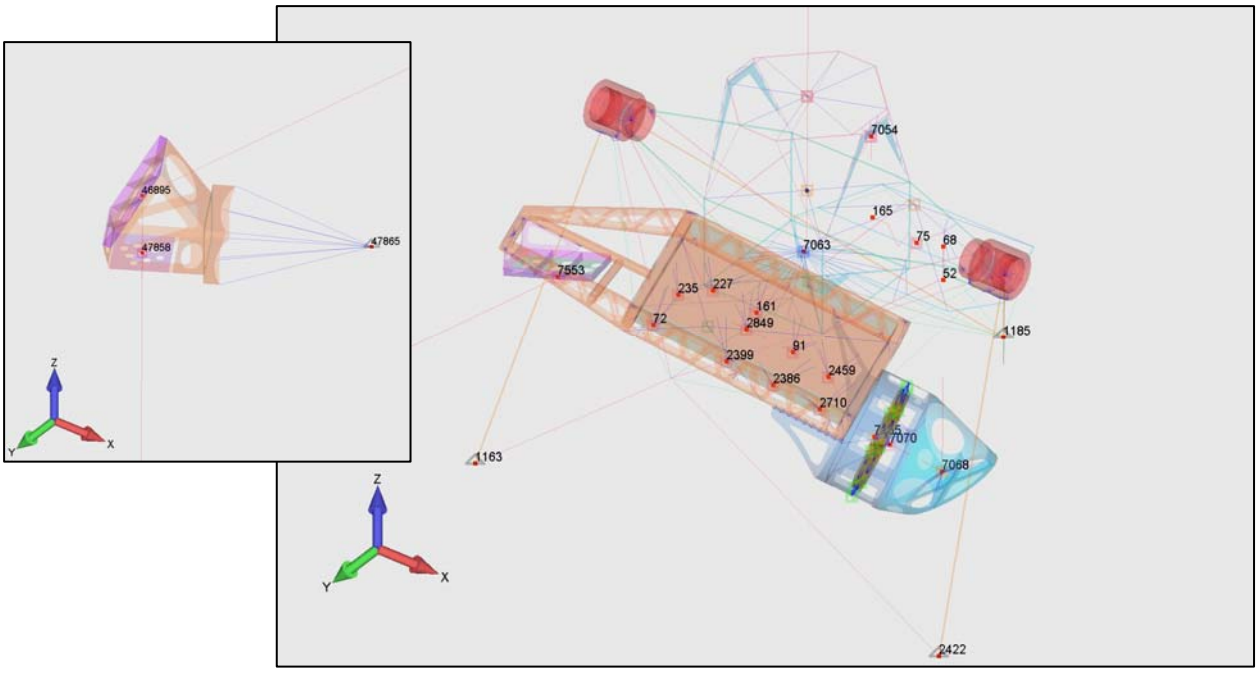

Figure 4.5-6: Illustration of the key nodes within the LGSF Tripod Fold Array (inset at left) and Top End Assembly (main panel) for which flexure displacements are given in Table 4.5-1.

Table 4.5-1: Displacements (m) and Rotation (radians) at Key LGSF Nodes

LOAD CASE		65deg Pointing - Zenith Pointing						
SUBASSEMBLY	ITEM	NODE	T1	T2	T3	R1	R2	R3
BTO	RELAY OPTICS LENS 3 GROUP	47858	-1.87E-03	-1.54E-02	8.12E-03	3.78E-06	4.08E-07	1.72E-06
BTO	TRIPOD FOLD MIRROR ARRAY	46895	-1.87E-03	-1.54E-02	8.12E-03	4.72E-06	-5.38E-07	3.18E-06
DOB	ACTIVE CENTERING MIRROR ARRAY	7553	-5.74E-05	-2.02E-02	2.69E-03	-2.42E-03	-5.50E-05	-8.80E-06
DOB	QUARTER WAVE PLATE ARRAY	72	-4.00E-05	-2.07E-02	3.06E-03	-2.46E-03	-8.19E-05	1.83E-05
DOB	FLIP OUT FOLD MIRROR	2339	-1.80E-05	-2.12E-02	3.57E-03	-2.48E-03	-8.18E-05	2.53E-05
DOB	BEAM SPLITTER 2 ARRAY	2386	-2.66E-05	-2.10E-02	3.37E-03	-2.48E-03	-8.48E-05	2.23E-05
DOB	BEAM DUMP ARRAY	2710	-8.76E-06	-2.14E-02	3.76E-03	-2.48E-03	-8.30E-05	2.61E-05
DOB	FOLD MIRROR 3	161	-1.58E-05	-2.10E-02	4.41E-03	-2.47E-03	-9.55E-05	2.11E-05
DOB	FOLD MIRROR 2	91	-9.49E-06	-2.12E-02	4.26E-03	-2.48E-03	-9.45E-05	2.30E-05
DOB	BEAM SPLITER 3	2849	-1.93E-05	-2.10E-02	4.06E-03	-2.47E-03	-9.06E-05	2.04E-05
DOB	NEAR FIELD CAMERA	235	-3.27E-05	-2.07E-02	3.77E-03	-2.47E-03	-8.98E-05	1.84E-05
DOB	FAR FIELD CAMERA	227	-2.46E-05	-2.08E-02	4.22E-03	-2.47E-03	-9.39E-05	1.76E-05
AG	AG CENTERING ARRAY	7155	1.40E-05	-2.17E-02	4.01E-03	-2.58E-03	-2.20E-04	2.75E-05
AG	35 ARCSEC FOLD MIRROR ARRAY	7070	2.12E-05	-2.17E-02	4.10E-03	-2.59E-03	-2.26E-04	1.75E-05
AG	AG OUTPUT FOLD MIRROR ARRAY	7068	4.44E-05	-2.20E-02	4.37E-03	-2.58E-03	-2.23E-04	3.25E-05
TOP END FRAME	COLLIMATING LENS GROUP	52	-2.68E-05	-1.95E-02	4.24E-03	-3.18E-03	3.09E-04	2.42E-04
TOP END FRAME	COLLIMATOR GROUP FOLD MIRROR	68	3.30E-05	-1.89E-02	4.25E-03	-3.18E-03	3.09E-04	2.42E-04
TOP END FRAME	K MIRROR GROUP	75	1.03E-05	-1.90E-02	4.25E-03	-2.18E-03	1.11E-04	8.66E-05
LLT	K MIRROR GROUP FOLD MIRROR	165	1.48E-05	-1.89E-02	4.28E-03	-2.18E-03	1.11E-04	8.66E-05
LLT	M2	7054	-3.52E-05	-1.79E-02	4.30E-03	-2.29E-03	-6.20E-05	-1.98E-05
LLT	M1	7063	-1.65E-05	-1.97E-02	4.28E-03	-2.20E-03	-1.58E-05	2.68E-05
BTO	CONNECTION POINT TO TELESCOPE	47865	-0.00187	-0.01537	0.008122	1.59E-06	-8.4E-06	-5E-06
TOP END FRAME	CONNECTION POINT TO TELESCOPE	1163	-4E-05	-0.02219	0.00237	-3.7E-05	4.87E-06	6.23E-06
TOP END FRAME	CONNECTION POINT TO TELESCOPE	1185	1.94E-05	-0.02221	0.00726	-3.2E-05	-5.2E-07	3.9E-09
TOP END FRAME	CONNECTION POINT TO TELESCOPE	2422	7.66E-05	-0.0222	0.00247	-3.7E-05	-6E-06	-6.4E-06

4.5.5 Conclusions of Flexure Analysis

The net results of the flexure analysis yield a displacement of the LGSF Top End structure of approximately 20 mm and a rotation of the LLT axis of approximately 2.2 mrad, not very different from the rough estimates provided in the Statement of Work of 15 mm and 2.0 mrad, respectively. Nonetheless, over the approximately 19 m lever arm represented by the horizontal truss members, this degree of rotation represents a significant (~46 mm) displacement of the line of sight over this distance, raising the concern that the laser beams could move off of the 50 mm diameter mirrors. However, the graphical illustrations in Figs. 4.5-4 and 4.5-5 are somewhat pessimistic, in that they represent an extrapolation of the internal lines of sight of the Tripod Fold Array and Top End Assembly. Since the actual laser beams propagate up the vertical truss, through the Tripod Fold Array and to the Top End, the relevant displacement is the much smaller transverse displacement of the Top End with respect to the Tripod Fold Array pointing beam. The large 2.42 mrad rotation of the Top End Assembly can be compensated by a tilt of the mirrors in the Pointing array by half that amount.

The answer to this issue would require a more rigorous treatment of the optical beam, including the effect of the relay lenses, traversing the displaced and rotated nodes in the LGSF. This was originally part of this study, but the recent decision to consider a relocation of the LSE and the ducting geometry between it and the Centering Array on the telescope structure (section 5.1) makes an optical study of limited value at this time, since it would need to be repeated for the revised geometry.

The other offshoot of the flexure analysis is the rather large differential rotation of the Diagnostic Bench/Asterism Generator with respect to the LLT under lateral loads, due to the shallow angle geometry of the supporting truss members. We recommend that these members be stiffened or their geometry improved in the Final Design phase of the project.

4.6 Modal Analysis of Seismic Events

In addition to the gravitational flexure, we also calculated the lower modal frequencies of the LGSF structure (not including the telescope) to establish the sensitivity of the structure to earthquake loads based on the response spectrum provided by TMT. The geometry of the three lowest modal frequencies are described below and illustrated in Figs. 4.6-1 through 4.6-3. As with the flexure analysis, animated versions of these figures can be found in Appendix D [6]. The response curve provided by TMT (Fig. 4.6-4) is for a "lifetime seismic event" modeled at the TMT M2 assembly.

Mode 1 (f_1 = 13.9 Hz): This is a side-to-side motion of the truss members supporting the electronics, amplified by the large weight (265 kg) of the electronics cabinets themselves. This drives a twisting motion of the two flexures supporting the LLT (Fig. 4.6-1).

Mode 2 (f_2 = 16.0 Hz): This is a motion in the Y direction of the truss members supporting the electronics, also resulting from the large weight of the electronics. This drives a tilt motion of the LLT structure in the same direction (Fig. 4.6-2). Stiffening the portion of the space frame

which supports the electronics boxes will increase both f_1 and f_2, reducing the excitation which might be produced by the wind loading spectrum.

Mode 3 (f_3 = 20.8 Hz): This is a rocking motion of the Diagnostic Bench/Asterism Generator subassembly which also drives a small motion of the LLT frame (Fig. 4.6-3). Modification of the members supporting this subassembly (section 4.5) could increase the frequency of this mode.

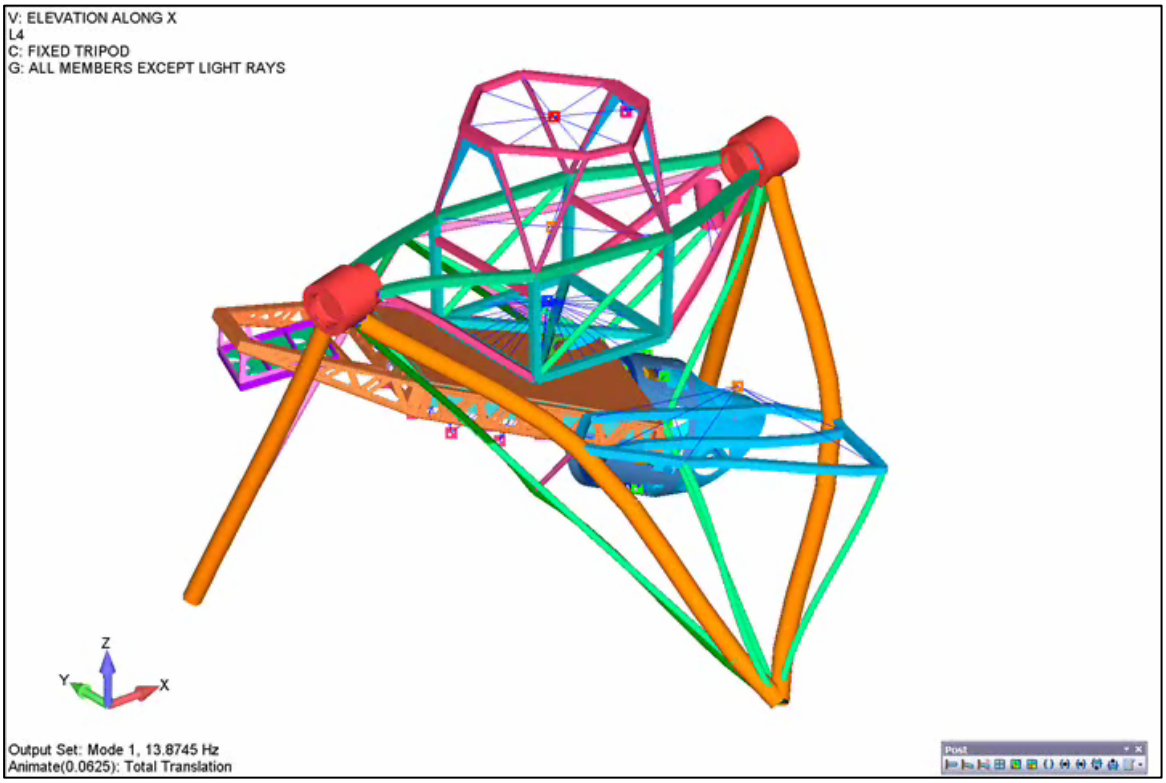

Figure 4.6-1: Illustration of the structural deformation corresponding to Mode 1 (f = 13.6 Hz), which is primarily a side-to-side motion of the electronics cabinets and support frame.

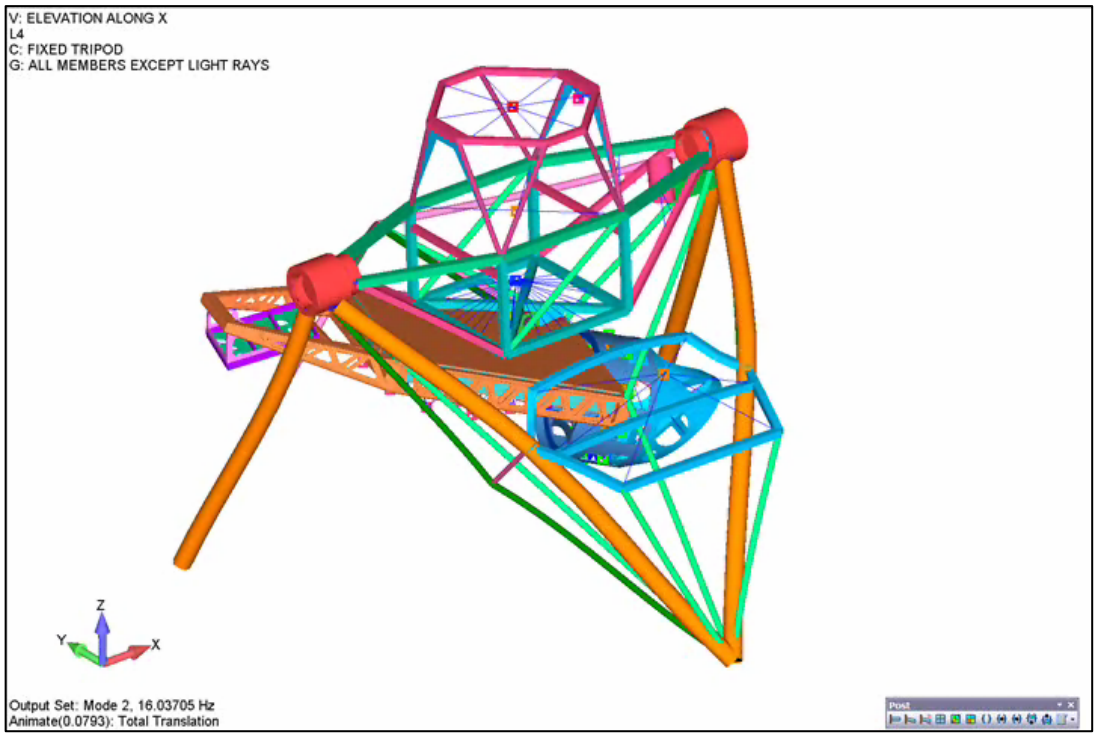

Figure 4.6-2: Structural deformation corresponding to Mode 2 (f = 16.0 Hz), primarily a ±Y direction motion of the electronics cabinets and support frame.

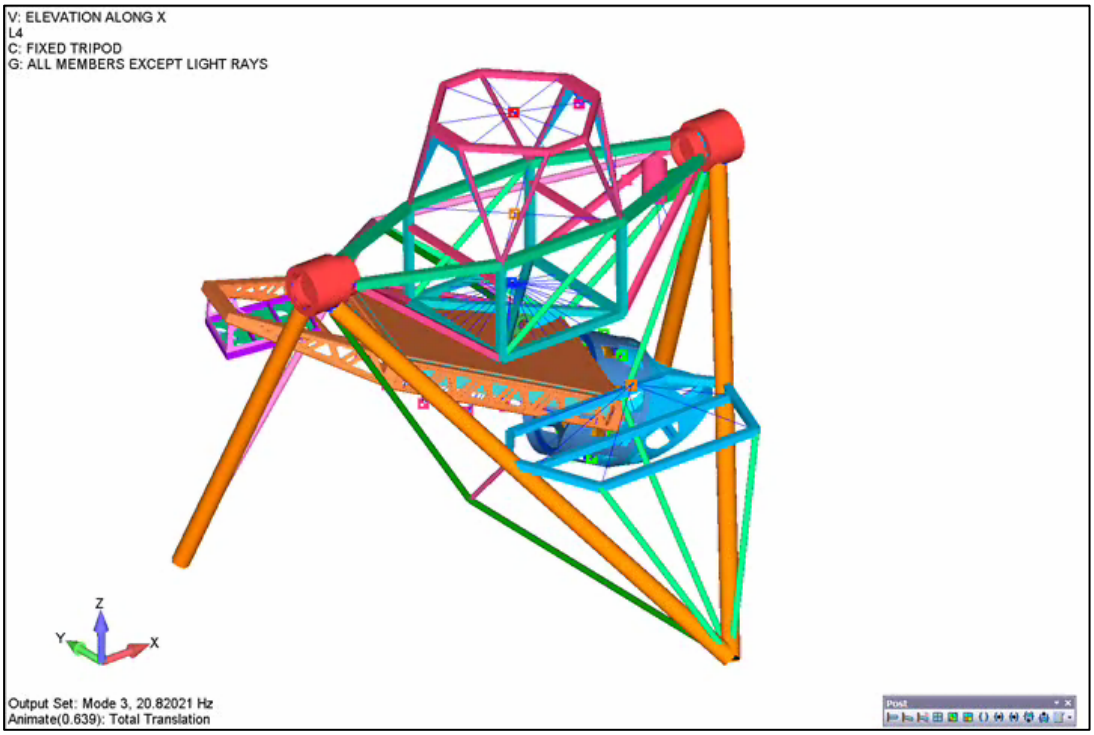

Figure 4.6-3: Structural deformation corresponding to Mode 3 (f = 20.8 Hz), a rocking motion of the Diagnostic Bench/Asterism Generator subassembly.

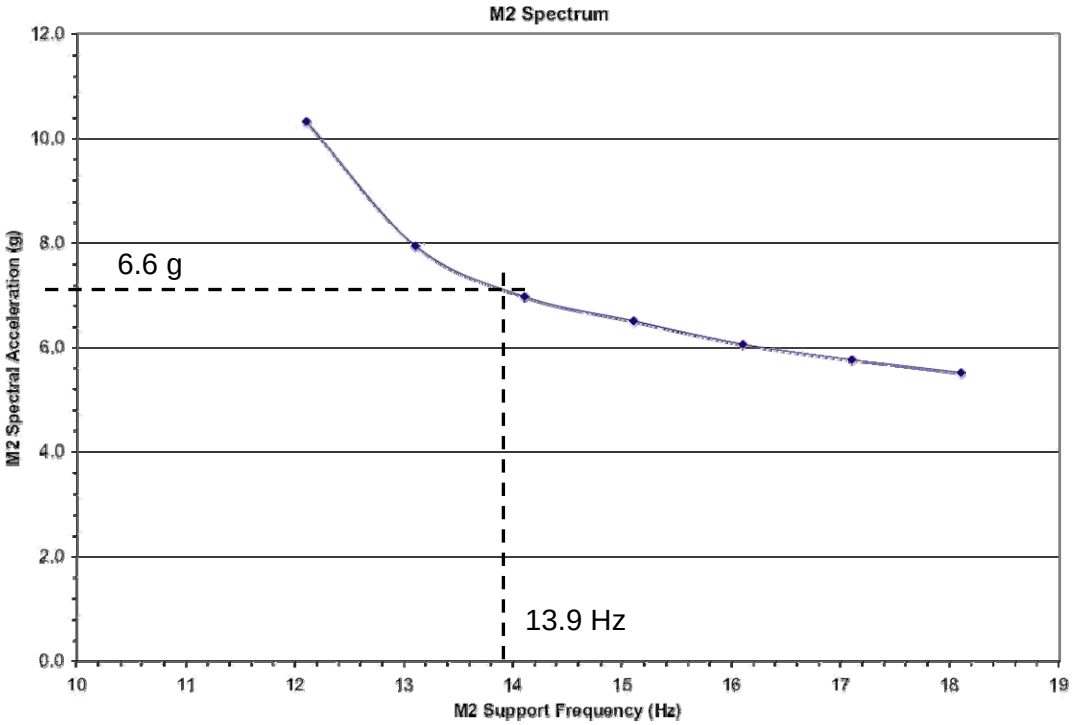

Figure 4.6-4: Response curve for the TMT top end (courtesy Dynamic Structures) for a "lifetime seismic event". The acceleration for the lowest LGSF mode at 13.9 Hz is 6.6 g.

The response curve in Fig. 4.6-4 shows the magnitude of the amplification of the primary seismic accelerations (0.8 g for input seismic periods in the range $0.1 < T < 0.45$s) by the telescope structure. Unfortunately, the response curve is sufficiently flat above ~ 15 Hz that even significant stiffening of the LGSF structure is unlikely to reduce the local accelerations below 5 - 6 g.

Because the mechanical amplification of the seismic input occurs within the telescope structure, changes in the design of the BTOTE are unlikely to reduce local accelerations much below those in Fig. 4.6-4. As noted in the last section, stiffening of the space frame supporting the electronics boxes will increase the frequencies of the lowest modes, but this would not appreciably lower the seismic loads. It is virtually certain that a major earthquake would require realignment of the LSGF optics (and most likely TMT itself) and possibly repair/replacement of some elements of the mechanical structure. The emphasis in the Final Design phase should be to minimize potential damage to elements within the LGSF and hazards to Observatory personnel or the telescope from pieces breaking off of the LGSF during an earthquake. Padded "earthquake clips" around the LLT M1 (which would not touch the mirror during normal use) could reduce the possibility of damage to that delicate (and massive) element. Safety clips or chains at other delicate points such as the LLT tilt drive flexure or the flexures supporting the

LLT space frame would provide some redundant support should the flexures bend or break during the event.

4.7 Accessibility

The conceptual designs for the TMT Enclosure and the telescope itself have reached a sufficiently mature stage that it is necessary to consider in the design of the LGSF the constraints imposed by the real observatory infrastructure. These constraints include those imposed by the various handling or access features (cranes, lifts, platforms) planned for the observatory on the lifetime operations such as:

- Initial installation of the LGSF on TMT
- Removal/reinstallation of subsystems of the LGSF for repair or upgrade
- Access to the various subsystems of the LGSF for routine maintenance
- Avoiding conflicts with other TMT systems (e.g., M2 supports or electronics) when carrying out the above steps

Since we are still in the conceptual design phase, it is premature to present specific designs that are more appropriately considered in the detailed design. However, we can address general aspects of how one would install and access the LGSF subsystems and identify necessary features (fixtures, lift points, etc.) and interfaces which will have to be kept in mind as the project progresses.

Appendix C presents a spreadsheet (courtesy C. Boyer) which is an initial compilation of the access and handling requirements for the LGSF subsystems. This is a living document which should be continuously updated as the design of the telescope progresses; in particular, it specifies a number of ICDs between the LGSF and various enclosure facilities which will need defining in the future.

From the viewpoint of accessibility, we discuss general LGSF "subsystems", which are defined more by geometry and physical location rather than function:

- Laser Service Enclosure (LSE): This has been defined previously. Given the probable change in location (section 5.1), we will discuss this in quite general terms.
- LGSF Vertical Path: This includes the beam path from the LSE through the Truss Pointing Array and up the vertical truss to the Tripod Fold Array at the junction of the vertical truss and tripod leg. The relay lenses would be included in this path, along with the electronics for the Truss Pointing Array and the prealignment cameras at the Tripod Array location. Access occurs with the telescope at zenith.
- LGSF Tripod (Horizontal) Path: This includes the beam path between the Tripod Fold Array and the BTO Top End. With the relocation of the Truss Centering Array onto the Diagnostic Bench Structure (Fig. 4.4-2), this region of the beam path should have no elements requiring periodic maintenance, unless the decision is made to access the Tripod Array and the associated prealignment cameras with the telescope pointing at the horizon.

- LGSF BTO Top End: This includes all of the Top End subassemblies, such as the Truss Centering Array, Diagnostic Bench, Asterism Generator, LLT, and electronics. Access is with the telescope pointing at the horizon.

4.7.1 Installation and Removal

4.7.1.1 LSE

Given the currently indeterminate location for the LSE, detailed comments would be purely speculative. The final location will require hard mounting points for the three Laser Systems, the Switchyard and (probably) electronics racks because of their weight and the requirement for mechanical stability. The LSE itself will probably be separately supported and will in effect be a clean enclosure for the Lasers, Switchyard, and electronics. Depending on its location, one of the walls or the roof (or a significant portion) will need to be removable to permit the installation or removal of the Laser Systems and electronics. The details will clearly depend on the location and whether the access is from the top or the side. Access from the side could pose challenges because of the size and weight of each of the Laser Systems.

4.7.1.2 LGSF Vertical and Horizontal Path

The beam ducting, access boxes, and mirror array supports (Fig. 4.4-5) will probably bolt onto bosses on the telescope truss, so initial installation can be done using the dome crane. Except for major damage, it should not be necessary to remove any of these assemblies. The Elastomer bellows between the access boxes and tubing sections may need replacement at infrequent intervals if damaged or worn out. The access boxes themselves should have removable panels (or hinged doors, which do not need to be completely removed) large enough to permit full access to the mirror/lens assemblies and the prealignment cameras for installation; the lenses/mirrors can be individually installed within the enclosures.

4.7.1.3 LGSF Top End Assembly

The current plans for assembly, integration, and test [2] call for the LGSF to be assembled and tested at the vendor facility prior to shipment to the observatory. This can be carried out with only one of the three Laser Systems and, although the full path length from the Laser Switchyard to the BTO Top End must be replicated, space constraints will likely prohibit a straight path on the truss routes. Therefore, two of the Laser Systems, the LSE itself, and the BTO truss ducting will probably be shipped directly to the observatory site.

The LGSF Top End components will be assembled and tested on the actual framework which will eventually be installed on the TMT top end. Furthermore, after the pre-ship testing is complete, the safest and most efficient strategy is to ship the entire assembly as a unit, with appropriate precautions. For example, one would remove all of the optical elements, particularly those with delicate AR coatings to prevent damage from the environment during shipping, and

delicate mechanical linkages such as the LLT flexure drive would be removed and replaced by staybars.

There is an extensive body of experience at the Gemini Observatory (among others) in the transport and installation of instrumentation of a size (1.5 m on a side) and weight (2000 kg) similar to that of the LGSF Top End Assembly. Furthermore, Gemini instrumentation is installed in a horizontal orientation, as will the LGSF Top End Assembly (dome clearance and obvious safety considerations preclude installation with the TMT at zenith). An outline of possible procedures for the LGSF Top End Assembly follows:

- The strategy for assembling, testing, shipping, and installation/removal of the LGSF Top End Assembly would be founded on a heavy-duty cart, probably a square-frame with large casters. This cart would have a trunnion subassembly carrying a frame (to which the Top End Assembly would mount) which could rotate from an upright to a horizontal orientation. In addition to the casters for rolling, the cart would have lift points to permit it to be craned into a shipping container, where it would be supported by inflatable air shocks to minimize g-forces during shipping.
- The Top End Assembly (Fig. 4.4-4) would rest on its three mounting pads during the assembly and integration process. A removable triangular frame (not shown in the Figure) would bolt to the support legs to hold them firmly in position whenever the assembly is not mounted on the TMT. All of the optomechanical and electronic subassemblies would be installed in the Top End at this point, and initial testing of the assembly can be carried out.
- For optical testing of the BTO, it will probably be desirable to have the assembly in a horizontal orientation for access to the output of the LLT for optical evaluation or the use of large flat mirrors for collimation. The Top End Assembly would have lift points which permit it to be craned into the cart and bolted into the frame using the three installation pads in a vertical orientation. The frame can then be oriented horizontally for optical testing or to arbitrary attitudes for flexure testing and a first-order calibration of the BTO Centering and Pointing Arrays.
- The Top End Assembly can be shipped to the post-ship assembly and test facility near the observatory in the cart in a vertical orientation. As noted above, delicate optics will be removed prior to shipping, and the LLT and electronics may also be removed and shipped separately. Depending on the actual installation schedule and the desire to test LGSF at the post-ship assembly location, the final optics may or may not be installed prior to shipping the assembly to the observatory.
- At the observatory, the cart can be moved onto the M2 access floor with the TMT in the horizon pointing orientation and the frame rotated so the Top End Assembly is also in a horizontal orientation. The assembly can then be lifted from the cart, using a set of lifting points specific to a horizontal orientation, by the dome crane and installed onto the M2 frame with the three mounting pads. The triangular frame staybar can then be removed.

4.7.1.3.1 LLT Removal

Except in the case of a major breakdown within the Top End Assembly or major rework of the M2 hexapod, it should not be necessary to remove the assembly from the telescope. Access for replacement or maintenance of the BTO elements should be possible with the assembly in place (section 4.7.2). However, in the event of a problem with one of the LLT optics, it may be advantageous to remove the LLT itself from the Top End Assembly. Since the LLT is mounted in a separate space frame for the flexure tilt correction, special lift points can be designed onto the LLT for this purpose. This would be carried out with the TMT in the horizon pointing orientation, using the dome crane. An LLT handling cart (which may be built in any case during the construction phase of the project) will be used for storage and transport of the LLT when it is removed from the telescope. Depending on the reach of the dome crane, the location of the LLT closer to the edge of the enclosure may require a special spreader bar (Fig. 4.7-1).

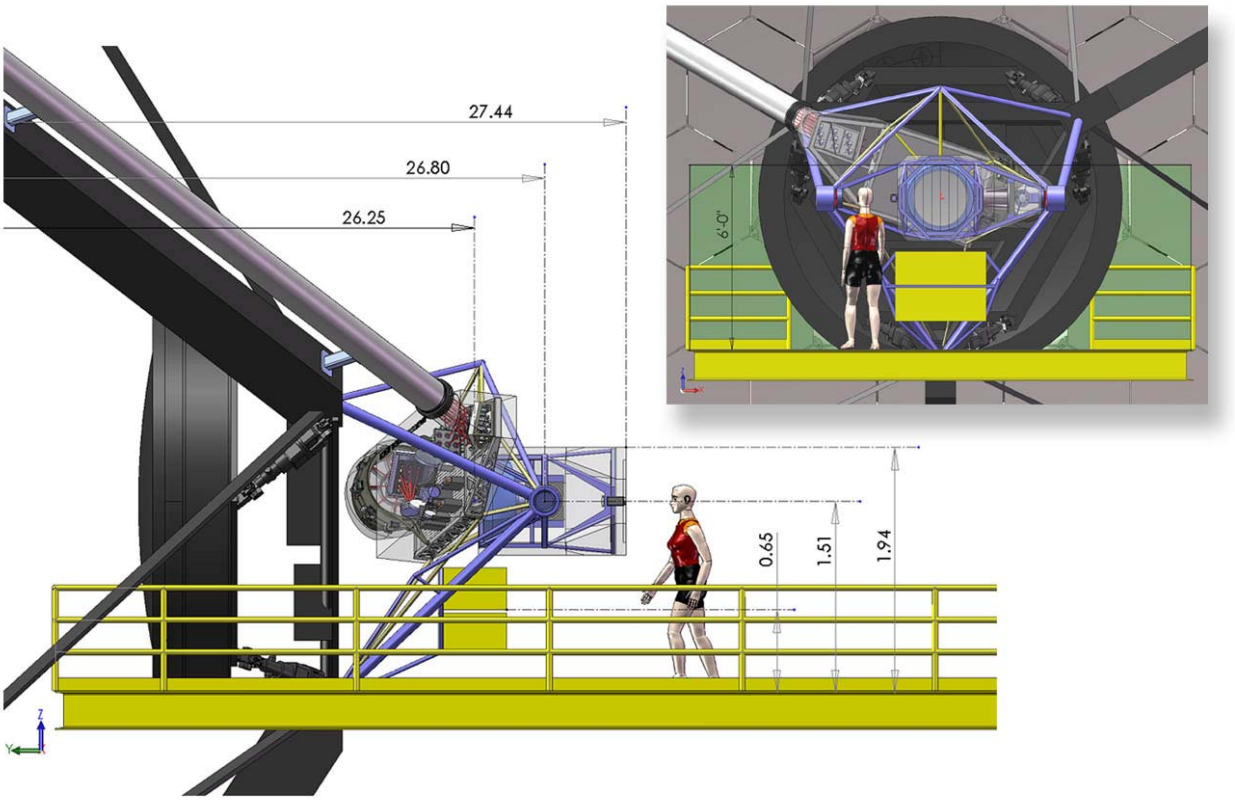

Figure 4.7-1: Layout of the M2 access platform (olive green, extending from right) in relation to the TMT and the LGSF Top End Assembly. The three dimensions noted are the distance from the center of the enclosure to the CG of the Top End Assembly, LLT, and LLT Window, respectively, and represent the required reach of the dome crane to access each of these subassemblies.

4.7.1.3.2 LLT Window

Although the LLT window is easily accessible for cleaning on a regular basis, it may be necessary to remove it in the case of extreme contamination, damage, or contamination on the inside surface. The LLT window is sufficiently light to not require the dome crane (and the greater reach to reach the window), but safety considerations dictate against a reliance on purely human lifting for removal or installation of an expensive optical element. The window should either be supported by a rolling boom crane or in a special cart with a hydraulic lift while it is being installed or removed.

4.7.2 Routine Maintenance

4.7.2.1 LSE

The LSE is designed for frequent (daily) access by maintenance personnel for carrying out any required work on the Laser Systems, electronics, or Switchyard. In its current on-telescope location (Fig. 2.3-1), the only constraint is that the telescope be in a zenith pointing condition, both for physical access to and working inside the LSE. With the LSE moved off of the telescope elevation structure (section 5.1), then more general access may be possible.

4.7.2.2 LGSF Vertical and Horizontal Path

Access to these areas, particularly the two enclosures housing the Truss Pointing Array and the Tripod Fold Array (as well as the relay lenses), will be necessary at moderate intervals for cleaning the optical elements. The frequency of such maintenance will be determined empirically during the telescope operation; at Gemini, this is carried out prior to each LGS observing run. In addition, access is required in the event of a mechanical problem with one of the mirror mounts or an issue with the Truss Pointing Array electronics assembly, which will be installed nearby [2].

The Truss Pointing Array enclosure and associated electronics will probably be accessed with the telescope at zenith, possibly from the enclosure mounted crane with a basket. The Tripod Fold Array enclosure has no active elements and should (ideally) require electronic maintenance at less frequent intervals. To clean the fixed mirrors, L3 relay lenses, or the prealignment cameras, this area would probably be accessed with the telescope horizon pointing, also using the enclosure mounted crane (TBD).

4.7.2.3 LGSF Top End Assembly

Physical access to the Top End Assembly will be quite easy from the access platform (Fig. 4.7-1). For a standard 1.62 m person standing on the access platform, the center of the LLT will be close to eye level. Therefore, physical access to the “higher” portions of the assembly, such as the Truss Centering Array or Diagnostic Bench, will require some additional elevation, such as a small ladder or retractable steps built into the platform. Conversely, some of the electronics will be too low for comfortable access, unless one sits on the (probably cold) platform.

Additional safety issues arise in the first case. The existing railing, which appears to be approximately 1 m high, is adequate for a person walking on the platform, but may be inadequate if personnel are standing on ladders or steps, unless the horizontal dimension of the platform is sufficiently large that a fall would not place one in danger of falling off the side of the platform. In addition, there is a cutout in the platform to clear the M2 assembly which would be nearly under someone working on the Diagnostic Bench. It is premature to propose specific access methods, only to point out that the need exists and that a safety review of any proposed access aids such as steps or ladders will be necessary.

General comments which we can make at this point in the design include:

- Access panels need to be large, particularly to gain access to all of the mirrors in the Asterism Generator for cleaning/replacement. Personnel will probably be dressed for cold weather.
- Space may preclude the use of hinged access panels. Need to have some way to avoid dropping panels off of the elevated platform (safety, damage to panel).
- Need to use captive fasteners on access panels
- Need to determine maintenance requirements for the electronic components; is it necessary to slide electronics out of rack? Use extender boards? Do we need to access the backplane?
- Require AC power either at TMT top end or on access platform to run any diagnostic electronics.

5.0 Future Directions

5.1 LSE Redesign and Relocation

The current location of the LSE on the telescope elevation structure poses a number of potential system-level problems in the design and operations areas. The most obvious is that the large size and weight of the current 50W sodium lasers and associated electronics (of which there will be three in the first light TMT configuration) necessitates a large, heavy enclosure. The LSE must be reasonably clean (for optics cleanliness), enclosed (to permit maintenance on the lasers without danger to other observatory personnel in the dome), and capable of extracting any heat from the lasers or electronics which is not removed by liquid cooling lines to meet the heat dissipation requirements. This structure has implications for the telescope weight and balance, requiring a compensating mass on the other side of the telescope for balance, and it will contribute to the wind loading on the telescope. Maintenance personnel could access the lasers and electronics only at zenith pointing, thus possibly limiting other daytime maintenance efforts. The only significant advantage of mounting the LSE on the telescope structure is the fixed beam transport path from the LSE to the telescope top end.

The possibility of moving the LSE from the telescope elevation structure to a fixed but nearby location has been discussed for some time and since the beginning of work on this contract, the TMT project has decided to seriously consider this step. Proposed locations are one of the Nasmyth platforms or a site on the azimuth structure below the telescope itself, with the latter

being more favorably considered. If implemented, as seems likely, the current LGSF concept will need modification, at least in the portion between the LSE and the current location of the pointing array at the bottom of the vertical telescope truss member.

We note these developments for completeness, but emphasize that this issue goes beyond the scope of this report, which was limited to completing the design of the top end of the LSGF with consideration of the effects of telescope flexure. To first order, this design should not be significantly dependent on a relocation of the LSE, with the exception of a revision of the relay lens design to accommodate the (presumably) greater path length from the LSE to the LLT input pupil.

5.1.1 Deployable Transport Ducting

Barring technical advances such as the development of hollow core photonic crystal fibers for transporting the laser beams from the LSE to the telescope top end, the only logical optical path from an LSE on the azimuth structure to the telescope elevation structure is through one of the two elevation axes. Since these are also used for the axial Nasmyth sites occupied by the APS/PFI and WFOS instrument/AO systems, there are two significant requirements for the LGSF optical feed in this region:

- The LSGF ducting must be deployable; i.e., it must be moved out of the path of the instrument which uses that axial Nasmyth port (which, by definition, must be a non-LGS AO instrument).
- The beam pattern on the elevation structure will rotate with respect to that on the azimuth/Nasmyth structure as the telescope moves in elevation. The beam transport in this area must accommodate this rotation.

5.1.2 Switchyard and Asterism Generator

Although any concept for the details of the optical transport from the LSE to the fixed portion on the telescope elevation structure is purely speculative, it would probably have to involve the use of tip/tilt mirrors in the critical region between the Nasmyth platform and the telescope elevation axis. Even if further engineering studies showed it to be possible to transport the beams in a more compact formation than the 3 × 3 array on 70 mm centers envisioned for the truss portion of the BTO, the envelope would still be quite large (with 25 mm diameter mirrors, the closest reasonable center spacing would be 35 mm, for an outside envelope 95 mm on a side). A K-mirror optical rotator of the sort used in the LLT input would be large and heavy and would have to be precisely aligned with the elevation axis. Since the beam will require a 90º bend at each of the two end points in any case, it is simpler to think in terms of individual tip/tilt mirror arrays similar to those used in the Centering and Pointing Arrays on the truss and top end. The tip/tilt range would have to be significantly larger than that for the Centering/Pointing Arrays (depending on the distance between the two sets of mirrors). This approach would also eliminate the three reflections of a K-mirror system.

Although more complex than a simple K-mirror, the use of tip/tilt mirrors provides additional flexibility and versatility. Slight misalignments which may result from the episodic removal and

redeployment of the transport ducting can be compensated by recalibration of the mirror pointing algorithms at the beginning of each deployment, using the Prealignment Cameras or the Diagnostic System. In contrast, a K-mirror would have to be carefully aligned each time it is deployed. It is also possible that creative use of the tip/tilt mirrors can also be used to assume some of the optical selection procedures presently carried out in the Laser Switchyard and Asterism Generator when switching from one asterism to another, eliminating some of the additional reflections which the off-telescope LSE and deployable transport will require.

5.2 Road Map to Final Conceptual Design Report

As noted in the Conceptual Design Report [2], the schedule for completing the LGSF is shorter than that for the TMT itself, thus permitting a slack period before beginning the final design process for LGSF. One driver for this approach is that one might anticipate technical advances (more compact or powerful laser systems, development of pulsed laser systems, development of hollow core photonic crystal fibers) which could greatly reduce the cost or complexity of the LGSF.

A second point, noted in the Conceptual Design Report, is that several aspects of the LGSF design were not initially addressed in detail because they depended on design features of the TMT which were undefined at that time. The present report is a case in point, since a detailed analysis of the gravity deflections and mechanism inaccuracies as they impact the LGSF design could not be accomplished until the telescope structure itself had been defined and subjected to flexure analysis. This report, which concentrates on those aspects of the design, should be considered an incremental addition to the original report.

This process will continue in the future. As the telescope structure continues to mature and decisions within TMT are made on (for example) the final location of the LSE, a separate study of the incremental changes to the LGSF design will be required. Once the final optomechanical concept is complete, it will be necessary to re-evaluate the design of the electronics, real-time controller, and (possibly) safety systems. As a result, the “slack” time in the LGSF schedule is not devoid of effort, but consists of keeping up with changes in the TMT design as well as with technical advances which may occur in the laser or beam transport fields. The goal is to consolidate the initial Conceptual Design Report with succeeding incremental design reports into a Final Conceptual Design Report prior to the detailed design phase of LGSF construction.

Appendix A –Physical Modeling of LGSF Optical Performance

A.1 Physical Propagation through Relay Lens System

We employed conventional ray tracing techniques to design the relay lens prescription with the goal of reimaging the laser system output at the input pupil of the LLT. In addition, we carried out physical modeling of the beam propagation to ensure that the relay lenses also maintained the beam profile and power density at the LLT input pupil.

A perfect TEM_{00} laser beam with a Gaussian profile will spread out as it propagates as:

$$w(z) = w_o\left[1+\left(\frac{\lambda z}{\pi w_o^{\,2}}\right)^2\right]^{\frac{1}{2}}$$

where w_o is the $1/e^2$ beam waist radius, λ the wavelength, and z the propagation distance (Fig. A-1).

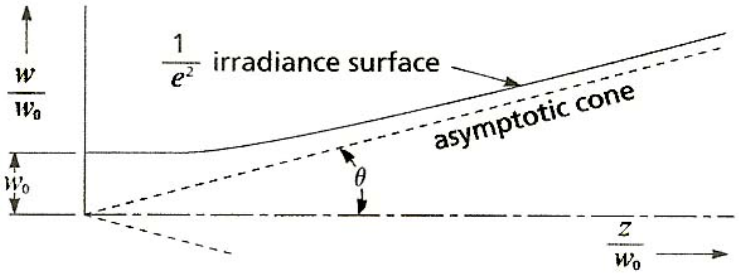

Figure A.1-1: Representation of the spread of a TEM_{00} laser beam with distance

The TMT LGSF will utilize laser beams with a $1/e^2$ beam waist diameter of 5.0 mm (w_o = 2.5 mm), so over the 44.5 m path length to the LLT, the beam waist will increase to 8.34 mm, with a consequent loss of power density (Table A.1-1).

Table A.1-1: LGSF Laser Beam Propagation without Relay Optics

Surface name	Position mm	Total power watt	Peak irradiance w/mm2	Beam waist x mm	90% encircled energy diameter mm	95% encircled energy diameter mm
Laser output		50	5.093	2.500	2.689	3.069
Pointing Mirror	2500	50	5.064	2.507	2.696	3.078
(Lens 1)	2700	50	5.060	2.508	2.697	3.079
(Lens 2)	2753	50	5.058	2.508	2.697	3.080
(Lens 3)	21237.98	50	3.623	2.965	3.189	3.635
Fixed Mirror	21500	50	3.601	2.975	3.200	3.649
Centering Mirror	40000	50	2.075	3.907	4.200	4.798
LLT Entrance	44500	50	1.825	4.172	4.482	5.116

As shown in Fig. A.1-1, the increase in beam waist with propagation distance changes its behavior in the vicinity of $z_o = \pi w_o^2/\lambda$, known as the Rayleigh range. Inside of this distance, the beam propagation is calculated by Fresnel diffraction; outside of this distance, the propagation is largely angular. At the lens surfaces, we still employed geometric ray tracing. The beam profile at the relay lens positions is illustrated in Fig. A.1-2, and the calculated beam waist throughout the optical path is presented in Table A.1-2

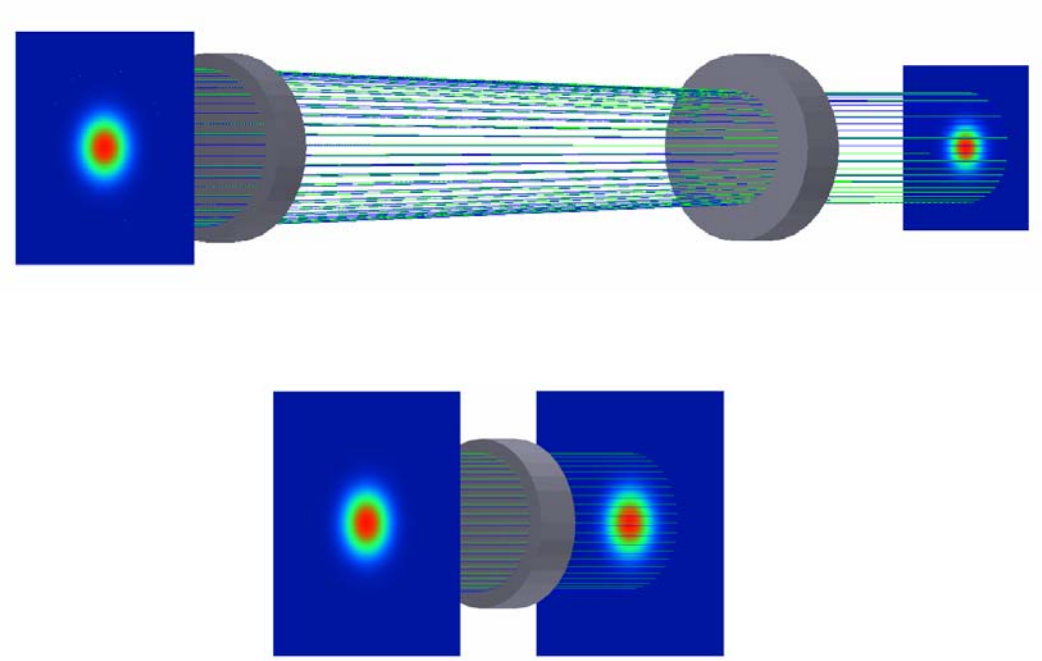

Figure A.1-2: LGSF beam profile at the input to relay lens L1 and output of relay lens L2 (top panel) and at the input and output of relay lens L3 (bottom panel). The minimum beam waist diameter of 3.6 mm occurs at L2.

Table A.1-2: LGSF Laser Beam Propagation with Relay Optics

Surface name	Position	Total power	Peak	Beam	90% encircled	95% encircled
	mm	watt	irradiance	waist x	energy diameter	energy diameter
			w/mm2	mm	mm	mm
Laser output		50	5.093	2.500	2.689	3.069
Pointing Mirror	2500	50	5.064	2.507	2.696	3.078
Lens 1	2700	50	5.060	2.508	2.697	3.079
Lens 2	2753	50	9.717	1.810	1.946	2.222
Lens 3	21237.98	50	3.435	3.045	3.279	3.748
Fixed Mirror	21500	50	3.459	3.034	3.267	3.735
Centering Mirror	40000	50	5.038	2.514	2.717	3.096
LLT Entrance	44500	50	5.131	2.491	2.692	3.069

These results confirm that the relay optics design maintains the original beam profile and power density at the input pupil to the LLT. Figure A.1-3 illustrates the input Gaussian profile and the calculated profiles at the LLT input pupil without and with the relay optics.

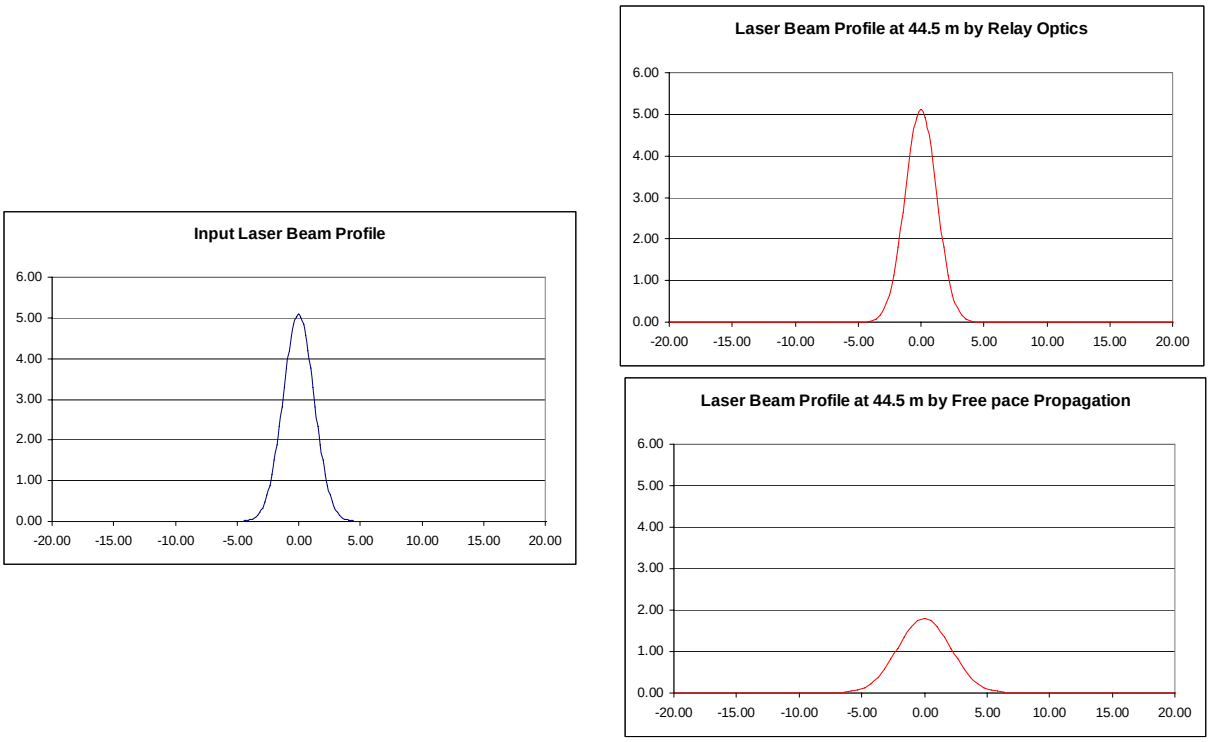

Figure A.1-3: Calculated beam profiles at the output of the laser system (left panel) and at the input pupil of the LLT over a propagation distance of 44.5 m with the relay lens system (top right panel) and without the relay optics (bottom right panel).

A.2 Wavefront Analysis of Laser Beam Propagation through the LLT

We carried out an analysis of the LLT optical performance by calculating the wavefront for the beam locations of NFIRAOS (on- and 35 arcsec off-axis) and GLAO (510 arcsec off-axis). For the purpose of the analysis, we used a top-hat input beam profile 8.33 mm diameter instead of the actual Gaussian laser beam profile with a $1/e^2$ beam waist diameter of 5.0 mm. The output beam diameter is 500 mm. The calculation used a 128 × 128 ray trace grid and the wavefront results were interpolated to 36 terms in the Zernike Polynomial (Table A.2-1).

The model for the propagation analysis is shown in Fig. A.2-1. Note that the local coordinate system is not the TMT system, but is defined with respect to the local optical axis (local z axis). The local x and y axes are perpendicular to and parallel to the LLT M1-M2 axis. One would expect the wavefront behavior in X to be symmetric about the origin, whereas the behavior in y samples different off-axis angles of the LLT primary. The wavefronts were therefore calculated on-axis and at +35 and +510 arcsec off-axis in X, ±35 and ±510 arcsec off-axis in Y (Figures A.2-2 through A.2-5).

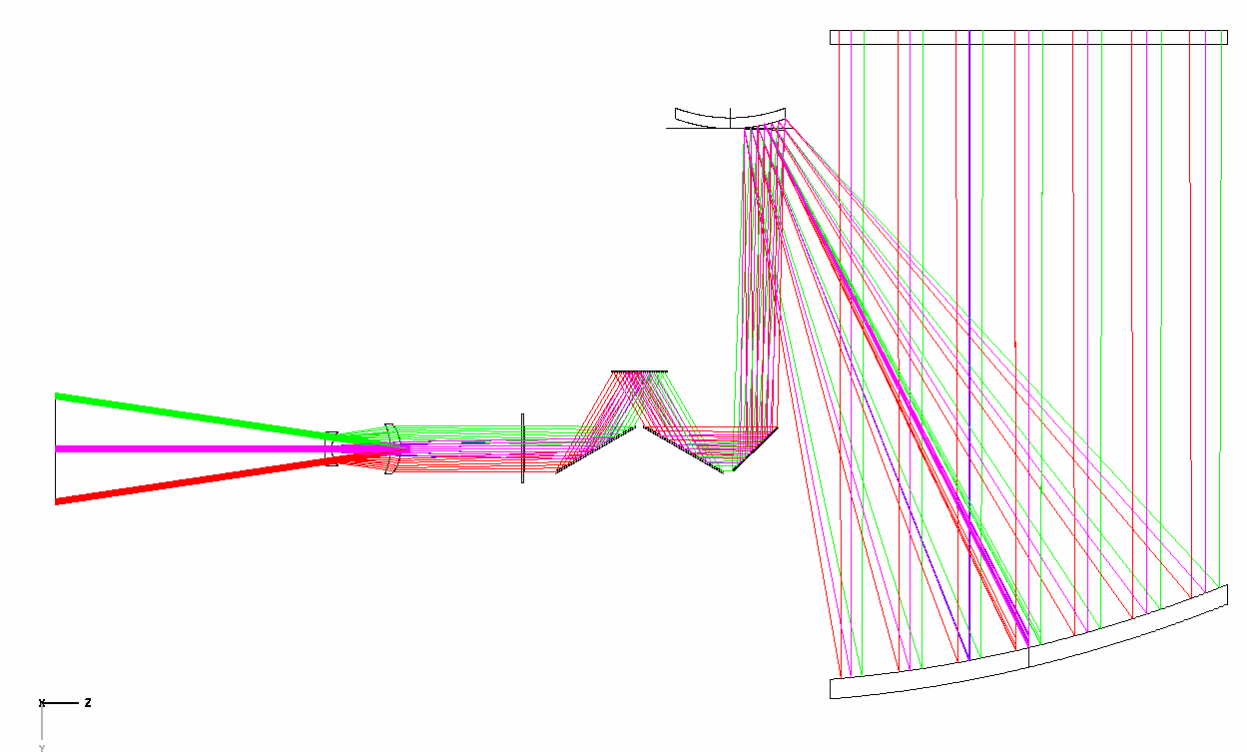

Figure A.2-1: Geometry of LLT wavefront analysis model. The input beam is a top-hat 8.33 mm diameter at the output of the Asterism Generator (left). The z axis of the coordinate system is the optical axis of the propagating beam.

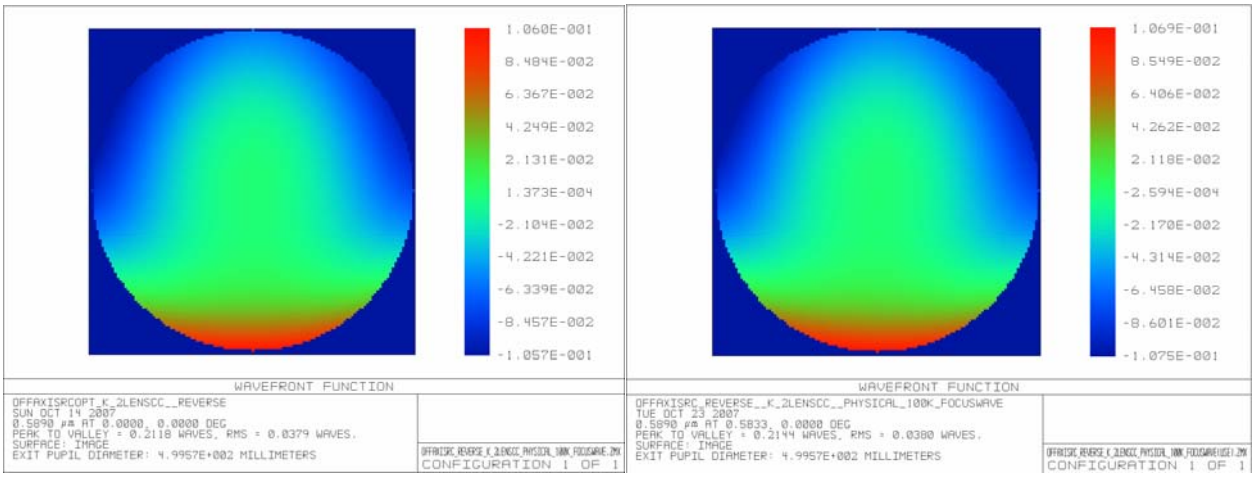

Figure A.2-2: Wavefront map for the on-axis (left panel) and X = +35 arcsec off-axis (right panel) beacons. The wavefront map is symmetric in X.

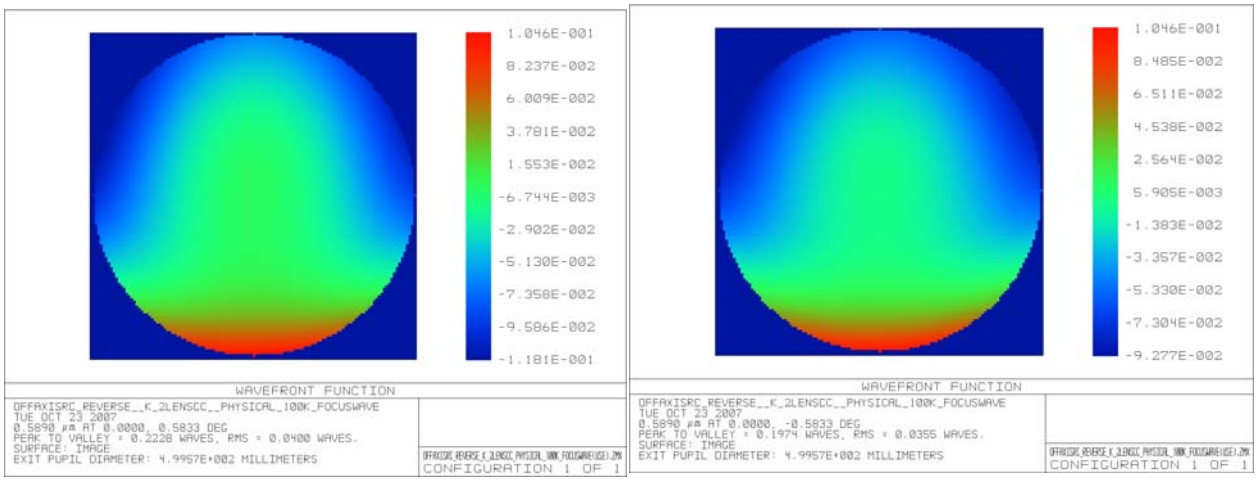

Figure A.2-3: Wavefront map for the Y = +35 arcsec off-axis (left panel) and Y = -35 arcsec off-axis (right panel) beacons.

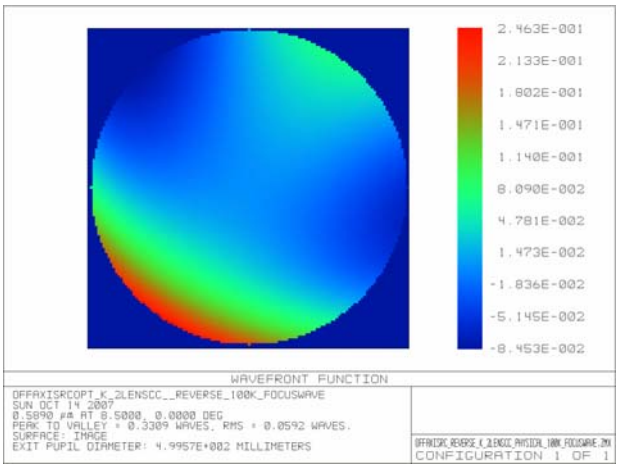

Figure A.2-4: Wavefront map for the X = +510 arcsec off-axis beacon.

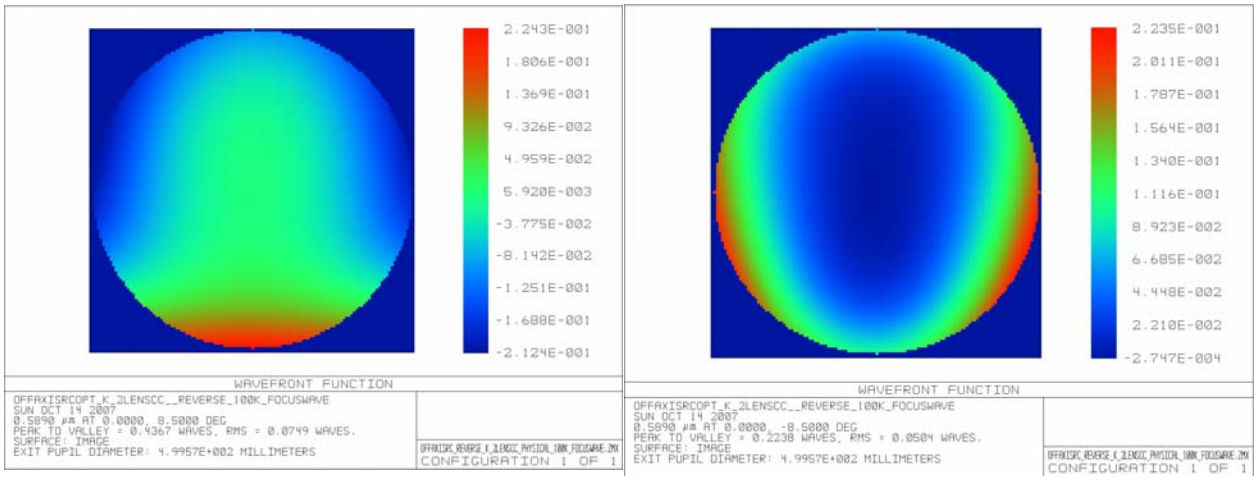

Figure A.2-5: Wavefront maps for the Y = +510 arcsec off-axis (left panel) and Y = -510 arcsec off-axis (right panel) beacons.

Table A.2-1: Zernike Coefficients for LLT Wavefront Map

Statistic performance								
		on axis	35" +y	35" -y	35" +x	510" +y	510" -y	510" +x
RMS (to chief) waves		0.03792309	0.04010985	0.03552054	0.03806194	0.0750995	0.05052948	0.05929045
RMS (to centroid) waves		0.02504105	0.02759457	0.02200414	0.0252718	0.05770392	0.04864372	0.04831331
Strehl Ratio (Est)		0.97554878	0.97038611	0.98106678	0.97510176	0.87682054	0.91081607	0.91196875
RMS fit error (waves)		0.00011996	0.00011869	0.0001195	0.00011997	0.00012075	0.0001223	0.00012073
Maximum fit error (waves)		0.00046513	0.00042346	0.00043993	0.00047603	0.00049169	0.00050071	0.00058316
Listing of Zernike Standard Coefficient Data								
Terms	**Mathematic forms**	**on axis**	**35" +y**	**35" -y**	**35" +x**	**510" +y**	**510" -y**	**510" +x**
Z1	1	-0.02236744	-0.02621017	-0.01883502	-0.02213073	-0.04198538	0.06214512	0.01803939
Z2	4^(1/2) (p) * COS (A)	0.0018666	0.00186702	0.00186788	0.00126973	0.00187947	0.00188451	-0.01515953
Z3	4^(1/2) (p) * SIN (A)	-0.0284187	-0.02904917	-0.02782152	-0.02843299	-0.04802771	-0.01354491	-0.03084429
Z4	3^(1/2) (2p^2 - 1)	-0.00835538	-0.0107866	-0.00631412	-0.00827806	-0.01903019	0.04099746	0.01558064
Z5	6^(1/2) (p^2) * SIN (2A)	-0.00000158	0.00015441	-0.00015631	0.00231487	0.00225068	-0.00225621	0.0379595
Z6	6^(1/2) (p^2) * COS (2A)	-0.02108917	-0.02296489	-0.01834938	-0.0212718	-0.05115603	0.02449388	-0.0212031
Z7	8^(1/2) (3p^3 - 2p) * SIN (A)	-0.00994152	-0.01019821	-0.0096905	-0.00994379	-0.01737042	-0.00417726	-0.0107964
Z8	8^(1/2) (3p^3 - 2p) * COS (A)	0.00065852	0.0006595	0.0006593	0.00041124	0.00066344	0.00066515	-0.00586215
Z9	8^(1/2) (p^3) * SIN (3A)	-0.00081566	-0.00081416	-0.00082065	-0.00081813	0.00509525	-0.00672395	-0.00079491
Z10	8^(1/2) (p^3) * COS (3A)	0.00012414	0.00012389	0.00012307	0.00012454	0.00012571	0.00012515	-0.00574544
Z11	5^(1/2) (6p^4 - 6p^2 + 1)	0.00352708	0.00353262	0.00352913	0.00352995	0.00401305	0.00398124	0.00399795
Z12	10^(1/2) (4p^4 - 3p^2) * COS (2A)	-0.00030928	-0.00031732	-0.00031394	-0.00030212	-0.00112343	-0.00112414	0.00050705
Z13	10^(1/2) (4p^4 - 3p^2) * SIN (2A)	0.00000017	-0.00000076	-0.0000019	0.00000125	-0.00000046	0.00000272	0.00000525
Z14	10^(1/2) (p^4) * COS (4A)	-0.00002285	-0.00002094	-0.0000215	-0.00002326	0.00013639	0.00015649	0.00015384
Z15	10^(1/2) (p^4) * SIN (4A)	-0.00000051	-0.0000002	0.00000077	-0.00000165	0	-0.00000002	-0.00001652
Z16	12^(1/2) (10p^5 - 12p^3 + 3p) * COS (A)	0.00000021	0.0000021	-0.00000016	-0.00002241	-0.0000011	0.00000073	-0.00028523
Z17	12^(1/2) (10p^5 - 12p^3 + 3p) * SIN (A)	0.00005927	0.00003832	0.00008069	0.00005867	-0.00022248	0.00034334	0.00006094
Z18	12^(1/2) (5p^5 - 4p^3) * COS (3A)	0.00000067	0.00000122	0.00000203	0.00000039	-0.0000006	0.00000072	-0.00004243
Z19	12^(1/2) (5p^5 - 4p^3) * SIN (3A)	0.00000938	0.00001256	0.00000668	0.0000089	0.00004829	-0.00003107	0.00000926
Z20	12^(1/2) (p^5) * COS (5A)	0.00000202	-0.00000036	0.00000017	-0.00000148	0.00000004	0.00000252	-0.00002741
Z21	12^(1/2) (p^5) * SIN (5A)	-0.00000084	-0.00000065	-0.00000075	0.0000002	-0.00002548	0.0000284	0.00000147
Z22	7^(1/2) (20p^6 - 30p^4 + 12p^2 - 1)	0.00002187	0.00002089	0.00001977	0.00002174	0.00004169	0.00004028	0.0000407
Z23	14^(1/2) (15p^6 - 20p^4 + 6p^2) * SIN (2A)	0.00000044	-0.00000023	-0.00000096	0	0.00000125	-0.00000004	-0.00000098
Z24	14^(1/2) (15p^6 - 20p^4 + 6p^2) * COS (2A)	0.00000365	0.00000026	0.00000182	0.00000301	-0.0000188	-0.00001985	0.00002454
Z25	14^(1/2) (6p^6 - 5p^4) * SIN (4A)	-0.00000135	0.00000036	0.00000114	0.00000037	-0.00000083	-0.00000107	0.0000006
Z26	14^(1/2) (6p^6 - 5p^4) * COS (4A)	0.00000072	0.00000038	-0.00000031	0.00000079	0.00000601	0.0000088	0.00000924
Z27	14^(1/2) (p^6) * SIN (6A)	-0.00000004	0.00000073	-0.00000168	-0.00000033	-0.0000001	0.00000033	-0.0000001
Z28	14^(1/2) (p^6) * COS (6A)	0.00000096	-0.00000192	0.00000047	0.00000006	-0.00000236	-0.00000219	0.0000038
Z29	16^(1/2) (35p^7 - 60p^5 + 30p^3 - 4p) * SIN (A)	-0.00000004	-0.00000032	-0.00000132	0.0000001	-0.00000635	0.00000419	-0.00000179
Z30	16^(1/2) (35p^7 - 60p^5 + 30p^3 - 4p) * COS (A)	0.00000104	0.00000171	0.00000096	-0.00000175	0.0000012	-0.00000101	-0.00000477
Z31	16^(1/2) (21p^7 - 30p^5 + 10p^3) * SIN (3A)	-0.00000007	0.00000031	-0.00000041	0.00000002	0.00000079	-0.00000211	-0.00000158
Z32	16^(1/2) (21p^7 - 30p^5 + 10p^3) * COS (3A)	-0.00000007	-0.00000168	0.00000115	-0.00000272	-0.00000093	-0.00000073	-0.00000251
Z33	16^(1/2) (7p^7 - 6p^5) * SIN (5A)	0.00000065	0.00000154	-0.00000148	0.00000023	-0.00000253	0.00000238	-0.00000032
Z34	16^(1/2) (7p^7 - 6p^5) * COS (5A)	-0.00000057	-0.00000108	-0.00000151	0.00000238	0.00000055	0.00000234	-0.00000128
Z35	16^(1/2) (p^7) * SIN (7A)	-0.00000049	-0.00000206	0.00000207	0.00000202	0.00000023	-0.00000062	0.00000042
Z36	16^(1/2) (p^7) * COS (7A)	-0.00000173	-0.00000137	0.00000188	-0.00000017	-0.00000051	-0.00000124	0.00000115

A.3 Energy Performance of LLT

A second analysis of the LLT performance was of the energy concentration/beam profile through the LLT and at the nominal 100 km range of the sodium layer, where the LLT is focused. For this calculation, we assumed the beam at the LLT input pupil to be Gaussian with a $1/e^2$ beam waist diameter of 5.0 mm. The clear aperture of the LLT was 560 mm (somewhat larger than the initial conceptual diameter of 533 mm) to ensure that there was almost no clipping of the beam, particularly for the off-axis GLAO beacons. All optical surfaces were assumed to be perfectly transmitting or reflecting, as required, and the atmosphere is assumed to be perfectly homogeneous and transmitting. For the purposes of the power density, we assumed an input power of 50 W.

The propagation of the laser beam through the LLT is diagrammed in Fig. A.3-1. The following figures show the laser beam profile at the input and output of the LLT, and at 100 km distance. As with the LLT wavefront, the beam profiles were calculated on-axis and at +35 and +510 arcsec off-axis in X, ±35 and ±510 arcsec off-axis in Y (Figures A.3-2 through A.3-5). Table A.3-1 presents the calculated power density and Strehl ratio of the laser beams at 100 km.

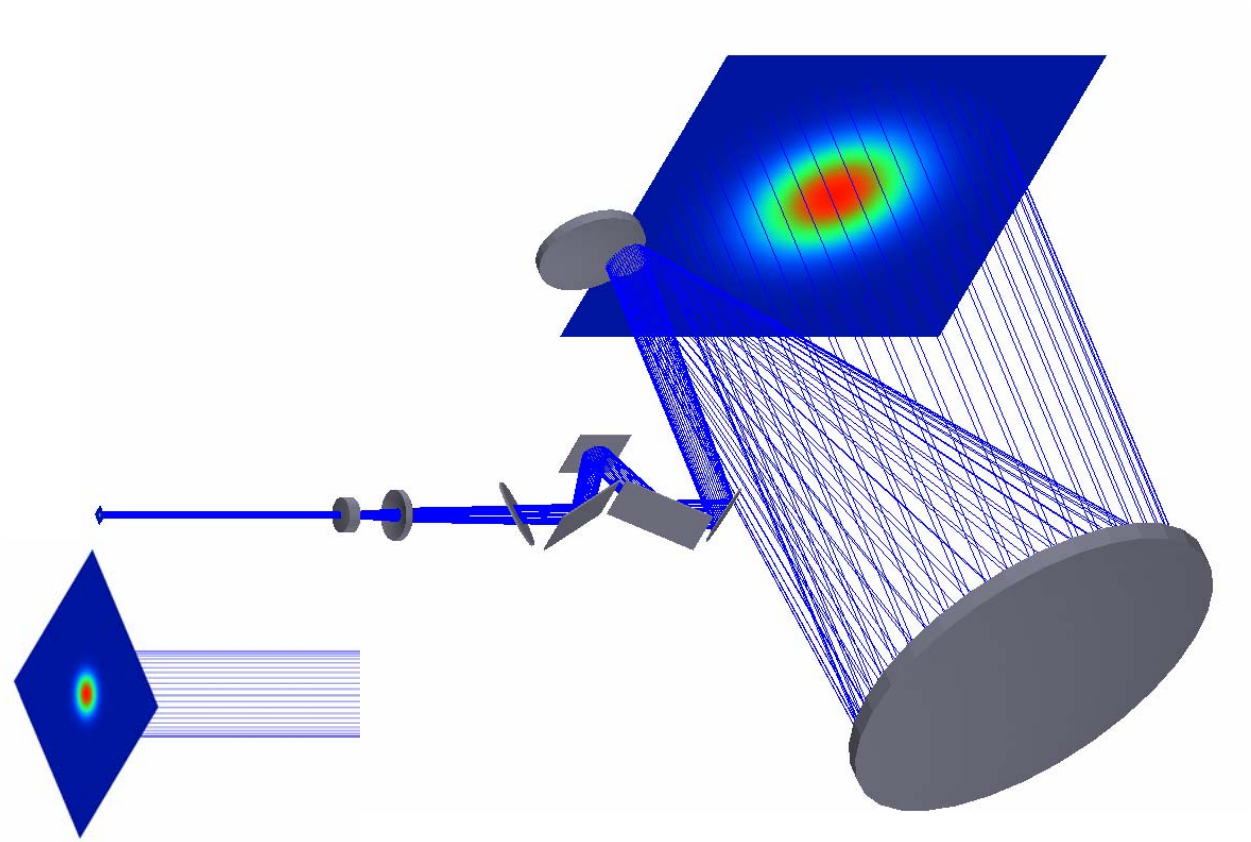

Figure A.3-1: Schematic of the Gaussian laser beam projection through the LLT for the on-axis beacon. The inset at lower left shows the magnified beam at the LLT input pupil.

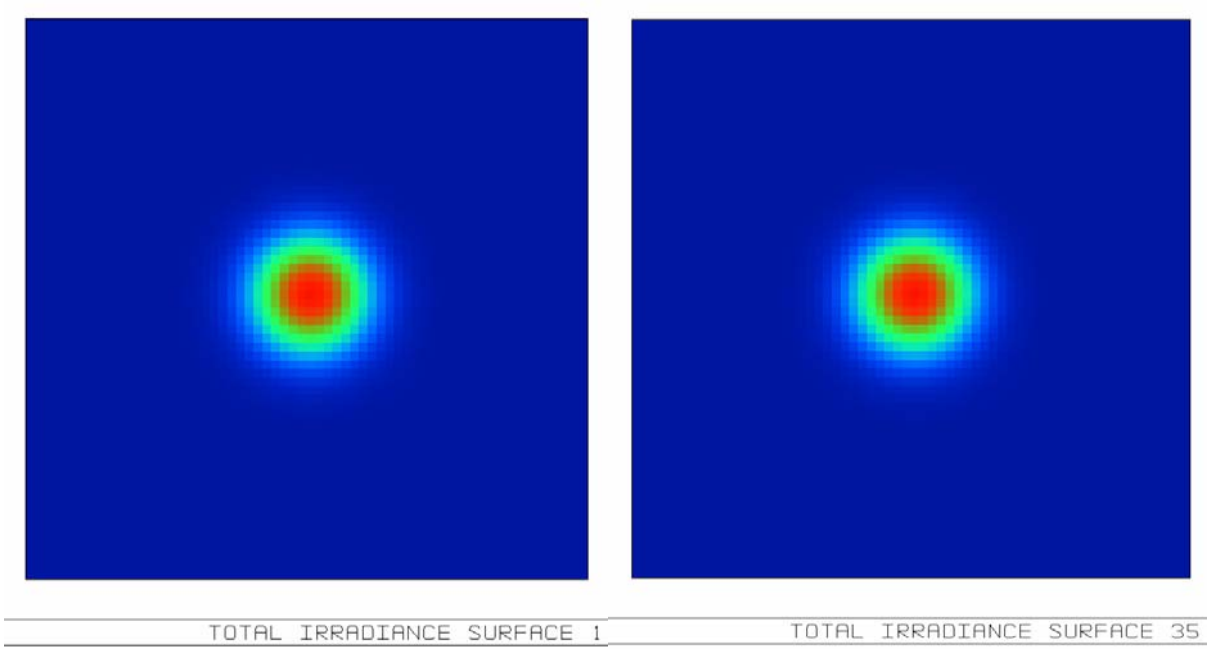

Figure A.3-2: (Left panel): Beam profile for the on-axis laser beacon at the LLT input pupil. The $1/e^2$ beam waist diameter is 5.0 mm, total power 50 W, and power density 5.09 W-mm^{-2}. (Right panel): Beam profile at the LLT primary. The $1/e^2$ beam waist diameter is 299.6 mm, total power 49.96 W, and power density 0.00142 W-mm^{-2}. The power loss is a result of vignetting by the 560 mm diameter LLT primary.

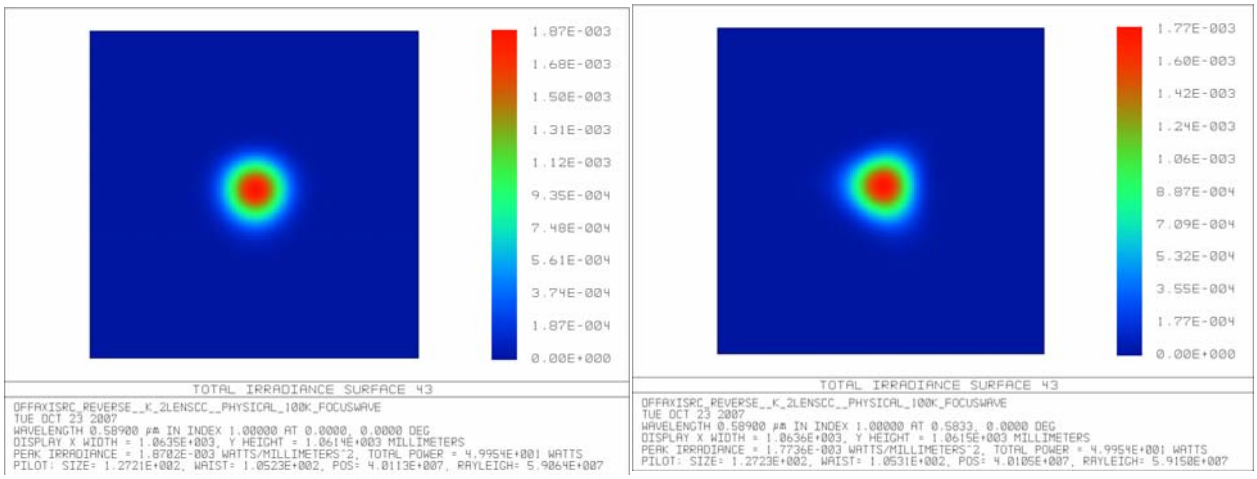

Figure A.3-3: Beam profiles at 100 km distance for the on-axis (left panel) and X = +35 arcsec off-axis (right panel) beacons. The profile is symmetric about off-axis angles in X.

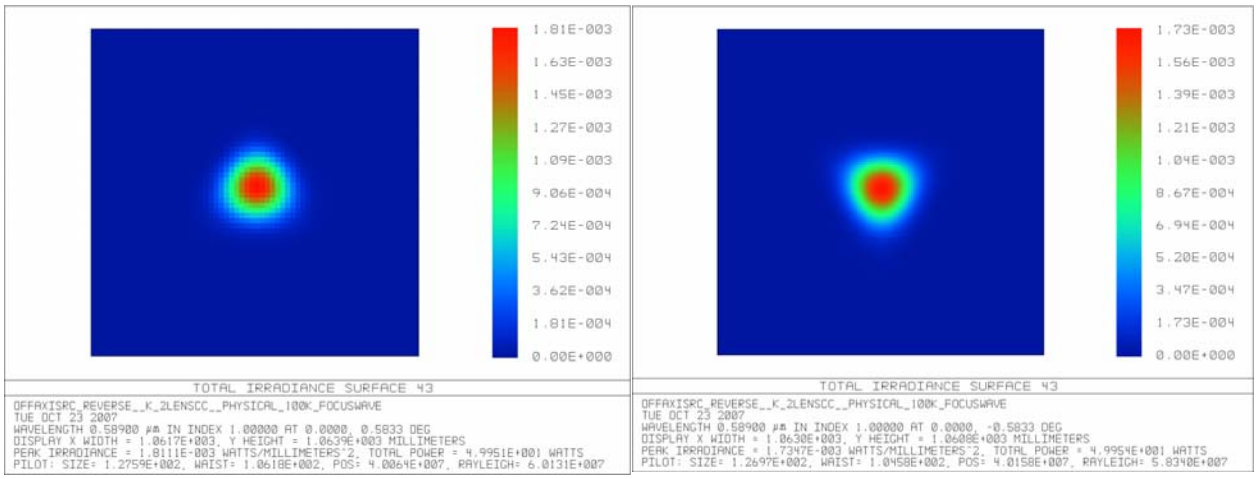

Figure A.3-4: Beam profile at 100 km distance for the Y = +35 arcsec off-axis (left panel) and Y = -35 arcsec off-axis (right panel) beacons.

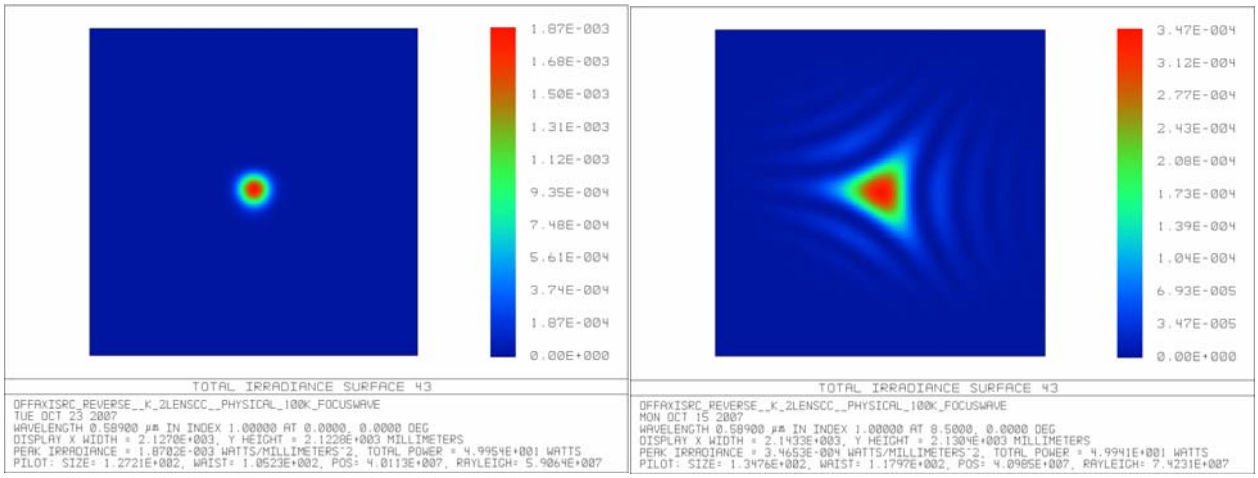

Figure A.3-5: Beam profile at 100 km distance for the on-axis (left panel) and X = +510 arcsec off-axis (right panel) beacons. The on-axis beam is the same as in Fig. A.2-2, but the scaling is reduced for comparison with the 510 arcsec off-axis beacons.

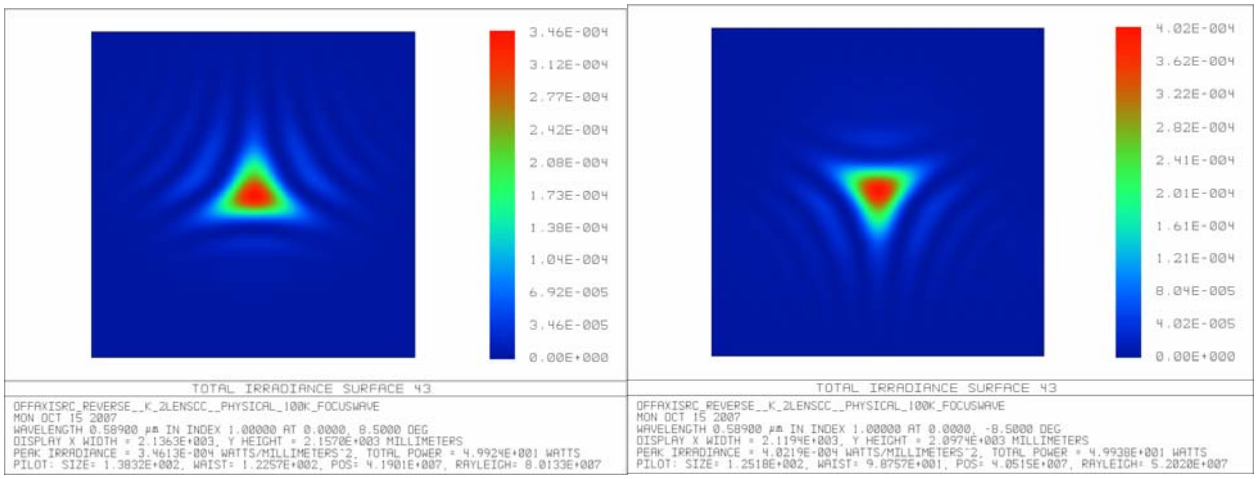

Figure A.3-6: Beam profile at 100 km distance for the Y = +510 arcsec off-axis (left panel) and Y = -510 arcsec off-axis beacons.

Table A.3-1: Energy Concentration of Laser Beacons at 100 km

Laser energy performance at 100 km sky					
	Peak irrediance w / mm^2	50 % energy encircle radius	80 % energy encircle radius	90 % energy encircle radius	Strehl ratio
On axis	0.0019	76.23 mm	115.07 mm	137.15 mm	0.976
35" +x	0.001774	78.39 mm	118.91 mm	142.22 mm	0.975
35" +y	0.001811	77.43 mm	117.61 mm	140.43 mm	0.971
35" -y	0.001735	79.33 mm	120.59 mm	144.60 mm	0.981
510" +x	0.000347	203.25 mm	445.04 mm	627.10 mm	0.906
510" +y	0.000346	211.63 mm	463.50 mm	666.68 mm	0.877
510" -y	0.000402	185.61 mm	416.92 mm	602.25 mm	0.911

Appendix B – Optical Performance of Enlarged LLT Field

The LLT in the original Conceptual Design Report [2] was designed to accommodate a maximum field of view of 432 arcsec radius, determined by the requirements of the GLAO system. Refinements of the GLAO requirements at the time of the CoDR increased this field of view to 510 arcsec radius, but there was insufficient time to update the LLT design to accommodate this requirement. This Appendix describes the modifications to the LLT design and the performance over this enlarged field.

The accommodation to the 18% larger field required enlarging the physical size of the outer ring of mirrors on the Asterism Generator by a corresponding amount, from 540 to 640 mm diameter. The off-axis aberrations could be controlled by adding an additional conic surface to one of the two lenses in the LLT collimator. These changes are shown in Fig. B-1.

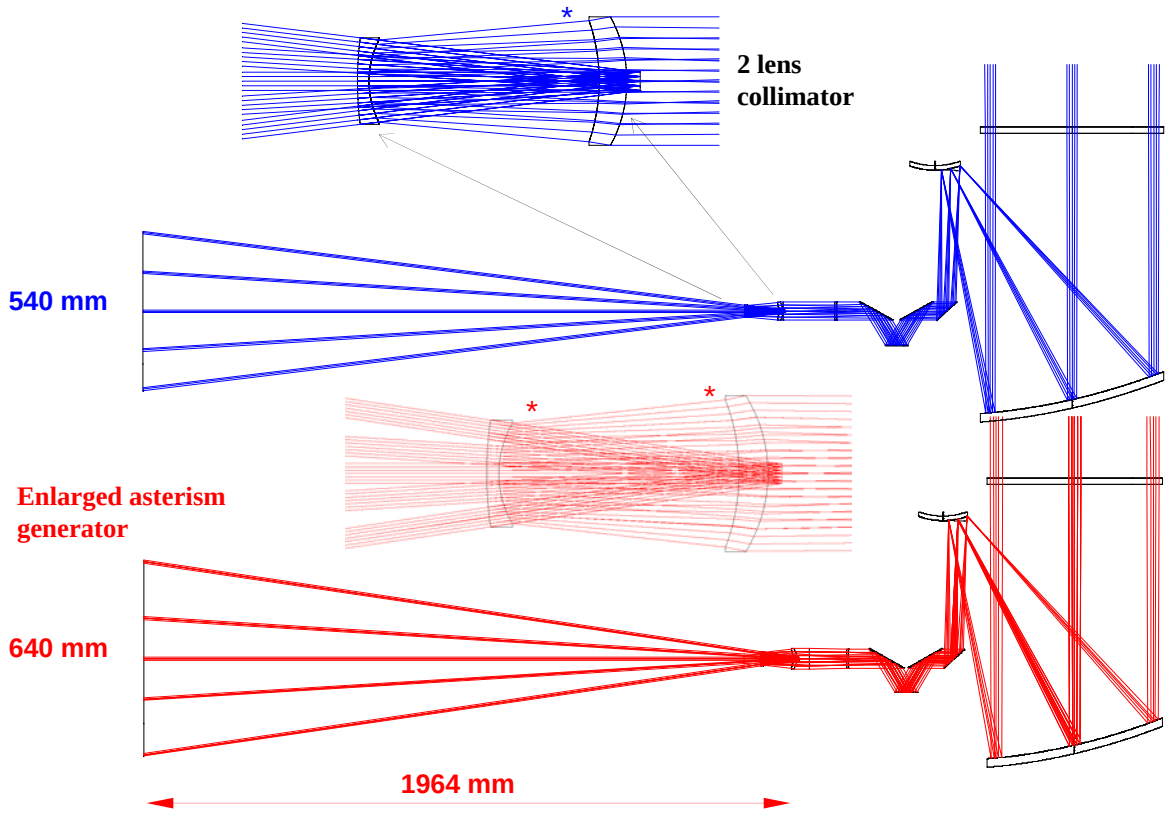

Figure B-1: Schematic LLT design for the original 7.2 arcmin radius GLAO asterism (blue, top) and for the enlarged 8.5 arcmin radius asterism (red, bottom). The insets in each design show the details of the two-lens collimator. Aside from the larger diameter of the lenses in the enlarged design, a second conic surface (*) was required to maintain image quality over the larger field. The physical size and focal length of the Asterism Generator have since been reduced by 25 % as part of this design effort to allow it to fit between the Diagnostic Bench and LLT.

As noted in section 4.2.3, the focal length, diameter, and output mirror spacing of the Asterism Generator were later decreased by 25% to permit it to fit between the Diagnostic Bench and LLT while keeping the field of view at 17 arcmin diameter.

The following figures (B-2 through B-4) illustrate the geometric ray tracing spot diagrams of the LLT for various locations in the field, as well as wavefront and Strehl plots, all at 589.3 nm wavelength. The LLT Y-axis is on a line through the M1-M2 axis, so calculations are carried out on both sides of the origin. The performance should be symmetric about the origin in the X-direction. Figure B-5 shows the on-axis performance near 550 nm, where the LLT would be used to observe a star for image quality and pointing accuracy evaluation using the Diagnostic System.

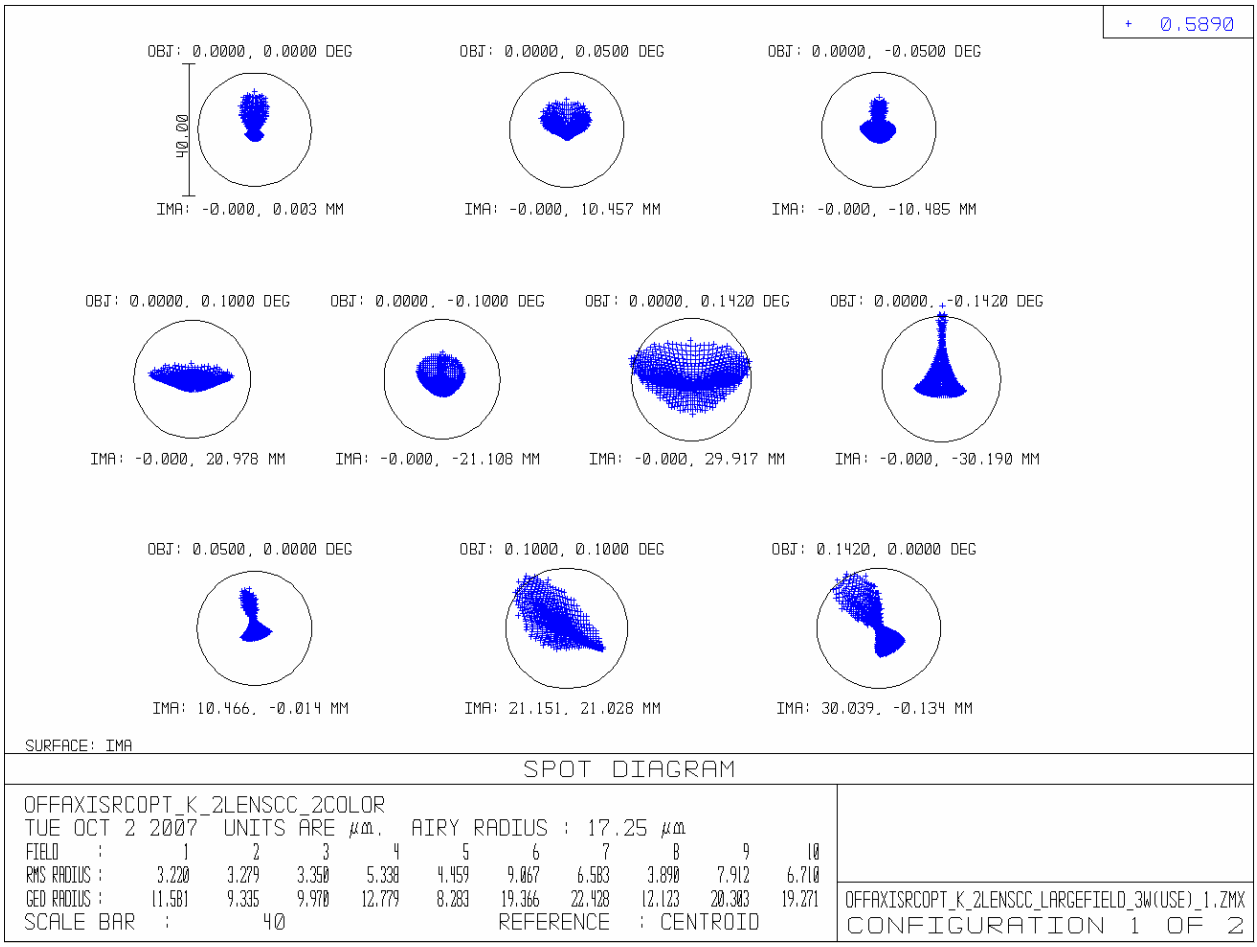

Figure B-2: Spot diagrams at 589.3 nm for various field locations in the revised LLT design.

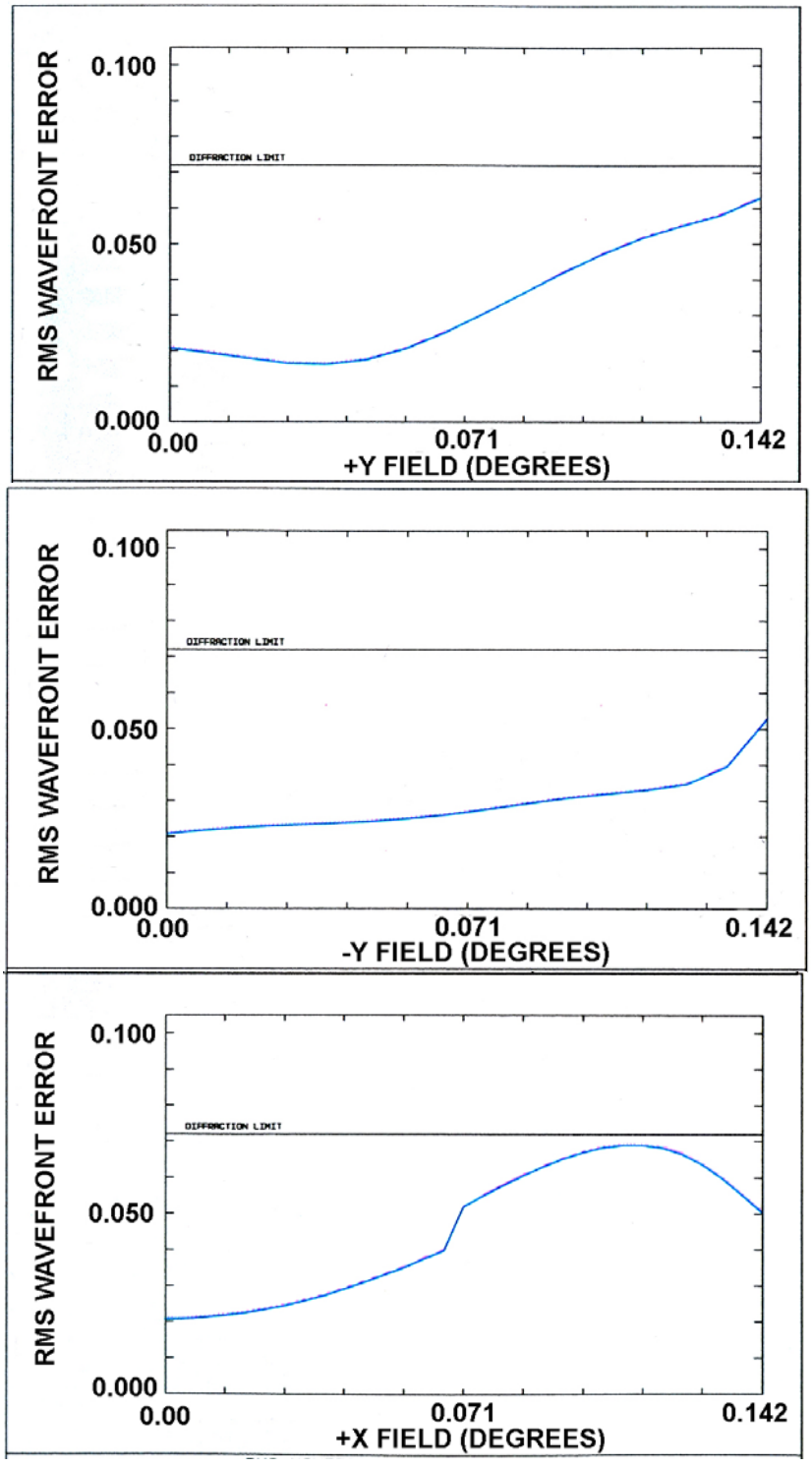

Figure B-3: Wavefront error (in waves) over the redesigned LLT field at 589.3 nm for the +Y field (upper panel), -Y field (middle panel) and +X field (lower panel). The error is symmetric in X. The horizontal line at 0.072 waves represents the diffraction limit.

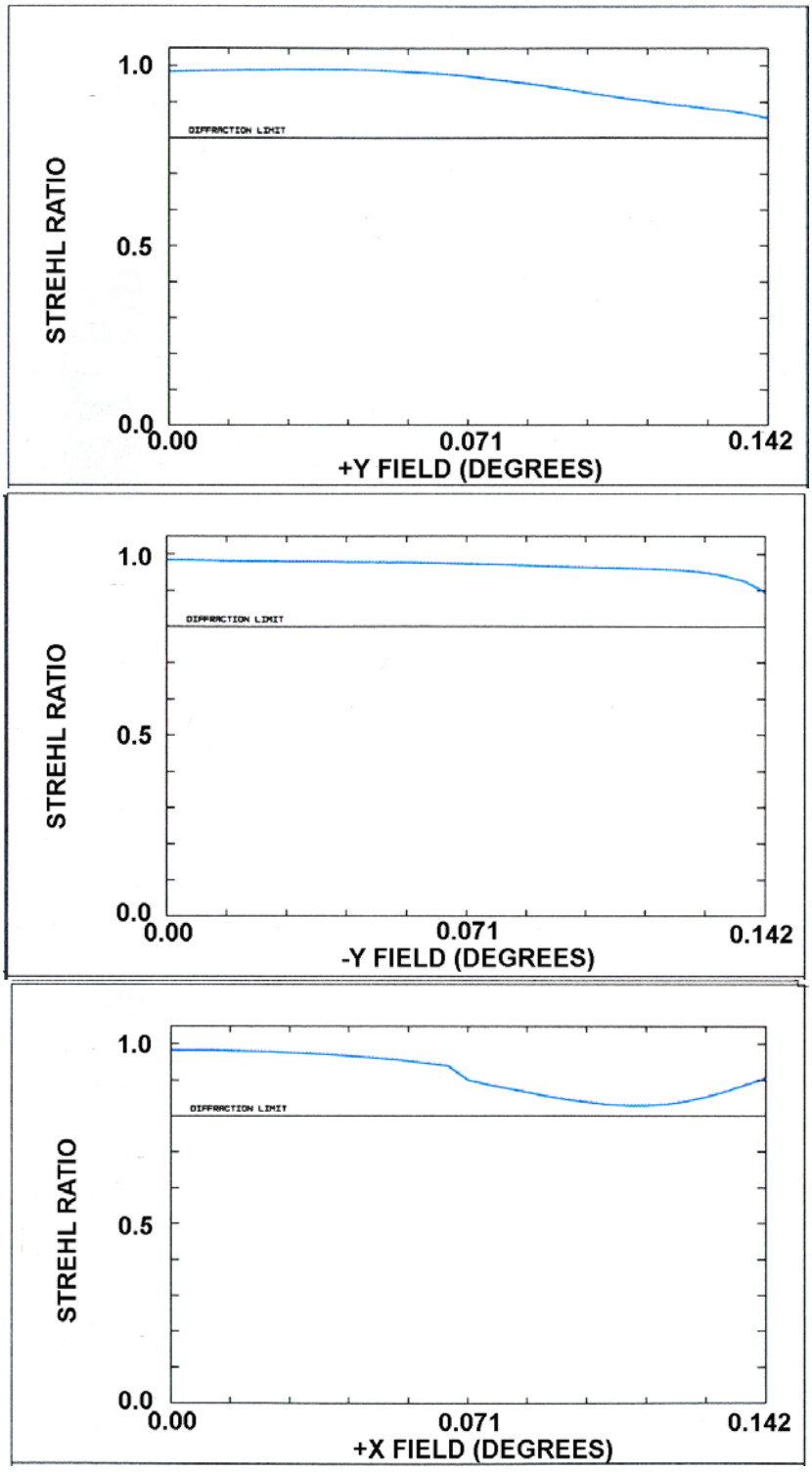

Figure B-4: Wavefront error plots over the redesigned LLT field at 589.3 nm. This is the same information as in Fig. B-3, but presented in terms of the Strehl ratio. The horizontal line at 0.8 represents the diffraction limit.

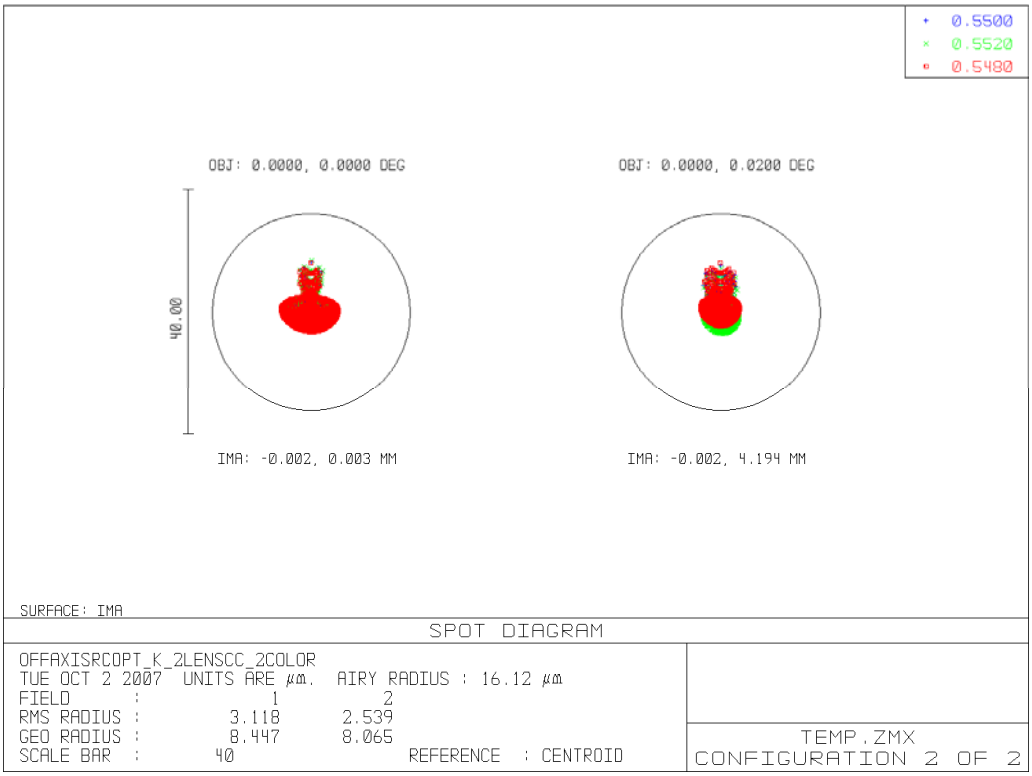

Figure B-5: Spot diagram for the redesigned LLT over the 540 – 560 nm wavelength range.

Appendix C – Access and Handling Requirements

LGSF sub-systems	Locations	Access and handling requirements	Document	Comments
Laser Service Enclosure (LSE): - Laser Room - 3 Lasers and electronics - Safety shutters - Switchyard (SWY) and electronics		Access when telescope zenith pointing	REQ-1-OAD-1495	
		Load capacity for access/handling equipment: 2t	REQ-1-OAD-6240	LSE assembled piece by piece. Heaviest component: laser bench 1.5t
		Installation from side and top using enclosure mounted crane	?	Enclosure mounted crane -> ICD ENC to LGSF
		Removal of components from top using enclosure mounted crane	?	Enclosure mounted crane -> ICD ENC to LGSF
LGSF BTO Vertical Path (VP): - SWY to BTO Path Optics - Truss Pointing Array (TPA) - Relay lenses (L1, L2 and L3) - Tripod Fold array - Sensors and Pre-Alignment Cameras (PAC)	1) SWY to BTO Path Optics: nearby LSE (bottom of the vertical leg and close to LSE roof) or within LSE 2) TPA: nearby LSE (bottom of the vertical leg and close to LSE roof) or within LSE 3) Relay lenses L1 and L2: nearby LSE: bottom of the vertical leg and close to LSE roof 4) Relay Lens L3: As close as possible of the fold array at the top of the vertical path 5) Tripod Fold array: intersection of the vertical path and tripod leg 6) PAC: with TPA and Tripod Fold Array 7) Sensors (temperature, pressure and smoke sensors, control switches...): several along the vertical path	Access when telescope zenith pointing	REQ-1-OAD-2992	
		Load capacity for access/handling equipment: 1t	?	Estimate for overall BTO path is 1t (LGSF CoDR report)
		Installation TBD	?	To be discussed with Kei
		Maintenance (cleaning, troubleshooting or removal of components) using the ladder or enclosure mounted crane with basket	?	Ladder: Described in TEL-STR to LGSF ICD Enclosure mounted crane -> ICD ENC to LGSF Should have a LGSF req that the mass of each individual BTO path component does not exceed TBD kg, that the volume does not exceed TBDxTBDxTBD and that each component can be handled by 1 person located in the enclosure mounted crane basket
LGSF BTO Tripod Path (TP): - - Sensors ?	Sensors (same as BTO VP): several along the tripod leg (TBD)	Access when telescope horizon pointing	REQ-1-OAD-2994	
		Load capacity for access/handling equipment: 1t	?	Estimate for overall BTO path is 1t (LGSF CoDR report)
		Installation TBD	?	Enclosure mounted crane with basket: ICD ENC to LGSF

		Maintenance (cleaning, troubleshooting or removal of components) using the enclosure mounted crane with basket	?	Should have a LGSF req that the mass of each individual BTO path component does not exceed TBD kg, that the volume does not exceed TBDxTBDxTBD and that each component can be handled by 1 person located in the enclosure mounted crane basket
LGSF BTO Top End: - Truss Centering Array (TCA) - Diagnostic bench - Asterism generator (AG) - LLT & LLT bench	1) TCA: at the entrance of the LGSF top end 2) PAC: with TCA	Access when telescope horizon pointing	REQ-1-OAD-2994	
		Load capacity for access/handling equipment: 1t	REQ-1-OAD-6220	Estimate for overall LGSF BTO TE is 1t (LGSF CoDR report plus electronics cabinets and supports)
		Installation TBD	?	Similar to M2 installation ?
		Maintenance (cleaning, troubleshooting or removal of components) using the Top End Access Platform and enclosure mounted crane	?	ICD-ENC-LGSF: -Top end access platform is deployed when telescope is horizon pointing and rotated by TBD degrees in Az. - Clearances between Top End Access Platform and LGSF - Top End Access Platform load Requirement for LGSF is 650kg - Additional deployable raised platform to access all components of the LGSF Top End Enclosure mounted crane.